Deutsches Geodätisches Forschungsinstitut (DGFI)

ANNUAL REPORT 2005/2006

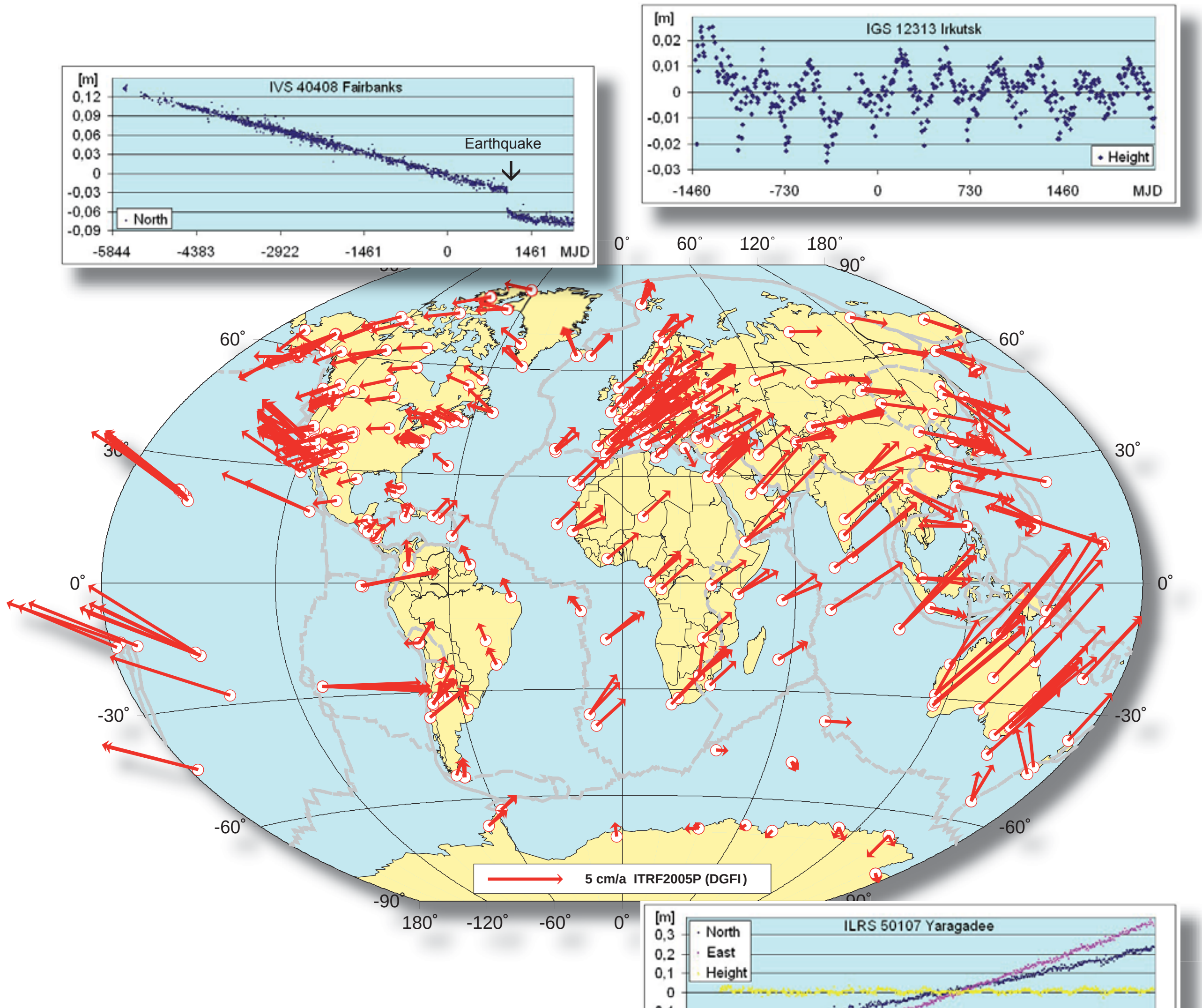

ITRF2005

DGFI computation of ITRF2005 based on weekly SLR, GPS, DORIS, and session-wise VLBI normal equations of station coordinates and EOP provided by the corresponding techniques' services (see topic 3.1).

Deutsches Geodätisches Forschungsinstitut (DGFI)
Alfons-Goppel-Str. 11, D-80539 München
Tel.: 089 23031-1107   Fax: 089 23031-1240
E-mail: mailer@dgfi.badw.de   Internet: http://www.dgfi.badw.de

ANNUAL REPORT 2005/2006

Table of Contents

2nd Edition

The Institute

The German Geodetic Research Institute (Deutsches Geodätisches Forschungsinstitut, DGFI) is an autonomous and independent research institution located in Munich. It is supervised by the German Geodetic Commission (Deutsche Geodätische Kommission, DGK) at the Bavarian Academy of Humanities and Sciences (Bayerische Akademie der Wissenschaften, BAdW). The research covers all fields of geodesy and includes the participation in national and international research projects as well as various functions in international bodies.

Research Programme

The general theme of the DGFI research programme is established for a long period (several years) in order to meet the continuous requirements of international activities and the demands of modern society. It is defined as "Geodetic research for observing and analysing the System Earth". This theme reflects the scientific orientation of Geodesy as the discipline of measuring and mapping the changing Earth, and responds to the challenges for a better representation of global change and geodynamic phenomena and processes. It includes the study of geometric and gravimetric observation techniques, fundamentals of geodetic reference systems, and analysis methods for estimating geodetic parameters in physical models.

Motivation

The present societal challenges to Geodesy are based on the increasing consciousness of helplessness of mankind against natural hazards. Extreme disasters can only be prevented if the characteristics and processes of earthquakes, tsunamis, flooding, etc. are well understood in order to envisage a prognosis of future events. Geodesy is capable of measuring effects of such processes by observing the variations of the Earth's rotation, the Earth's surface geometry, and the Earth's gravity field. As these variations are very small, all efforts have to be undertaken to exhaust the full information included in the geodetic measurements. This can only be done by a thorough study of the techniques, models and results, and by the development of sophisticated methods for observing and analysing the parameters describing the dynamics of the System Earth.

Practical Applications

The basic requirement for all geodetic measurements and derived parameters (time-variable position coordinates, gravity values, etc.) are unique reference systems. A fundamental research of DGFI is therefore dedicated to this field. The frames realizing the reference systems are also used in many practical applications. The celestial reference frame enables to describe the orientation of Earth in space. It is necessary for space travel, global navigation, astrometry etc. The terrestrial reference frame serves as the basis for all precise positioning in surveying, engineering, navigation, and geo-information systems. It allows the unification of all national and continental reference systems, which is a prerequisite for globalisation of society and economics. The Earth's gravity is represented with respect to physical reference surfaces, e.g., the geoid as an equipotential surface or the mean sea level in a state of equilibrium. It is also the reference for physical heights used in practical applications (levelling, barometric heights). The DGFI research activities support these applications.

University Connections

DGFI is cooperating very closely with all German universities offering geodetic education. This is mainly done under the umbrella of the DGK but also in bilateral arrangements. Members of DGFI give lectures and courses at various universities. Doctoral or Diploma theses are supervised by DGFI members. Interdisciplinary cooperation is installed with university institutes for Geophysics, Meteorology and Oceanography.

Research Group Satellite Geodesy (FGS)

Most intensive cooperation exists with the Technical University of Munich (TUM), in particular within the Research Group on Satellite Geodesy (Forschungsgruppe Satellitengeodäsie, FGS). It is a consortium formed by TUM's Institute of Astronomical and Physical Geodesy (IAPG) and Research Establishment (Forschungseinrichtung) Satellite Geodesy (FESG), the Geodetic Institute of the University of Bonn (GIUB), the Federal Agency (Bundesamt) for Cartography and Geodesy (BKG), and the German Geodetic Research Institute (DGFI).

International Integration

The research of DGFI is integrated within several international services, programmes and projects, in particular of the International Association of Geodesy (IAG). DGFI recognizes the outstanding role of the scientific services of IAG for practice and research, and cooperates in several of these services as data, analysis and research centre. Members of DGFI have taken leading positions and supporting functions in IAG's scientific commissions, services, projects, working groups and study groups. DGFI also participates in the research programmes and bodies of the European Union (EU) and the European Space Agency (ESA). It cooperates in several United Nations' (UN) and inter-governmental institutions and activities.

Structure of the Programme

The present research programme for the years 2005-2006 was set up during an internal workshop on May 17 and 18, 2004. It was evaluated and revised by the Scientific Council (Beirat) of DGK, and approved by the DGK General Assembly on November 18, 2004. It consists of the three long-term research fields

1. Earth System Observations,
2. Earth System Analysis,
3. International Services and Projects.

System observations include the modelling of observation techniques, methods and approaches of data processing and data combination, definition and realization of reference systems, and provision of consistent parameters. System analysis deals with the study of the properties and interactions of system elements which are reflected by the corresponding geodetic parameters and their correlations. The participation in international services and projects and the maintenance of information systems and science transfer are indispensable requirements for a research institute. The research fields are subdivided into specific topics, twenty in total. DGFI scientists are working simultaneously in several scientific topics in order to ensure the connection between the different fields and the consistency of methods, models and results.

1 System Observations

The major research field system observations includes fundamental investigations on the modelling, data analysis and combination of the different space geodetic observation data, such as the Global Navigation Satellite Systems (GNSS), Satellite Laser Ranging (SLR), Very Long Baseline Interferometry (VLBI), satellite altimetry and gravity sensors (SST, gradiometry). These observations are the basis allowing a highly precise determination of the geometry, the rotation and the gravity field of the Earth and its variations in time.
The research activities are divided into six topics. In topic 1.1 the work concentrates on the modelling of the different observation types to achieve a unification of the models and to improve the consistency between the techniques. Fundamental research concerning the realization of the terrestrial and the celestial reference frame is subject of topics 1.2 and 1.3, respectively. In topic 1.4 the activities concentrate on the development of combination methods for a consistent parameter determination. Subject of topic 1.5 is the modelling for earth gravity field parameters. Methods for the height determination aiming at the unification of height systems are investigated in topic 1.6.

1.1 Modelling for space geodetic observations

DGFI combines observation and normal equations of different space techniques for the determination of a consistent geodetic reference system. In order to minimize systematic differences between combined techniques, the physical modelling has to be uniform. This requires changes in software which is not written in-house for all space techniques. We collaborate with the Technical University Munich and the GeoForschungsZentrum Potsdam for the generation of well adapted GPS equations. As soon as a uniform modelling is realized, the comparison of different techniques allows to improve the processing of individual space techniques. The combination reasearch is mainly done within the GGOS-D project (see also 1.4 and 3.7).

Update of SLR processing

Up to now the colours of bichromatic laser systems were handled as two different observing stations - either of them being furnished with a virtual domes number, and afterwards the station coordinates had to be equated in the generated system of equations. In order to automatize the two-colour handling in the DGFI software DOGS-OC, the station identification in that program was extended to a trinomial identifier composed of site ID, occupation ID, and frequency or wavelength. Thus, the two colours of an instrument can be handled either as one or as two stations according to the requirements. For computing biases and tropospheric refraction, they are regarded as two stations, whereas they operate as a single station in coordinate determination and pass analysis. Thus we can easily discover a relative bias between the two colours (see 3.4).

As a fortuitous bonus of looking into the passage-wise residual plots, we recognized a lot of duplicate passages in the laser data consisting of different data releases which were wrongly given the same release flag. These doublets were systematically eliminated from the data.

Effect of various analysis options on estimated TRF and station position parameters

Geodetic computations often give a variety of options, between which the user has to choose. Such options can be subject of conventions, like the IERS Conventions, or technique dependent conventions proposed by the technique services (e.g. IVS, IGS, ILRS). Some options are obviously preferable to other ones. But, neither can all options be objectively judged as right or wrong, nor are the effects of all options on geodetic target parameters known in detail. This is why it is necessary to clarify the impact of analysis options on the estimated parameters (e.g. terrestrial reference frame, TRF, and position time series) in terms of systematic differences, scale, annual signals and station position repeatabilities. Several analysis options are investigated: tropospheric mapping functions, tropospheric parameterization models, atmospheric loading, thermal deformation and a refined stochastic model of VLBI observations (mainly elevation dependent re-weighting). All computations at DGFI used OCCAM 6.1 and the DOGS-CS software with VLBI data from 1984 till 2005. For all applications, like for geophysical studies or combination issues, systematic effects must be considered thoroughly.

VLBI evaluations significantly depend on the chosen tropospheric mapping function (MF), which can cause systematic effects: When the VMF1 (Vienna Mapping Function 1) is replaced by the NMF (Niell Mapping Function), some station heights of a computed TRF change by up to 13 mm (figure 1.1.1). Between VMF1 and GMF (Global Mapping Function), there are no significant height differences. Discrepancies between station height time series computed with VMF1 and NMF reveal annual periodical signals with amplitudes up to 5 mm, see figure 1.1.2 (usually with similar characteristics, but noticeably smaller in size by one or two thirds for VMF1-GMF). The differences of the position time series are well reflected by the scale time series (figure 1.1.3): The use of different MF causes the amplitudes to disagree by about 0.1 ppb for annual as well as semi-annual signals. Concerning station position repeatability, VMF1 is clearly superior to the other MF: With VMF1, the overall WRMS of the heights is between 5 % and 7 % better. Comparing VMF1 to NMF and GMF, the height WRMS for stations between 30° and 50° latitude is better by up to 23 %.

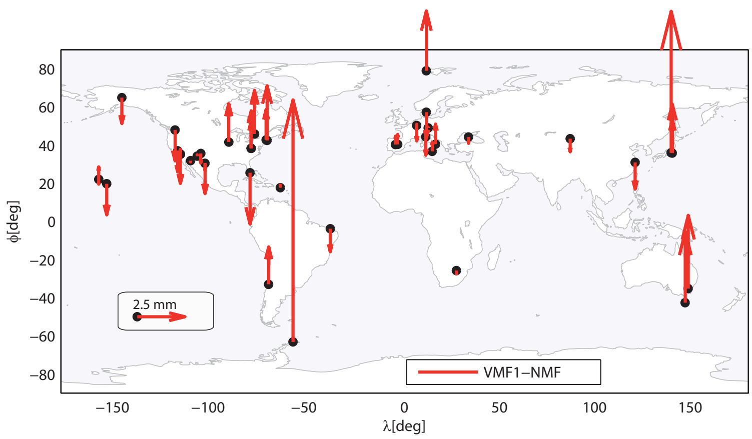

Fig. 1.1.1: TRF height differences: Comparing solutions with VMF1 and NMF.

Fig. 1.1.2: Time series of height differences in Tsukuba (Japan): Solutions VMF1 vs. NMF (red) and GMF (green). Displayed are moving medians computed every 7 days for values of 70 days each.

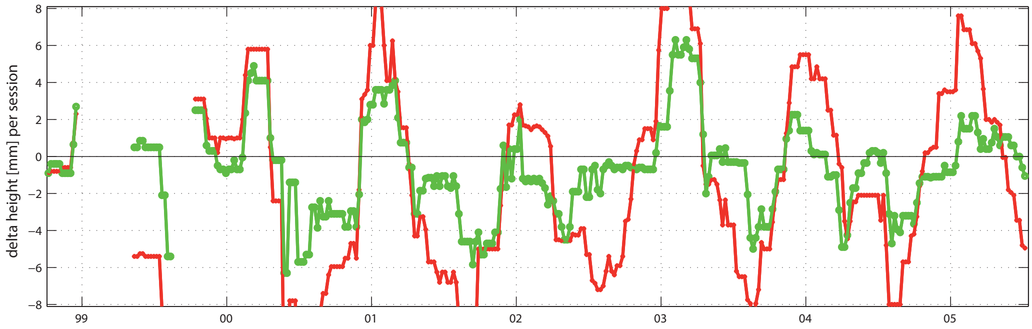

Fig. 1.1.3: Differences between session-wise scale estimates: Solutions VMF1 vs. NMF (red) and GMF (green). Displayed are moving medians computed every 7 days for values of 70 days each.

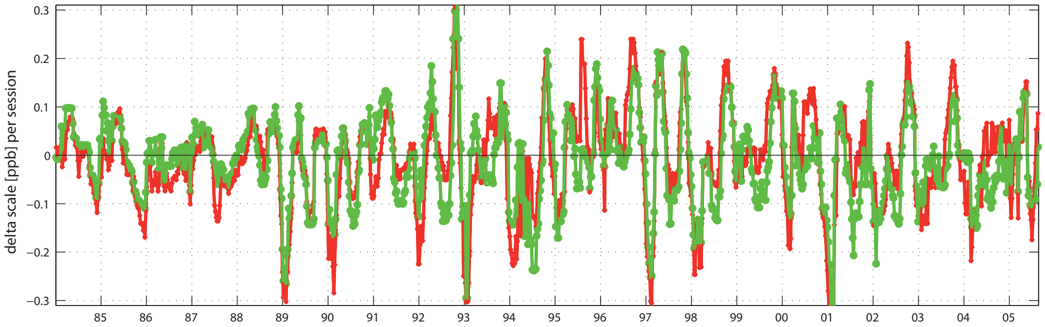

The approach using non-zero a priori values for the horizontal troposphere gradients is applicable from a theoretical point of view and should yield more realistic results. Compared to solutions with zero values, this approach affects TRF estimates mainly by a small tilt in north-south direction of up to -2 mm. These systematic effects are due to the common practice to stabilize gradient estimates towards their a priori values, because they are sometimes weakly defined by the VLBI observations themselves.

Using constant a priori ZD (zenith delay) instead of a ZD derived from surface meteorological data may change the station heights of an estimated TRF to almost random values, because of the correlations between the estimated ZD and station height components. With the ZD data used in this investigation, the station heights generally change less than 1 cm (the maximum is 38 mm), the overall scale is shifted by about 0.2 ppb. Periodic and annual signals in differences of height position time series can be found reaching up to 4 mm (figure 1.1.4).

Fig. 1.1.4: Time series of height differences in Ny-Alesund (Spitsbergen, Norway): Solution using ZD from surface met data vs. solution using constant a priori ZD. Displayed are moving medians computed every 7 days for values of 70 days each.

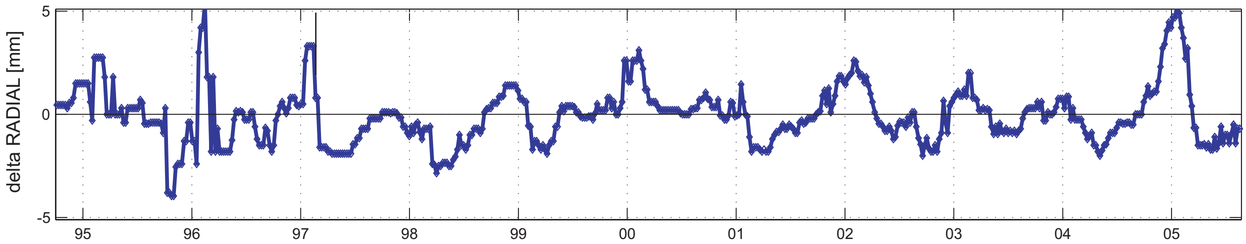

Decreasing the temporal resolution of the estimated ZD from 1 hour to 2 hours does not affect systematically any type of parameter investigated. It leads to episodic signals and noise in station position time series and degrades their repeatabilities by about 3%.

Thermal deformation corrections reduce the annual amplitudes in station position time series by up to 0.7 mm in height and 0.4 mm in the horizontal components. Episodic signals reach up to 3 mm in height (see figure 1.1.5) and 1 mm in the horizontal components. But this correction can be used in VLBI solutions for combination in the IVS or the IERS, only if a clear and reasonable definition of the reference temperature exists. In future, even local tie measurements from VLBI reference points to those of other techniques should comprise calibrated temperature measurements.

Fig. 1.1.5: Time series of height differences in Algonquin Parc (Canada): Solution using thermal deformation corrections and not using. Displayed are moving medians computed every 7 days for values of 70 days each.

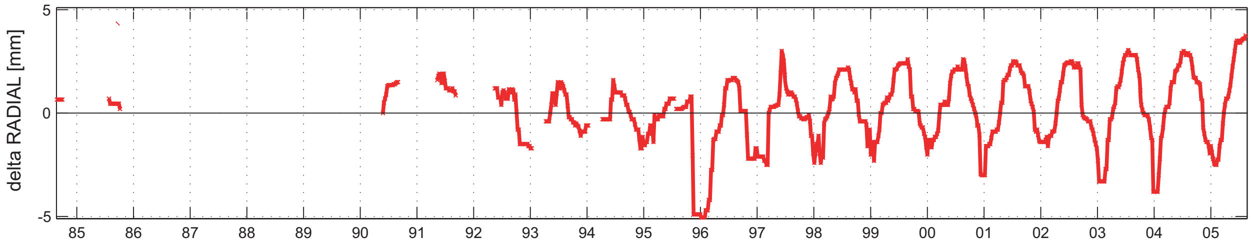

Atmospheric loading corrections generally reduce the amplitudes of the annual signals in height by up to 0.7 mm, but not in the horizontal components. Implied episodic differences in station position time series reach up to ±5 mm in height (see figure 1.1.6) and ±1 mm in the horizontal components. Using this correction improves the overall station height repeatability by 2% RMS and 4% WRMS, for some stations even between 5% and 10%, whereas the repeatabilities of horizontal components do not change. Comparable to thermal deformation, a reasonable application to geodetic data analysis requires a well-founded definition of the reference pressure.

Fig. 1.1.6: Time series of height differences in Gilmore Creek (Alaska): Solution using atmospheric loading corrections and not using. Displayed are moving medians computed every 7 days for values of 70 days each.

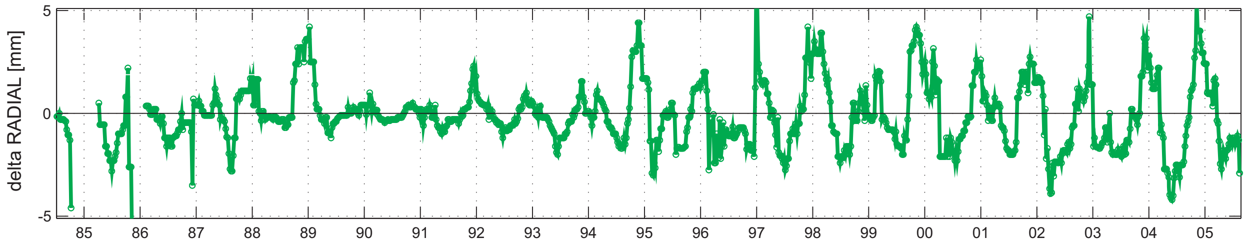

Another investigated option was the refined stochastic model (mainly elevation dependent re-weighting). The effects on the TRF are comparable to the ones of using a priori non-zero horizontal tropospheric gradients, but with different sign: TRF estimates are tilted in north-south direction by up to 1.5 mm, the scale increases by about 0.1 ppb. The station position repeatabilities overall improve by 3% RMS and 4% WRMS in height and horizontal components (which is the best improvement of the solution setup options analysed in this investigation). For some stations the gain is even between 10% and 15%.

1.2 Foundations of terrestrial reference systems

The work in 2005/2006 was focussed on the improvement of the methodology and data analysis related to the computation of the ITRF2005 (see also 3.1). A major part of the work is also related to the IERS Combination Research Centre (see 3.1) and the GGOS-D Project (see 1.4), which started in September 2005. After a detailed adoption of parameterization and modelling, consistent time series with a time span of one year are now available for GPS, VLBI and SLR. They are analysed and combined. Additionally a theoretical study concerning the combination of normal equations based on identical observations was performed.

Intra-technique combination

The computation strategy for ITRF2005 at DGFI is based on the combination of weekly (GPS, SLR and DORIS) and session-wise (VLBI) input data. The free normal equations are accumulated in a first step to technique-specific multi-year solutions. A possibly poor network geometry of the multi-year solution turned out to be a problem. In case of VLBI, the network seemed to have a singularity. Fig. 1.2.1 shows the correlation matrix of the Japanese network including station positions and velocities. Fig. 1.2.2. gives the corresponding map of the station network. The correlation matrix demonstrates that the network is fragmented into two parts. The upper one contains the stations Shintotsukawa, Mizusawa, Kashima und Tsukuba and the lower the stations Gifu and Aira. The network solution could be solved, but the accuracy of the resulting station positions and velocities is very poor. This example shows that the network geometry and possible singularities need to be examined carefully.

Fig. 1.2.1: Correlation matrix of Japanese network (station positions and velocities).

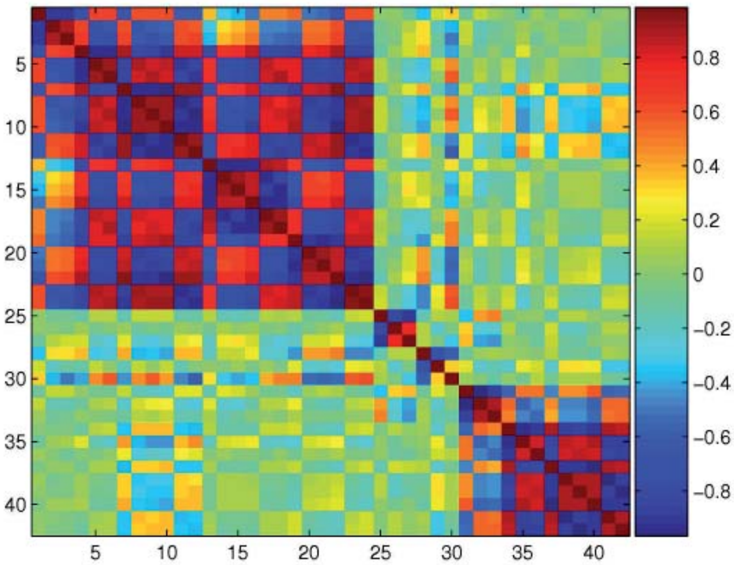

Inter-technique combination

The input for the inter-technique combination is the free normal equations of the technique-specific multi-year solutions resulting from the intra-technique combination. In a first step, absolute weighting factors are estimated for each technique. This becomes necessary since most of the input time series do not contain the full statistical information. Thus the real variance level cannot be reconstructed. For the computation of the weighting factors, the standard deviation of the positions and velocities of good stations was derived from the station position time series obtained

Technique	Weighting factor	Scaling factor for standard deviation
GPS	1/ 84.6	1/ 9.2
SLR	1/282.2	1/16.8
VLBI	1/ 16.8	1/ 4.1
DORIS	1/ 1.0	1/ 1.0

Tab. 1.2.1: Absolute weighting factors for technique specific multi-year solutions.

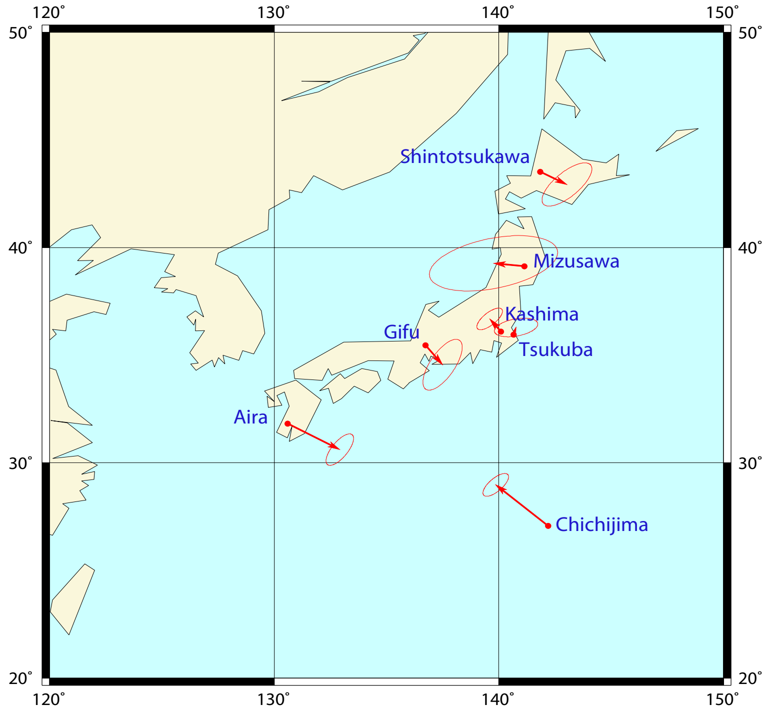

Fig. 1.2.2: Japanese station network.

from the intra-technique combination. The values are related to the standard deviations from the multi-year solutions. The resulting weighting factors are given in Tab. 1.2.1.

For the combination of the different techniques, a careful selection of the local ties (terrestrial measurements) is very important, because only the connection of the networks enables the realization of a consistent datum for the combined network. The ITRF2005 is the first realization which is based on a consistent combination of station coordinates and Earth orientation parameters (EOP). The EOP, as a global parameter common to all techniques, enable not only the connection of the techniques, they are also very suitable for the local tie selection. A refined strategy based on the analysis of EOP time series and the deformation of the networks due to the combination was used for the local tie selection. The aim is to minimize the offsets between the time series of the pole values of different techniques and to minimize the deformation of the networks (expressed by the RMS difference between the technique only and the combined solution) due to the combination. Tab.1.2.2 gives the final values. They demonstrate that a consistency between TRF and EOP of about 1 mm can be achieved for GPS/VLBI and GPS/SLR and of about 3 mm in case of GPS/DORIS. The RMS of the difference is 1mm and 0.3 mm/a in maximum.

Tab.1.2.2: Mean pole offsets and r.m.s. difference between technique only and combined solution for the combination of terrestrial networks of GPS and SLR, VLBI and DORIS.

Technique	pole offset w.r.t. GPS [micro as]		RMS of difference [mm, mm/a]	
	x-pole	y-pole	position	velocity
GPS	0	0	0.2	0.0
SLR	-47	24	1.0	0.2
VLBI	18	18	1.0	0.2
DORIS	116	142	0.4	0.3

Improved stochastic model for intra-technique combination

Within the intra-technique combination procedure, it has to be considered, that the input data provided by different analysis centres (AC) are based on the same observation data. Up to now the data sets are mostly handled as independent. Thus the standard deviations of the combined parameters become too small. In cooperation with Prof. H. Kutterer (University Hannover) we developed a new stochastic approach, assuming that the variance of the input data sets of different AC have a common part resulting from the variance of the observations (observation noise) and an individual part coming from the individual analysis strategy (analysis noise). Fig.1.2.3 shows the development of standard deviations of different parameters if solutions of one to ten AC are combined. (A) assumes that the observation data are independent, or (B) considering identical observations correctly and implying an analysis noise of 100% of the observation noise. The improved stochastic model for intra-technique combination will provide combined products with reliable stochastic information as input for the inter-technique combination.

Fig. 1.2.3: Behaviour of standard deviation combining one to ten solutions. A, upper panel: traditional stochastic combination model, B, lower panel: improved stochastic combination model.

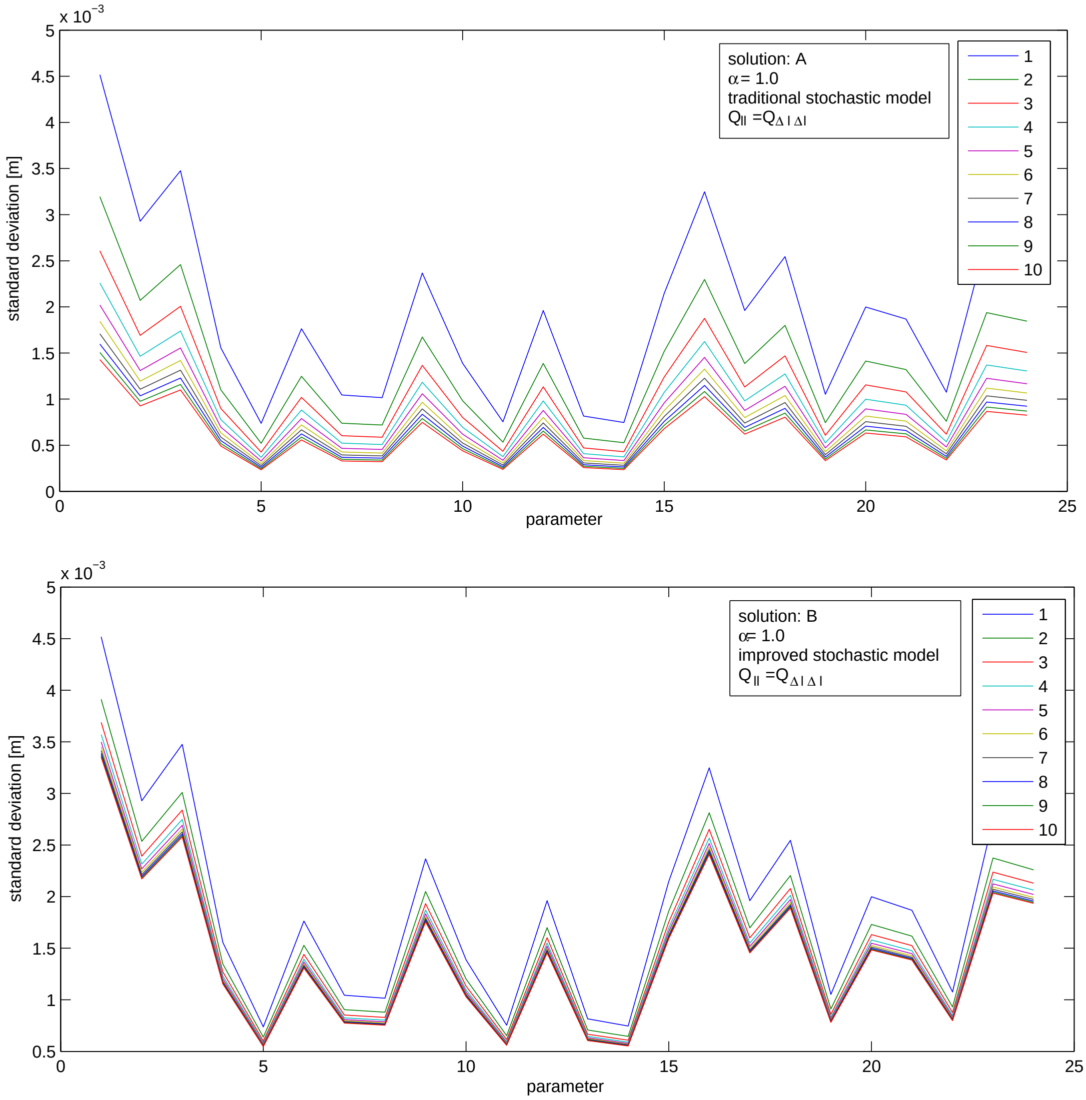

1.3 Realization of a celestial reference system

IAU and IVS working groups on a new realization of the ICRS

The International Celestial Reference System (ICRS) is realized by the coordinates of several hundreds of radio sources observed by VLBI (for the last realization “ICRF-Ext1”, data until 1998 were used). The IAU, the IERS as well as the IVS aim at a new realization of the ICRS in the next years, which shall be generated by combining several VLBI solutions if feasible. DGFI actively takes part in the corresponding IAU and IVS Working Groups by contributing solutions, as well as doing research, especially to optimize the homogeneity of the celestial and the terrestrial reference frames under the umbrella of the IERS.

Effect of various analysis options on VLBI-determined CRF

The next VLBI-determined realization of the International Celestial Reference System (ICRS) is intended to be prepared thoroughly. It will presumably serve as an important link between Earth-oriented and space-oriented sciences via other celestial reference frames (e.g. GAIA) to be created in the next decade. Such satellite-based celestial reference frames are planned to be of even higher precision than it can be achieved with VLBI observing at the Earth’s surface. This connection will be realized by the very stable VLBI station network referred to the International Terrestrial Reference Frame (ITRF).

In this context, the effect of various analysis options on VLBI-determined CRF (celestial reference frames) were investigated. Although some of these options had been discussed earlier by other scientists (see also 1.1), the purpose of this work was to analyse their influence on the estimated CRF with best possible comparability by using exactly the same solution (data, software, setup, …).

13 CRF solutions were computed at DGFI with the VLBI software OCCAM 6.1 (least-squares method), using 2847 daily sessions between 1984 and 2006, with 52 telescopes observing 2769 sources. Normal equations were set up per session to get the TRF, Earth orientation and CRF parameters in one common equation system. These session-wise normal equations were accumulated to one complete equation system with DOGS-CS and solved with NNT (no-net-translation) and NNR (no-net-rotation) conditions to 25 stations w.r.t. ITRF2000 and NNR conditions to 199 ‘stable’ sources w.r.t. ICRF-Ext1. The variables to be compared were the position differences between two solutions, the formal error differences, and the differences of the absolute values of the correlations between the estimated declinations (DE) and right ascensions (RA).

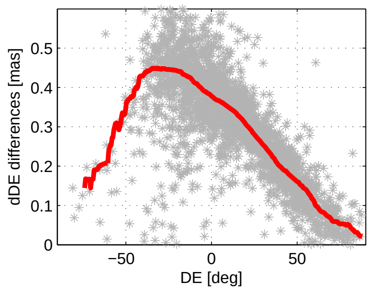

Fig. 1.3.1: Differences between 2769 declination estimates of two CRF solutions: with no gradients estimated - with gradients estimated slightly constrained.

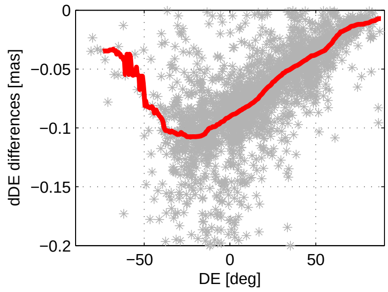

Fig. 1.3.2: Differences between 2769 declination estimates of two CRF solutions: with gradients esimated fully unconstrained - with gradients estimated slightly constrained.

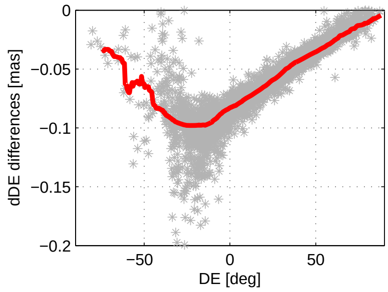

Fig. 1.3.3: Differences between 2769 declination estimates of two CRF solutions: using constant a priori gradient values (mean of 1990-1995) - using 0 a priori gradient values.

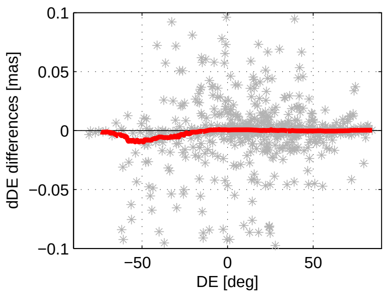

Fig. 1.3.4: Differences between 669 declination estimates of two CRF solutions: without using the 21 sessions of the VCS (VLBA Calibrator Surveys) - with using the VCS sessions.

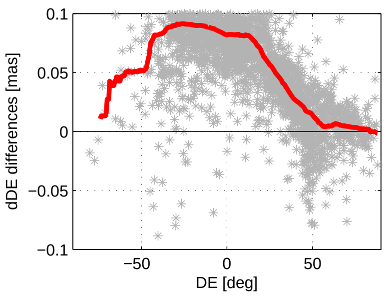

Fig. 1.3.5: Differences between 2769 declination estimates of two CRF solutions: all stations fixed to a preliminary solution of ITRF2005 - estimating positions and velocities for all stations.

The following analysis options were investigated:

- different troposphere mapping functions and gradient models,
- impact of elevation-dependent weighting (refined stochastic model),
- choice of the data set (neglecting the 534 sessions before 1990 and 21 astrometric sessions),
- handling of sources that may not be assumed to have time-invariant positions,
- handling of the station network (estimate the station positions per session, as positions and velocities over 20 years, or fix them to a priori values).

The biggest, clearly systematic effects in the estimated source positions up to 0.5 mas were found to be due to different gradient models (see figures 1.3.1, 1.3.2 and 1.3.3, grey stars indicate the differences between the declination estimates of the 2769 sources in the solution, the solid red lines are median values computed each 0.5° for all values inside a ±12.5° band). The choice of the data set does generally not have a significant influence. This holds also (with several exceptions) for different options how to treat sources which are assumed to have time-invariant positions (see figure 1.3.4). Furthermore it turned out that fixing station positions to values not consistent to the solution itself can noticeably affect CRF solutions (see figure 1.3.5). The coordinates and velocities of the ITRF2005 used here were taken from a preliminary version.

1.4 Combination of space geodetic observations

The investigations for the combination of space geodetic observations focussed on estimation and processing methods for weekly and multi-year intra-technique and inter-technique combination. The rigorous variance component estimation (VCE) was tuned for use as a fail/pass criteria tool for the automatic processing in the weekly intra-technique combination. For the weekly inter-technique combination the analysis of the usefulness of VCE as a fail/pass criteria tool was started.

Weekly intra-technique combination

Rigorous VCE should produce positive variance factors in a converging iteration process. That means that the converging factor converges to the value 1. This happens in the weekly intra-technique combination of SLR observations in most cases. In figure 1.4.1 the variance factors of the solutions of six SLR analysis centres (AC) for 2006 are presented. The variance factors for the solutions of two AC scatter between about 2 and 70. This implies a more or less strong down-weighting of the solutions within the combination.

Tab. 1.4.1a: Example of negative variance factors for week 040605 (June 5, 2004): variance factor (vf) -0.54724 with its variance -0.08143 for analysis centre (AC) ASI is negative.

AC	vf	var (vf)
asi	-0.54724	-0.08143
dgfi	1.39871	0.02983
gfz	17.27833	0.46013
jcet	10.32468	0.19957
nsgf	14.39704	0.30590

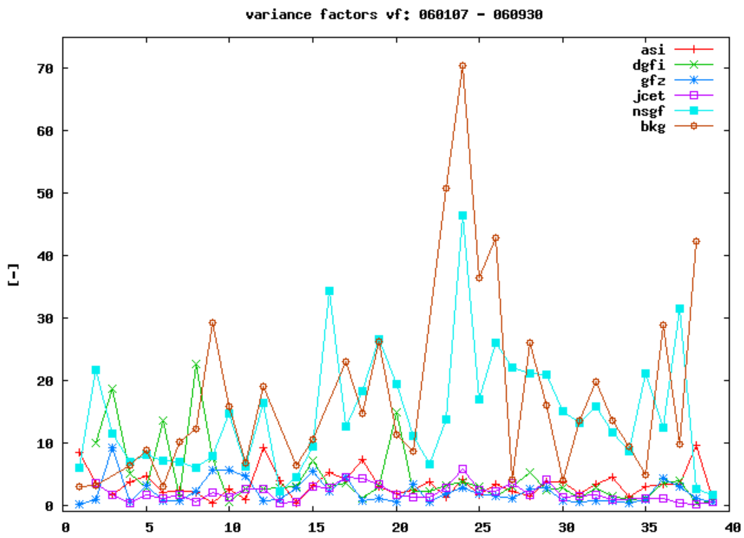

Fig. 1.4.1: Variance factors for the solutions of six analysis centres in 2006.

Tab. 1.4.1b: Part of JCET diagonal values of the minimal constraints covariance matrix for week 040605: For station 1868 and for the X, Y, and Z coordinates the values are too large w.r.t. those of station 1864.

Type	Station	Value
X	1864	0.0957859001015673
Y	1864	0.1894779664834140
Z	1864	0.1486869336499610
X	1868	214.2452851681370000
Y	1868	1621.0866860218700000
Z	1868	515.8737133131860000

In some cases negative variance factors may occur. There are two subcases: some diagonals of the covariance matrix of a minimally constrained input solution are either negative or relatively large. After one year of experience, the negative diagonals could always be related to the coordinates of one or more stations, or to all seven EOP. In the coordinate case the respective stations are eliminated from the solution. In the EOP case the whole solution is deleted from the combination.

Tab. 1.4.1c: After elimination of station 1868: variance factor for week 040605: variance factors (vf) reach reasonable values.

AC	vf	var(vf)
asi	2.13392	0.06577
dgfi	1.56153	17.70496
gfz	1.28750	0.03986
jcet	13.14136	0.35086
nsgf	14.66828	0.46992

In the subcase of relatively large diagonals, the values of one or more stations are about 100 to 1000 times larger than the rest of the diagonal values (s. Tab. 1.4.1) The respective station (here station 1868) is eliminated, and the new minimally constrained solution leads to positive variance factors (s. Tab 1.4.1c).

Tab. 1.4.2a: Example of an unrealistically small variance factor for week 060909 (September 9, 2006): variance factor (vf) 0.00666 with its variance of 0.00015 for analysis centre (AC) DGFI is too small.

AC	vf	var(vf)
asi	4.40058	0.22007
bkg	23.91065	1.50911
dgfi	0.00666	0.00015
gfz	3.20274	0.10010
jcet	2.79295	0.10956
nsgf	8.48917	0.37260

In the case of relatively small variance factors the values are 100 to 1000 times smaller than the others (s. Tab 1.4.2a). Investigations revealed that in one of the input solutions there is a station with relatively large absolute increments and large standard deviations (s. Tab 1.4.2b), and this station is not solved for in the other input solutions. After the elimination of the station the variance factors are reasonable (s. Tab. 1.4.2c).

All these fail/pass actions can be automatically performed in the weekly intra-technique processing.

Tab. 1.4.2c: After elimination of station 7309: variance factor for week 060909 (September 9, 2006): variance factor (vf) 3.45377 with its variance of 0.10967 for analysis centre (AC) DGFI reaches usual value.

AC	vf	var(vf)
asi	3.33795	0.14951
bkg	28.83627	1.18359
dgfi	3.45377	0.10967
gfz	4.22178	0.12278
jcet	1.15727	0.06450
nsgf	12.44800	0.44350

Tab. 1.4.2b: Part of DGFI solution parameters for week 060909: For station 7810 and for the X, Y, and Z coordinates the estimated increments and their standard deviations (sd) are usual, but for station 7308 they are too large. Units are meters.

Station	type	value	increment	sd	residual
7810	X	4331283.5310	-0.0112	0.1736	0.0003
7810	Y	567549.9176	-0.0042	0.2160	-0.0003
7810	Z	4633140.3647	0.0011	0.1987	0.0003
7308	X	-3942019.6763	-78.4233	1.4564	0.0007
7308	Y	3368097.6449	-71.9271	1.4278	0.0003
7308	Z	3702191.4164	-4.1802	0.8386	0.0008

Weekly inter-technique combination

With the experiences of automatic intra-technique processing, investigations on the usefulness of VCE for automatic fail/pass actions in the inter-technique combination started. The situation here is more complex than in the intra-technique case. The weekly and one-day session input solutions analysed here are products of intra-technique combinations as delivered by IGS for GPS, ILRS for SLR, IVS for VLBI and an individual IGN solution for DORIS. Week 051112 (November 12, 2005) was arbitrarily chosen for the first analyses. The number of parameters (3D station coordinates and daily EOP) for each technique is quite different: 182 for DORIS, 781 for GPS, 77 for SLR, and for the two one-day VLBI session solutions 23 each. The structure of the original covariance matrices is also quite different: minimally constrained for the unconstrained normal equation system delivered by ILRSB and IVS, over-constrained for DORIS and GPS.

Additionally, local tie information has to be considered. About 50 SINEX site files as delivered by the IERS for the ITRF2005 solution were analysed. The structure of the site covariance matrices reach from diagonal and diagonal block to full matrices.

At first a simulation study was performed in order to investigate the sensitivity of VCE for certain actions. For that purpose the local tie site solutions are composed to four block solutions in order to diminish the number of variance factors to be estimated. All a priori parameters are set identical. The simulated (estimated) parameters are the sums of a priori and normal-distributed random noise values with zero means and standard deviations of 0.01 m for station and local tie coordinates, 0.01 mas for the polar motions, and 0.01 ms for UT and LOD. The results of a first simulation with original covariance matrices are presented in Tab. 1.4.3.

Tab. 1.4.3a: Before simulation analysis: Variance factors vf with their variances var(vf) and convergence factors cf with their variances var(cf) for original covariance matrices of analysis centres IGN, IGS, ILRSB, IVSA, IVSb and of four local tie blocks.

Input	vf	var(vf)	cf	var(cf)
Ign	1876801.24330	35748.59511	1.000	0.019
Igs	220.04844	3.69829	1.000	0.016
Ilrsb	42.34879	1.56847	1.000	0.037
Ivsa	1946.99908	185.42848	1.000	0.095
Ivsb	53.83881	7.17851	1.000	0.133
ties 1	2.77979	0.11582	1.000	0.041
ties 2	3229.63142	195.73524	1.000	0.060
ties 3	0.23121	0.01927	1.000	0.083
ties 4	1.77249	10043349254.01921	2.052	5666251639.3835

Tab. 1.4.3b: After simulation analysis: Variance factors vf with their variances var(vf) and convergence factors cf with their variances var(cf) for original covariance matrices of analysis centres IGN, IGS, ILRSB, IVSA, IVSb and of four local tie blocks.

Input	vf	var(vf)	cf	var(cf)
ign	166.09677	3.16375	1.000	0.019
igs	191.60485	3.14106	1.000	0.016
ilrsb	33.20235	1.30205	1.000	0.039
ivsa	25.29186	2.40875	1.000	0.095
ivsb	0.53839	0.07179	1.000	0.133
ties 1	2.77979	0.11582	1.000	0.041
ties 2	0.21071	0.01081	1.000	0.051
ties 3	0.23121	0.01927	1.000	0.083
ties 4	30.33537	0.74902	1.000	0.024

Tab. 1.4.3c: After outlier simulation: Variance factors vf with their variances var(vf) and convergence factors cf with their variances var(cf) for original covariance matrices of analysis centres IGN, IGS, ILRSB, IVSA, IVSb and of four local tie blocks.

Input	vf	var(vf)	cf	var(cf)
ign	166.09677	3.16375	1.000	0.019
igs	191.60485	3.14106	1.000	0.016
ilrsb	33.20235	1.30205	1.000	0.039
ivsa	25.29186	2.40875	1.000	0.095
ivsb	0.53839	0.07179	1.000	0.133
ties 1	2.77979	0.11582	1.000	0.041
ties 2	42643.32734	2186.83730	1.000	0.051
ties 3	0.23121	0.01927	1.000	0.083
ties 4	30.33537	0.74902	1.000	0.024

An analysis of the covariance matrices of IGN and Ties_2 block revealed unrealistically large scattering of the diagonal values at some stations. The coordinates of these stations were adapted. The large variance factor of IVSA was due to too large standard deviations. They were set to 0.001 m. For the Ties_4 block, VCE did not converge. The reason was that one of the site covariance matrices was singular. This matrix was deleted.

The results of the next simulation may be seen in Tab. 1.4.3b. They show that VCE is sensitive to all actions performed.

A last simulation should give some information on the reaction of VCE to outliers. In the Ties_2 block, outliers of 1 to 3 m were added to the station position of a local tie site solution. Tab 1.4.3c shows that VCE is very sensitive to these outliers.

The simulation study reveals that VCE is sensitive to the actions described above. But further investigations are required until VCE can be used as an fail/pass criteria tool in the automatic inter-technique combination.

Multi-year combination

The methodology applied for the ITRF2005 computation (see 3.1) is based on combining datum-free normal equations (weekly or 24 h sessions) data sets and the common adjustment of station positions, velocities and Earth Orientation Parameters (EOP). The computations are performed with the DOGS-CS software (see below). The input data sets for ITRF2005 are provided by the international services (IGS, ILRS, IVS) and by individual DORIS analysis centres. The services performed intra-technique combinations based on solutions of individual analysis centres which are mostly computed with different software packages. Thus a unification of the used standards, models and parameterization was not yet achieved on the international level.

GGOS-D

Within the project "Integration of Space Techniques as a Basis for a Global Geodetic-Geophysical Observing System (GGOS-D)" unified processing standards, models and parameterizations were defined and implemented in the different software packages in use by the contributing institutions (see 1.1). GGOS-D is a joint project of Bundesamt für Kartographie und Geodäsie (BKG), Geodätisches Institut der Universität Bonn (GIUB), Deutsches Geodätisches Forschungsinstiut (DGFI), embedded in the Forschungsgruppe Satellitengeodäsie (FGS), and the GeoFor schungsZentrum Potsdam. It is financed by the German Ministry of Education and Technology (BMBF) within the R & D programme GEOTECHNOLOGIEN. Two consistent observation time series are generated independently with different software packages for VLBI, SLR and GPS. DGFI computes the observation time series for VLBI (OCCAM) and SLR (DOGS-OC). The currently available series for 2004 will be extended over the entire data time span to serve as input for the computation of a refined realization of the terrestrial reference frame. For GGOS-D the parameter spectrum of the ITRF2005 computation has to be extended to include also quasar coordinates, the lower degree spherical cooefficients of the Earth gravity field, and non-linear station motions.

Updates of the combination software

Updates of DOGS-AS (Analysis Software):

- refinement of the VCE method for use as fail/pass actions in automatic intra-technique combination,
- new methods for the simulation studies,
- new methods for the inter-technique combination.

Updates of DOGS-CS:

Concerning the DOGS-CS software the versions 4.07 and 4.08 were issued which stand out by an expanded command syntax. The continuation of a command is now marked with „\“ at the end of line. A mask representing an ordered list of parameters, such as the coordinates of a site, may hence contain list brackets with multi-digit elements separated by commas.

There are two routines handling general transformations of the vector of unknowns, ‚cs_trafo‘ and ‚cs_inpar‘. They obtained new features for time series of parameters and a special transformation of epoch which accounts for a regularization used for the transformed variable.

A new program, ‚cs_vasort‘, was added for re-arranging the variables in a given system of equations.

The routine ‚cs_solview‘ for the postprocessing of solutions was supplemented with tests for „local ties“.

1.5 Modelling for parameters of the Earth gravity field

This theme deals with the estimation of parameters of gravity field models from data of the modern satellite missions CHAMP, GRACE and (in future) GOCE. In the last year's annual report we presented first results based on the kinematic GPS orbits of CHAMP, kindly provided by D. Svehla and M. Rothacher (TU Munich), following the energy balance approach. To be more specific, CHAMP's kinematic orbits were converted into a time series of disturbing potential values along the orbit by subtracting a reference geopotential model. Whereas this procedure means the evaluation of high-low satellite-to-satellite tracking (SST) measurements, the appropriate evaluation of GRACE data requires the involvement of the high-precise KBR (K-band range, range-rate) measurements between the two satellites, i.e. low-low inter-satellite SST measurements.

Before developing an appropriate software package for the evaluation of GRACE data at DGFI we discussed in cooperation with the Institute of Astronomical and Physical Geodesy at the TU Munich several approaches. Since we are dealing with approaches derived by other groups or institutions we add relevant references. Some of the main issues are presented in the following:

Energy balance approach

In theme 2.2 we use residual geopotential data over South America derived from GRACE KBR measurements following the *energy balance approach* and kindly provided by S.-C. Han (Ohio State University). According to Han et al. (JGR, 111, B04411, doi:10.1029/2005JB003719, 2006) the GRACE geopotential difference V_{12} in an inertial system Σ_i can be written as

$$V_{12} = \frac{1}{2}\left|\dot{\boldsymbol{x}}_1^i\right|^2 - \frac{1}{2}\left|\dot{\boldsymbol{x}}_2^i\right|^2 - F_{12} - R_{12} + C_{12} \tag{1}$$

with $\boldsymbol{x}_1^i, \boldsymbol{x}_2^i, \dot{\boldsymbol{x}}_1^i, \dot{\boldsymbol{x}}_2^i =$ position and velocity vectors of the two GRACE satellites in Σ_i. The quantities F_{12} and R_{12} are the energies associated with the dissipative forces and the rotational potential; C_{12} means a constant. Equation (1) is introduced as a constraint into the adjustment of the KBR observations, namely the range-rate observations $\dot{\rho}$ between the satellites. The observation equation for $\dot{\rho}$ reads by introducing the measurement error v

$$\dot{\rho} + v = (\dot{\boldsymbol{x}}_{12}^i)^T \boldsymbol{e}_{12}^i \tag{2}$$

with the line-of-sight unit vector $\boldsymbol{e}_{12}^i$ and the relative velocity vector $\dot{\boldsymbol{x}}_{12}^i = \dot{\boldsymbol{x}}_1^i - \dot{\boldsymbol{x}}_2^i$. The equations (1) and (2) require both the high-precise KBR measurement and the velocity vectors. Since the latter are of much lower accuracy, the relative velocity vector $\dot{\boldsymbol{x}}_{12}^i$ is adjusted simultaneously with the geopotential difference V_{12} for each epoch using prior informations for $\boldsymbol{x}_{12}^i = \boldsymbol{x}_1^i - \boldsymbol{x}_2^i$, $\dot{\boldsymbol{x}}_{12}^i$ and V_{12}; more details are presented in Han (2006).

Fredholm integral solution

Equation (2) means the observation equation for the KBR range-rate observation $\dot{\rho}$. The corresponding observation equation for the KBR range observation ρ reads

$$\rho + v = (\boldsymbol{x}_1^i - \boldsymbol{x}_2^i)^T \boldsymbol{e}_{12}^i \tag{3}$$

Newton's equation of motion formulated in the inertial system Σ_i can be generally written as

$$\ddot{\boldsymbol{x}}^i(t) = \boldsymbol{b}^i(t, \boldsymbol{x}^i, \dot{\boldsymbol{x}}^i, V(\boldsymbol{x}^i, t), \boldsymbol{f}^i, ...) \tag{4}$$

with $\boldsymbol{f}^i$ = non-conservative accelerations. The *Fredholm integral solution* of equation (4) reads

$$\begin{aligned} \boldsymbol{x}^i(\tau) &= (1-\tau)\boldsymbol{x}^i(t_A) + \tau\, \boldsymbol{x}^i(t_B) \\ &- T^2 \int_0^1 K(\tau, \tau')\boldsymbol{b}^i(\tau', \boldsymbol{x}^i, \dot{\boldsymbol{x}}^i, V(\boldsymbol{x}^i, \tau'), \boldsymbol{f}^i, ...)\, d\tau' \end{aligned} \tag{5}$$

with $\tau = (t - t_A) / T$ = normalized time variable, $T = t_B - t_A$ and $t_B > t_A$. The kernel $K(\tau, \tau')$ is defined as

$$K(\tau, \tau') = \begin{cases} \tau(1-\tau') & \text{if } \tau \le \tau' \\ \tau'(1-\tau) & \text{if } \tau' \le \tau \end{cases} . \tag{6}$$

In the next step the solution (5) is introduced into the observation equation (3) for the position vectors $\boldsymbol{x}_1^i$ and $\boldsymbol{x}_2^i$ of the two GRACE satellites. Furthermore, the geopotential $V(\boldsymbol{x}^i, \tau')$ in the integrand of equation (5) can be split into a reference field and a correction term. The latter can be modelled, e.g., as a spherical harmonic expansion or by means of localizing base functions. The corresponding series coefficients and the boundary position vectors $\boldsymbol{x}^i(t_A)$ and $\boldsymbol{x}^i(t_B)$ are the unknowns of this approach which have to be estimated from the KBR range observations; for more details see, e.g., Mayer-Gürr et al. (J Geod, 78, 2005).

Semi-analytical approach

In the *semi-analytical approach* the geopotential can be modelled by the along-track representation

$$\begin{aligned} V(u, \Lambda, r) &= \frac{GM}{R} \sum_{n=0}^{\infty} \sum_{m=-n}^{n} \left(\frac{R}{r}\right)^{n+1} \\ &\times \sum_{k=-n}^{n} \overline{K}_{nm}\, \overline{F}_{nmk}(I)\, e^{i(ku+m\Lambda)} \end{aligned} \tag{7}$$

with u, Λ, r = argument of latitude, longitude of the ascending node, radial distance; the inclination functions $\overline{F}_{nmk}(I)$ are related to the inclination I. Finally $\overline{K}_{nm}$ denote the spherical harmonic coefficients of degree n and order m. Along the nominal orbit, equation (7) can be rewritten as

$$V(u, \Lambda) = \sum_{m=-n}^{n} \sum_{k=-n}^{n} A_{mk}^V\, e^{i\psi_{mk}} , \tag{8}$$

wherein

$$A_{mk}^{V} = \sum_{n=\max(|m|,|k|)}^{\infty} H_{nmk}^{V} \, \overline{K}_{nm} \tag{9}$$

are the lumped coefficients and H_{nmk}^{V} the transfer coefficients; $\psi_{mk} = ku + m\Lambda$. Equation (8) means a two-dimensional (2-D) Fourier transform which should be related to the nominal orbit, because in this case the lumped coefficients and the transfer coefficients are constant. Topologically the domain of the 2-D Fourier series (8) is a torus, since u, $\Lambda \in [0, 2\pi]$ holds. Finally, the observation equation for the KBR range measurement ρ of this approach can be written as

$$\rho - \rho_0 + v = \sum_{n=0}^{\infty} \sum_{m=-n}^{n} \sum_{k=-n}^{n} H_{nmk}^{\Delta\rho} \, \Delta\overline{K}_{nm} \, e^{i\psi_{mk} t} \; . \tag{10}$$

Herein ρ_0 is computed a priori from the kinematic or reduced-dynamic orbits using a reference gravity model based on the spherical harmonic coefficients $\overline{K}_{nm}$. The associated corrections $\Delta\overline{K}_{nm}$ are the unknowns of this approach. The transfer coefficients $H_{nmk}^{\Delta\rho}$ are computed analytically from the Hill equations defined on the nominal orbit. Finally it is worth to be mentioned that due to the transfer coefficients, the resulting normal equation becomes block-diagonal; for details see, e.g., Sneeuw (PhD thesis, DGK 527, 2000).

Besides these three approaches we also studied the *acceleration approach* (see, e.g., Ditmar et al., J Geod, 78, 2004) and the *gradiometer approach* (see, e.g., Sharifi and Keller, J Geod, 79, 2005) in more detail.

Since both, the Fredholm integral solution and the semi-analytical approach depend much less on the satellite velocities than the energy balance approach we consequently decided to work on the Fredholm integral solution and the semi-analytical approach.

1.6 Unification of height systems

The existing height systems do not support the high accuracy requirements of modern Geodesy. They refer to local (isolated) levels, are stationary (without considering variations in time), and their accuracy (10^{-6} … 10^{-7}) is about two orders of magnitude less than that of the realization of geometric reference systems (10^{-9}). These height systems become obsolete to realize the integrated geodetic observation of the Earth system, which requires a unified precise global vertical reference, free of biases and consistent in space and time. Although the vertical component of the geometrical reference system (i.e. ellipsoidal heights) presents many advantages in comparison with the (levelled) physical heights (quickly and low cost determination, smaller systematic errors over long distances, etc.), the ellipsoidal heights cannot replace the physical heights because of their 'geometrical' nature. So, it is mandatory to actualize the existing physical heights through transformation into a global (unified) vertical reference system, which must support, besides the physical heights derived from levelling and gravity reductions, those obtained from the new geodetic procedures (e.g., GNSS positioning, satellite altimetry, etc.).

A global zero height level

The first step to establish a global vertical reference system is the definition and realization of a global vertical datum: the zero height level. The 'natural' reference level is given by an equipotential surface of the Earth's gravity field, which can be arbitrarily selected, but in general is as close as possible to the mean sea surface. Following the oceanographic realization of the geoid definition given by Gauss and Listing, the selected reference surface should correspond to the level surface in relation to which the average permanent sea surface topography (SSTop) is zero when sampled globally over all marine areas. If the SSTop is assumed identical with the normal heights of the sea surface, the condition to satisfy can be written as:

$$\int (SSTop)^2 \, d\sigma = \int \left(\frac{W_0 - W_i}{\gamma_i} \right)^2 d\sigma = \min \,, \qquad (1)$$

and the corresponding reference potential value (i.e. W_0) can be estimated through:

$$W_0 = \int \frac{W_i}{\gamma_i^2} d\sigma \Big/ \int \frac{1}{\gamma_i^2} d\sigma \,. \qquad (2)$$

γ_i is the normal gravity value generated by a conventional level ellipsoid (i.e. GRS80) and W_i is the actual gravity potential at each point describing the mean sea surface. The W_i values can be computed by applying a global gravity model (e.g., EGM96, EIGEN-GL04, etc.) and a mean sea surface model (e.g., CLS01, KMS04, DNSC06, etc.). In this approach, W_0 is the mean value of the potential obtained at the gridded sea surface, but an equipotential surface averaging the sea surface topography in a geometric sense is not determined. It should be realized by solving the Gravity Boundary Value Problem (GBVP), i.e. by the geoid determination.

Figure 1.6.1 shows the residuals of the potential values computed at the sea surface with respect to the W_0 value derived by solving the given formulae and applying the following parameters:

Global gravity model:
EIGEN-GL04S (GRGS/GFZ),
spectral resolution n =150,
reference epoch of the coefficients 2000.0

Mean sea surface model:
Derived from Topex/Poseidon data at AVISO,
latitudinal coverage between φ = 60° N/S,
spatial resolution 1° x 1°,
reference epoch of the mean sea heights 2000.0

Constants:
$GM = 398\ 600{,}4415 \times 10^9\ m^3s^{-2}$
$\omega = 7\ 292\ 115 \times 10^{-11}\ rad\ s^{-1}$.

The estimated W_0 value corresponds to $62\ 636\ 853{,}4 \pm 0{,}04\ m^2\ s^{-2}$, with a standard deviation for the unit weight of $\pm\ 6{,}49\ m^2\ s^{-2}$. This last quantity represents the variation of the SSTop (~ 65 cm) in a quadrangle of 1° x 1° at the equatorial region (φ = 0°).

Fig. 1.6.1: Residuals of the potential values computed at the sea surface with respect to the W_0 value $62\ 636\ 853{,}4 \pm 0{,}04\ m^2\ s^{-2}$. The potential differences were divided by the corresponding normal gravity values in order to represent the residuals in units of length [m].

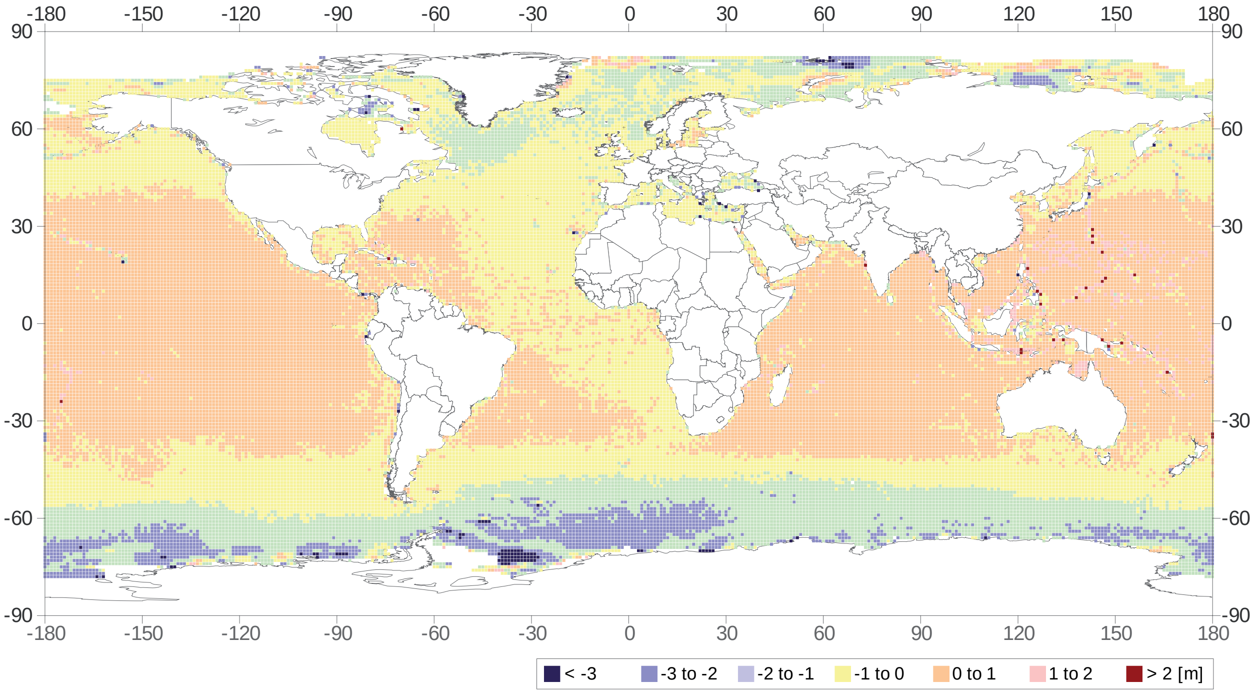

Height datum unification

The fundamental purpose of the vertical datum unification is to refer all geopotential numbers (physical heights) to one and the same equipotential surface (figure 1.6.2). The estimation of the datum discrepancies (i.e. potential differences between the local height datums and the global vertical reference system, terms δW_I and δW_J in the figure 1.6.2) is based on the combination of ellipsoidal heights (derived from space techniques), geopotential numbers (derived from levelling and gravity reductions) and the solution of the GBVP. The corresponding relationship is given by

$$W_0 - W_j = \delta W_j \; ; \quad \left[\frac{\delta W_j}{\gamma_p}\right] = h_p - \left[\frac{W_0^j - W_p^j}{\gamma_p}\right] - \left[\frac{T_p^j}{\gamma_p}\right] \; . \quad (3)$$

The index j represents the different vertical datum zones ($j = 1, \ldots, J$), p indicates the evaluation point, W_0^j is the reference level of the datum j, γ is the normal gravity, and T_p^j is the anomalous potential at the point p referred to the level j. In order to get reliable δW_j values, the linearization of the GBVP in all datum zones should be based on the same reference surface and normal gravity (potential) field. Otherwise, the differences between the level ellipsoids can be misinterpreted as level inconsistencies.

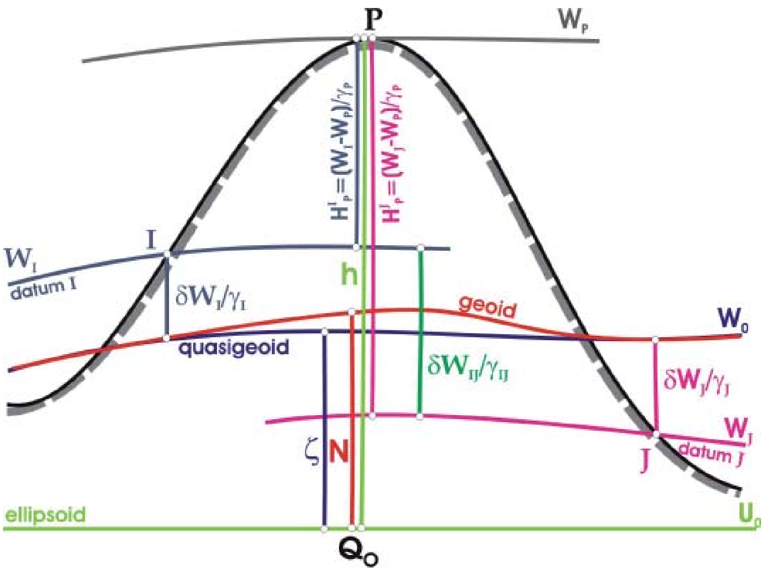

Fig. 1.6.2: Discrepancies between two classical height datums (W_I, W_J) and the global reference level W_0.

The δW_j values can be determined in four approaches:

- At the fundamental points (tide gauges) of the classical height systems: In this case, the ellipsoidal height is derived from GNSS positioning, the geopotential number is zero for the reference tide gauge and close to zero for other included tide gauges. The geopotential numbers (physical heights) and the (quasi)geoid refer to the local level W_0^j.

- In the marine areas close to the tide gauges: Here, the ellipsoidal heights are given by satellite altimetry, the geoid refers to the local level W_0^j, and the physical heights correspond to the SSTop, which should refer to the global geoid W_0. This global geoid is computed by solving the GBVP on marine areas based on satellite data only, i.e. satellite-only global gravity models and satellite altimetry data.

- At the fiducial stations of the geometrical (terrestrial) reference frame (TRF): At these points, the ellipsoidal heights are obtained from GNSS positioning and the physical heights are derived from spirit levelling combined with gravity reductions. The physical heights and the (quasi)geoid refer also to the local level W_0^j.

- At connection points between two classical height systems: This is a variation of the last case. At these points the physical heights and the (quasi)geoid undulations referred to the two neighbouring vertical datums (i.e. W_0^J, W_0^I) must be known, so that the discrepancy between the two datums is represented by δW_{IJ} (figure 1.6.2). The ellipsoidal heights are also derived form GNSS positioning.

In all the four cases, the (quasi-) geoid must be estimated by solving the GBVP, and the ellipsoidal heights must refer to the conventional TRS. The final datum discrepancies δW_I, δW_J, … are estimated by a combined adjustment of the observation equation systems generated in each approach.

Figure 1.6.3 shows the datum discrepancies computed at the reference tide gauges of the existing height systems in South America. The height anomalies were derived from the EIGEN-CG03 and the EGM96 models. The differences between the δW_I terms at the same tide gauge reflect the discrepancies between the two gravity models.

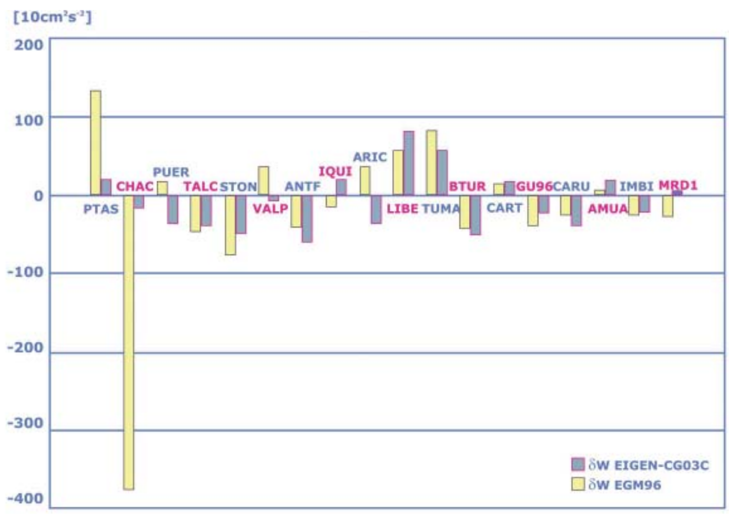

Fig. 1.6.3: Datum discrepancies between the height systems in South America and the global reference level W_0 (values determined at the reference tide gauges). Abbreviations: PTAS: Punta Arenas (Chile), CHAC: Chacabuco (Chile), PUER: Puerto Montt (Chile), TALC: Talcahuano (Chile), STON: San Antonio (Chile), VALP: Valparaíso (Chile), ANTF: Antofagasta (Chile), IQUI: Iquique (Chile), ARIC: Arica (Chile, used also by Bolivia), LIBE: La Libertad (Ecuador), TUMA: Tumaco (Colombia), BTUR: Buenaventura (Colombia), CART: Cartagena (Colombia), GU96: La Guaira (Venezuela), CARU: Carupano (Venezuela), AMUA: Amuay (Venezuela), IMBI: Imbituba (Brazil), MRD1: Mar del Plata (Argentina).

2 System Analysis

The processes of the system Earth are in general described by mathematical and physical models. Today, an increasing number of parameters used to characterize state and temporal evolution of these processes become measurable through observations of precise geodetic space techniques. The present research field "system analysis" shall investigate the interrelationship between geodetic observations and model parameters. The thorough analysis of parameters – most rigorously estimated by combining different geodetic space techniques – promises to overcome the weakness of individual observation approaches as, for example, low sensitivity or insufficient sampling rates. Moreover, system analysis can help to improve the signal-to-noise ratio, to identify model deficiencies, and to introduce novel or extended parameterization with the final goal to obtain a more precise description of processes of the system Earth.

The seven research topics pick up urgent problem areas for this type of analysis. The new parameterization of Earth orientation by means of the celestial ephemeris origin requires the development of new parameter series and software adoption (Topic 2.1). Wavelets are appropriate base functions for a local high resolution description of the gravity field, and the combination of satellite models and surface gravity data is to be elaborated (Topic 2.2). The geographically different evolution of the mean sea level shall be described kinematically (Topic 2.3). New gravity field missions provide integrated observations of water mass redistribution in the system Earth. Forward modelling and global mass balance can help to improve the weakest components of the global water cycle, the solid Earth hydrology (Topic 2.4). Single layer models of the ionosphere are an insufficient description of the highly variable electron content which can be derived from two-frequency GPS observations (Topic 2.5). Actual plate kinematic models shall be extended to the vertical tectonic motions based on a new model for the deformations of the solid Earth (Topic 2.6). Finally, Topic 2.7 focuses on the analysis of time series for geodetic parameters to improve the identification and decomposition of physical signal, systematic and random errors.

2.1 Relation between CRS and TRS

The transition from the vernal equinox to the celestial ephemeris origin as the first axis of the celestial intermediate system, which has no sidereal motion on the true equator, requires a detailed investigation how the true vernal equinox moves on the true equator according to the precession and nutation of the celestial intermediate pole.

The sidereal motion of the true vernal equinox on the true equator

The rotation of the traditional celestial intermediate system (= true equatorial system with the first axis in the true equinox) is described by the precession matrix $\mathbf{P} = \mathbf{R}_3(-z)\mathbf{R}_2(\theta)\mathbf{R}_3(-\zeta)$ with the secularly changing precession parameters ζ, θ, z and the nutation matrix $\mathbf{N} = \mathbf{R}_1(-\varepsilon-\Delta\varepsilon)\mathbf{R}_3(-\Delta\psi)\mathbf{R}_1(\varepsilon)$ with the additional precession parameter ε and the periodically changing small nutation parameters $\Delta\varepsilon$, $\Delta\psi$. The third coordinate of the rotation vector of the true equatorial system with respect to the true equatorial system is the polar component of its rotation, i.e. the sidereal angular velocity w of the true equinox on the true equator.

This angular velocity is found to be in a linearized form (regarding the nutation parameters $\Delta\varepsilon$, $\Delta\psi$, but not their temporal derivatives, as very small)

$$
\begin{aligned}
w = & -\cos\theta\,\dot{\zeta} - \dot{z} + (\sin\theta\sin z\,\Delta\varepsilon + \sin\theta\cos z\,\Delta\psi)\dot{\zeta} \\
& + (\cos z\,\Delta\varepsilon - \sin z\sin\varepsilon\,\Delta\psi)\dot{\theta} + \sin\varepsilon\,\Delta\psi\,\dot{\varepsilon} \\
& - \cos\varepsilon\,\Delta\dot{\psi} + \sin\varepsilon\,\Delta\varepsilon\,\Delta\dot{\psi}\,.
\end{aligned} \tag{1}
$$

The IAU 1976 precession model (but not the new IAU 2000 precession model) fulfills the condition

$$\sin\theta\cos z\,\dot{\zeta} = \sin z\,\dot{\theta}\,.$$

That simplifies the above relation to

$$
\begin{aligned}
w = & -\cos\theta\,\dot{\varsigma} - \dot{z} + \sin\theta\sin z\,\Delta\varepsilon\,\dot{\varsigma} \\
& + \cos z\Delta\varepsilon\,\dot{\theta} + \sin\varepsilon\,\Delta\psi\,\dot{\varepsilon} \; - \cos\varepsilon\,\dot{\Delta\psi} + \sin\varepsilon\,\Delta\varepsilon\,\dot{\Delta\psi}
\end{aligned}
\tag{2}
$$

in the case of the old precession model of 1976.

The integral of the sidereal velocity w is the angle between the celestial ephemeris origin and the vernal equinox. The undetermined integration constant corresponds to the arbitrary definition of the celestial ephemeris origin at an initial epoch.

The first two terms in (1) and (2) are the purely secular precession terms ("general precession in right ascension"). They describe the sidereal motion of the mean equinox on the mean equator.

The third and fourth terms contain secular components multiplied by one periodic factor each. So they are essentially periodical. They originate from the transformation of the precessional rotation of the mean equator into the true equatorial system: The precessing mean equinox is projected onto the precessing and nutating true equator. Therefore the sidereal motion of the projected mean equinox on the true equator contains periodical terms due to nutation.

The last three terms in (1) and (2) are the periodic nutation terms ("nutation in right ascension"). They describe the nutational part of the sidereal motion of the true equinox on the true equator. The fifth and sixth terms are directly integrable:

$$
\int (\sin\varepsilon\,\Delta\psi\,\dot{\varepsilon} - \cos\varepsilon\,\dot{\Delta\psi})\,dt = -\cos\varepsilon\,\Delta\psi \quad . \tag{3}
$$

$\cos\varepsilon\,\Delta\psi$ is the traditional "equation of the equinoxes", which is, in a linear approximation, the angle on the true equator between the true equinox and the orthogonal projection of the mean equinox. "Linear approximation" means: Products and higher than first powers of the nutation parameters $\Delta\varepsilon$, $\Delta\psi$ are neglected, and, consequently, the small right spherical triangle formed by the true equinox, the mean equinox and its projection on the true equator can be regarded as a plane triangle. As Figure 1 shows, the length of the leg on the true equator is equal to $\cos(\varepsilon+\Delta\varepsilon)\,\Delta\psi = \cos\varepsilon\,\Delta\psi$. So it is in a linear approximation the true right ascension of the mean equinox.

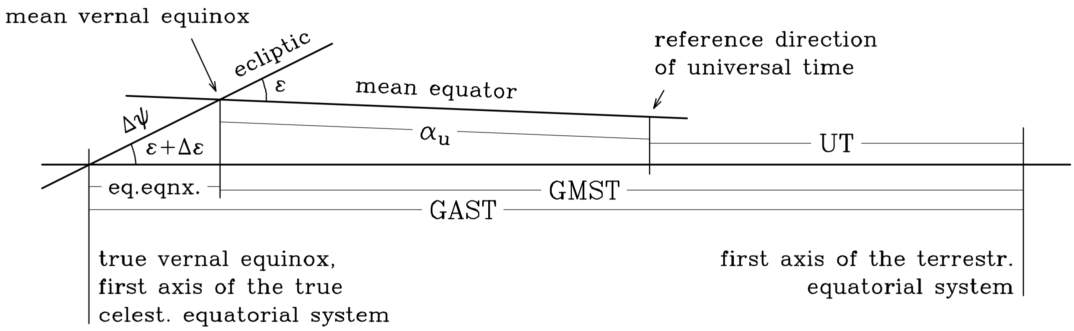

Fig. 2.1.1: Traditional reference directions on the true equator.

These first two nutation terms are purely periodical. The last nutation term, $\sin\varepsilon\,\Delta\varepsilon\,\Delta\dot{\psi}$, however, consists of a secular and a periodic part. With restriction to the predominant in-phase parts, $\Delta\varepsilon$ and $\Delta\psi$ are sums of the nutation components:

$$\Delta\varepsilon = \sum_i a_i \cos(\omega_i t)\,, \quad \Delta\psi = \sum_j b_j \sin(\omega_j t)$$

so that

$$\Delta\varepsilon\,\Delta\dot{\psi} = \sum_{i,j} a_i b_j \omega_j \cos(\omega_i t)\cos(\omega_j t)\ .$$

These products have for $i = j$ non-vanishing mean values resulting in secular terms. The other products are periodical with mean values of zero.

Table 1 shows a classification of the different terms of the sidereal angular velocity w occurring in (2).

Tab. 2.1.1: Classification of the terms of the siderial angular velocity w of the true equinox on the true equator.

No.	Term	Name		Kind of variability
1	$-\cos\theta\,\dot{\zeta}$	general precession in right ascension		secular
2	$-\dot{z}$			
3	$\sin\theta\sin z\,\Delta\varepsilon\,\dot{\zeta}$	projectional variation of precession		periodical
4	$\cos z\,\Delta\varepsilon\,\dot{\theta}$			
5	$\sin\varepsilon\,\Delta\psi\,\dot{\varepsilon}$	derivative of the equation of equinoxes	nutation in right ascension	periodical
6	$-\cos\varepsilon\,\Delta\dot{\psi}$			
7	$\sin\varepsilon\,\Delta\varepsilon\,\Delta\dot{\psi}$			secular / periodical

Until some years ago, we defined Greenwich apparent sidereal time (GAST) as the Greenwich hour angle of the true vernal equinox and Greenwich mean sidereal time (GMST) as the Greenwich hour angle of the mean vernal equinox. So their difference, the equation of the equinoxes, was the true right ascension $\cos\varepsilon\ \Delta\psi$ of the mean equinox. Since the reference direction of GMST, namely the projection of the mean equinox on the true equator, has not only a secular, but also a periodical sidereal motion on the true equator, GMST was redefined so that its difference from GAST is no longer only $\cos\varepsilon\ \Delta\psi$, but the sum of all periodical terms of the integral of the angular velocity w. Thus GMST is no longer the hour angle of the mean equinox, but the hour angle of a reference direction which has only a secular sidereal motion on the true equator.

With the numerical parameters of the IAU precession and nutation models of 1976/80, we find the following expressions of the secular terms and the other secularly changing coefficients in (2):

$$\begin{aligned} -\cos\theta\,\dot{\varsigma} &= -2306.''2181 - 0.''60376\,t + 0.''054887\,t^2\,, \\ -\dot{z} &= -2306.''2181 - 2.''18936\,t - 0.''054609\,t^2\,, \\ \sin\theta\sin z\,\dot{\varsigma} &= 0.''250562\,t^2 + 0.''0001312\,t^3\,, \\ \cos z\,\dot{\theta} &= 2004.''3109 - 0.''85330\,t - 0.''250780\,t^2 \end{aligned} \qquad (4)$$

and the secular part of the last term

$$(\sin\varepsilon\,\Delta\varepsilon\,\Delta^{\cdot}\psi)_s = 0.''003850 + 0.''0000042\,t \quad .$$

So the integral of the secular terms is

$$\int \{-\cos\theta\,\dot{\varsigma} - \dot{z} + (\sin\varepsilon\,\Delta\varepsilon\,\Delta^{\cdot}\psi)_s\}\,dt =$$
$$-4612.''4323t - 1.''39656t^2 + 0.''000093t^3 \ ,$$

and the integral of the "projection terms" is

$$\int (\sin\theta\sin z\,\Delta\varepsilon\,\dot{\varsigma} + \cos z\,\Delta\varepsilon\,\dot{\theta})\,dt =$$
$$(-0.''002649 + 0.''000001t)\sin\Omega$$
$$+0.''000013\sin(2\Omega) + 0.''000004\sin(2F - 2D + 2\Omega)$$

(with restriction to terms whose coefficients have absolute values larger than 0".5 $*$ 10^{-6}. The time coordinate *t* is always reckoned in julian centuries since J2000.0.

2.2 High resolution gravity field models

The basic idea of a multi-resolution representation (MRR) is to decompose a given input signal into a number of detail signals each related to a certain frequency band. Thus, we expect that different detail signals would be more sensitive to particular input signals in dependency on their spectral behaviour and noise characteristics. In the last year's annual report we presented spatial-temporal, i.e. four-dimensional (4-D) gravity fields from GRACE data based on this expectation, i.e. we estimated different detail signals in fact from different data sets. This year we present a spatio-temporal gravity field model by introducing one-dimensional series expansions for scaling and wavelet coefficients. To be more specific, we determine a regional 4-D gravity model from GRACE data using the spherical wavelet technique for the spatial part. In addition, we model the time dependency either by annual and semi-annual sine and cosine terms, i.e. a Fourier series, or by introducing one-dimensional B-splines. Consequently, in both cases we end up with a 4-D geopotential model of tensor product type. Since the spherical scaling functions and wavelets are derived from spherical harmonics, our approach accommodates for loading computations in the spectral domain as easily as for spherical harmonics.

Spatio-temporal gravity field

The MMR states that the level-$(i+1)$ approximation V_{i+1} of a signal like the geopotential V can be decomposed into the smoother level-i approximation V_i and a detail signal v_i absorbing all the fine structures of V_{i+1} missing in V_i. Consequently, the MRR of V can be written as

$$V(\mathbf{r},t) = V_{i'}(\mathbf{r},t) + \sum_{i=i'}^{I} v_i(\mathbf{r},t) + \Delta V(\mathbf{r},t) \tag{1}$$

($\mathbf{r}$ = position vector, t = time). For practical applications we may identify the first term on the right-hand side of (1) as a reference model and omit the last term. The level-i detail signal

$$v_i(\mathbf{r},t) = \sum_{k=1}^{N} d_{i,k}(t)\ \psi_{i+1,k}(\mathbf{r}) = \psi'_{i+1}(\mathbf{r})\ \mathbf{d}_i(t) \tag{2}$$

is computed as a series expansion in terms of the level-i wavelet functions $\psi_{i,k}$. Starting with the coefficient vector $\mathbf{d}_I(t) = (d_{I,k}(t))$ of highest level I, the vectors $\mathbf{d}_i(t)$ of the lower levels $i < I$ are computable via the pyramid algorithm. Within the approach we presented in the last year's annual report, we estimated the coefficient vectors $\mathbf{d}_i(t)$ of the levels $i = i', \ldots, I$ from different data sets covering level-dependent observation time intervals. Here, however, we model each element $d_{I,k}(t)$ either as a

1) Fourier series, consisting of an annual and a semi-annual oscillation or a as

2) series expansion in B-spline functions, which are compactly supported.

In both cases the detail signal (2) can be rewritten as

$$V(\mathbf{r},t) = \phi'_{I+1}(\mathbf{r})\mathbf{D}_{I;J}\phi_J(t) \quad (3)$$

wherein the first vector on the right-hand side consists of the level-$(I+1)$ scaling functions w.r.t. space; the last vector contains the time-dependent base functions, e.g., the sine and cosine terms in case of the Fourier series. In our second approach we choose normalized endpoint-interpolating quadratic B-spline functions as shown in Fig. 2.2.1 for temporal level value $J = 3$. These base functions are compactly supported and restricted to the unit interval.

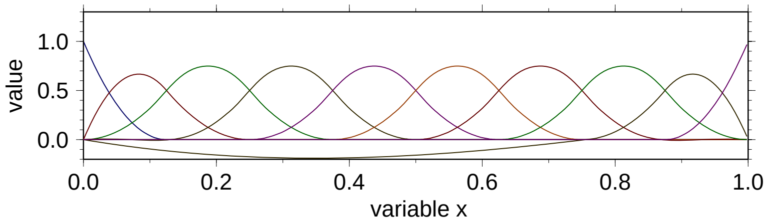

Fig. 2.2.1: Normalized endpoint-interpolating quadratic B-spline functions of level J = 3 within the unit interval.

Fourier series modelling

In case of the Fourier series approach, the matrix $\mathbf{D}_{I,J}$ comprises the spatio-temporal scaling coefficients $d_{I,k;l}$ which describe for $l = 1$ the annual behaviour of the scaling coefficients $d_{I,k}(t)$ introduced in Eq. (2) and for $l = 2$ the semi-annual behaviour. For the spatial part in Eq. (3) we choose the Blackman representation with base $b = 2.1$ and highest level $I + 1 = 5$, i.e. we solve for signal parts until degree 40 according to the definition of the generalized Blackman scaling function.

We analyse residual GRACE geopotential difference observations, processed from KBR-measurements, accelerometer data and precise orbits via the energy balance approach, kindly provided by Shin-Chan Han from the Ohio State University. Geographically we select a region in South America which includes the Amazon Basin (see Fig. 2.2.3). We choose a total observation interval between February 2003 and June 2005 with a sampling rate of 5 seconds. The observations are reduced by a priori time-variable models, e.g., for atmosphere and oceans, and are assumed to reflect mainly hydrology variations. The data show (Fig. 2.2.2) large gaps w.r.t. time, in particular in June 2003 and the second half of 2004. Furthermore, we introduce GGM01C as static reference model.

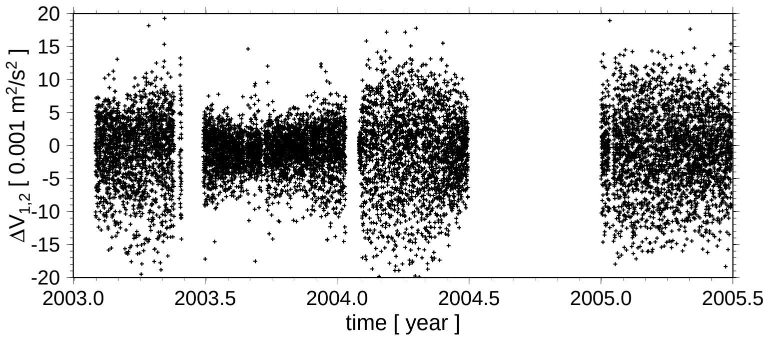

Fig. 2.2.2: Time series of the residual GRACE geopotential difference observations within the region of interest related to the observation interval between February 2003 and June 2005.

Since the resulting normal equation is ill-conditioned due to the downward continuation and probably not of full rank due to the distribution of the scaling functions, a regularization has to be applied. For that purpose we introduce prior information for the unknown scaling coefficients and formulate a linear model with unknown variance components for the satellite input data and the prior information. The quotient of the variance components is interpretable as regularization parameter. The results of the estimation process are the input of the wavelet decomposition, i.e. the computation of the satellite detail signals. Furthermore, from the estimated spatio-temporal scaling coefficients we compute the amplitudes and phases of the annual and semi-annual oscillations. We notice from Fig. 2.2.3a, that the highest annual variability occurs along the Amazon river. In Fig. 2.2.3b we detect phase differences of 180° between northern and southern regions of the Amazon.

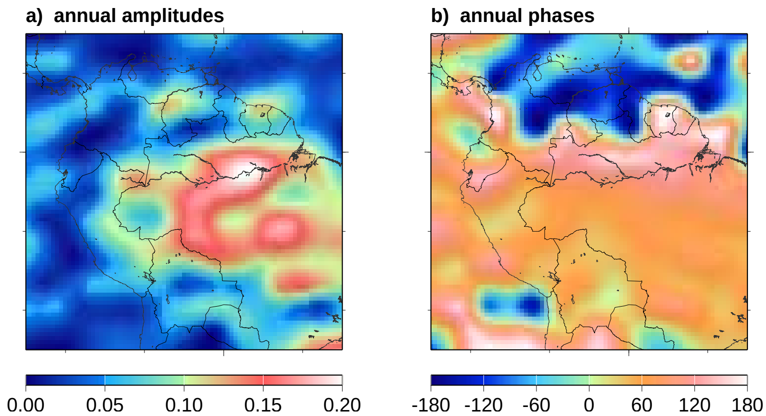

Fig. 2.2.3: Distribution of the (a) annual amplitudes and (b) annual phases of the scaling coefficients $d_{4,k}(t)$.

Applying the static gravitational and the vertical load Love numbers (Farrell, 1972) the residual GRACE geopotential differences can be transformed into height deformations at the Earth's surface. Since we study the geopotential with respect to GGM01C, the height deformations are related to GGM01C, too. Figure 2.2.4 shows 'snap shots' of the level-5 height deformations $\delta h_5(\mathbf{r},t_j)$, i.e. until degree $n = 40$, at selected times $t = t_j$ within one year, again considering annual and semi-annual oscillations for the scaling coefficients. The results reveal that the height deformations vary in the Amazon basin of about 10 mm.

Figure 2.2.5 shows the corresponding values of the level-4 height deformations $\delta h_4(\mathbf{r},t_j)$ considering signal parts until degree n = 19. Finally, Fig. 2.2.6 depicts the level-4 detail signal of height deformations, which means the difference $\delta h_5(\mathbf{r},t_j) - \delta h_4(\mathbf{r},t_j)$. It shows high-frequency variations of about 7 mm; its frequency band covers the range between the degree values 10 and 40.

Fig. 2.2.4: Level-5 height deformations with a 10-day time spacing considering an annual and a semi-annual oscillation of the scaling coefficients.

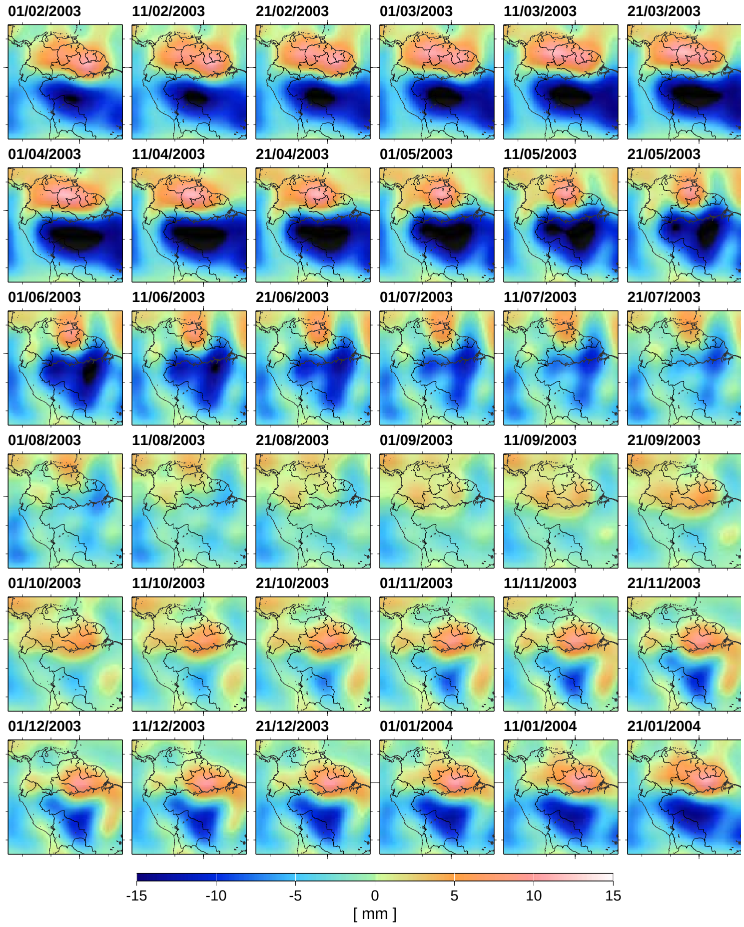

Fig. 2.2.5: Level-4 height deformations with a 10-day time spacing considering an annual and a semi-annual oscillation.

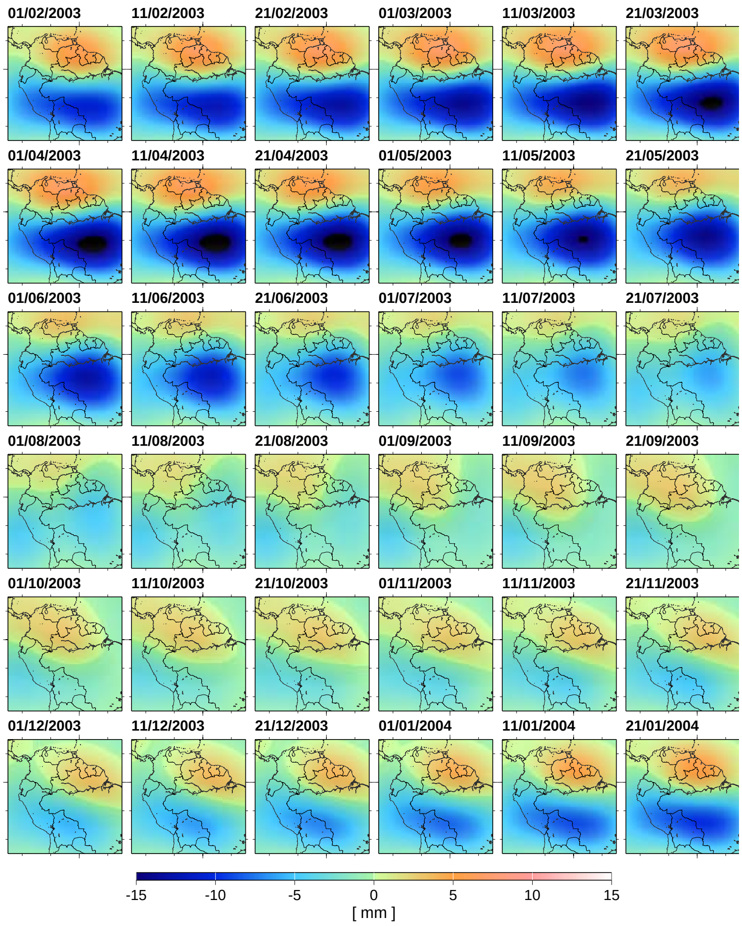

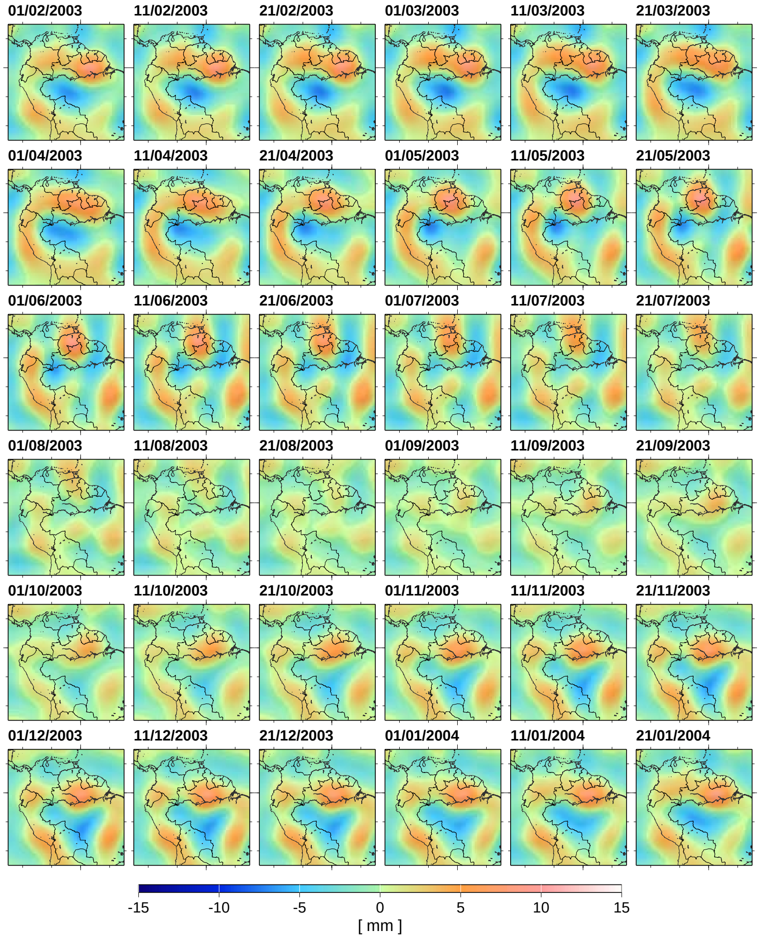

Fig. 2.2.6: Level-4 detail signals with a 10-day time spacing considering an annual and a semi-annual oscillation.

B-spline modelling

A disadvantage of this approach is that the Fourier series modelling does not allow a MRR w.r.t. time, i.e. Eq. (1) means a 3-D (spatial) MRR of the geopotential, because each detail signal v_i is modelled by the same vector $\Phi_J(t)$. This restriction can be overcome by substituting the normalized endpoint-interpolating B-spline functions introduced before as scaling functions for the sine and cosine terms of the Fourier series. In contrast to the Fourier series, the resulting B-spline expansion allows a 1-D MRR w.r.t. time, and Eq. (1) means a 4-D (spatio-temporal) MRR of the geopotential. In this case the matrix $\mathbf{D}_{I;J}$ introduced in Eq. (3) comprises the spatio-temporal scaling coefficients $d_{I,k;J,l}$ of spatial level I and temporal level J. Applying the corresponding two-scale relations w.r.t. space and time, a spatio-temporal, i.e. 4-D, MRR can be derived.

Here we choose for the spatial part again the Blackman representation until level $I + 1 = 5$, for the temporal part we choose the B-spline expansion until level $J = 5$, i.e. we have altogether 34 B-spline functions within the time interval of approximately 2.5 years. From the comparison with Fig 2.2.4 we clearly detect deviations from a strong annual (seasonal) behaviour.

Fig. 2.2.7: Height deformations of spatial level I+1 = 5 and temporal level J = 5 with a 10-day time spacing; compare this result with Fig. 2.2.4.

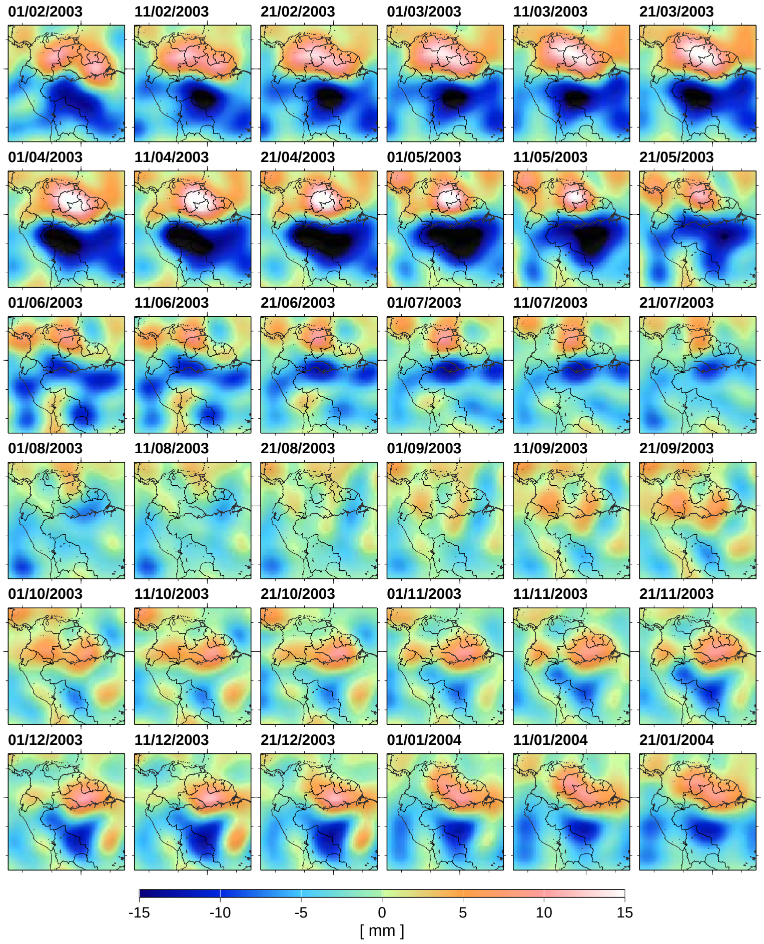

2.3 Kinematics of the mean sea level

An essential prerequisite for a *kinematic* description of the mean sea level is the cross-calibration of all altimeter missions in order to fully utilize the combined space-time sampling of altimeter systems with different orbit characteristics. The multi-mission cross-calibration is performed by means of the 'discrete crossover analysis' (DCA), already described in the previous annual report. The method applied here is innovative because

Innovative Multi-mission cross-calibration

- it realizes for the first time a common least squares adjustment of all single and dual satellite crossover differences performed between all altimeter systems operating simultaneously,
- the total set of these crossover differences establishes a rigid network with high redundancy allowing to estimate radial errors for all satellites with a sufficiently dense sampling – even for TOPEX/Poseidon whose orbit is no longer taken as free of errors (in contrast to the procedure followed so far by other investigations).

Extensions

The most recent realization of the multi-mission cross-calibration was extended to a 13 years period covering TOPEX cycles 001 - 481 (c.f. table 2.3.1). ENVISAT and ERS-1 data (as far as processed with the OPR version 6 software) were included in the analysis, and the ephemeries of ERS-1 and ERS-2 were replaced by orbits based on the DEGM04 gravity field as generated by DEOS.

Table 2.3.1: Altimeter mission data used for the present analysis. The orbits of TOPEX/Poseidon and Jason1 are still based on JGM3. Data from ERS-1 and ENVISAT were added and the orbits of ERS-1 and ERS-2 are based on the DEGM04 gravity field.

Mission (Phase)	Cycles	Period	Source	Harmonization / Replacements
TOPEX/Poseidon	001-481	1992/09/23-2005/10/08	MGDR-C AVISO	Chambers SSB correction, FES2004
Jason1	001-135	2002/01/15-2005/09/14	GDR-A PODACC	FES2004
ERS-1 (C & G)	083-101 144-155	1992/04/14-1993/12/20 1995/03/24-1996/04/28	OPR-V6 CERSAT	DEOS orbits, FES2004, pole tide 1.5ms time bias
ERS-2	000-087	1995/04/29-2003/09/15	OPR-V6 CERSAT	DEOS orbits, FES2004, pole tide, 1.3ms time bias
ENVISAT	010-040	2002/09/30-2005/09/19	GDR ESA/CNES	FES2004
GFO	100-122	2003/01/01-2003/12/31	GDR NOAA	FES2004

Discrete crossover analysis (DCA)

After harmonizing the data of all altimeter systems (details are indicated in table 2.3.1), single- and dual-satellite crossover differences with a time delay of at most 3 days are performed between all satellites. The crossover differences are then modelled just by the radial errors x_i and x_j of the two passes intersecting at the crossovers. No continuous error model is used. To avoid uncontrolled jumps of the errors, differences x_{i+1} - x_i between consecutive errors are minimized simultaneously with the crossover differences by a weighted least squares approach. With growing time difference, both crossover and consecutive differences are down-weighted by decaying weight functions with different half-weight width. Additional weights for the crossover differences are derived from their standard deviations and by cos φ, to compensate the increasing number of crossovers at high latitude.

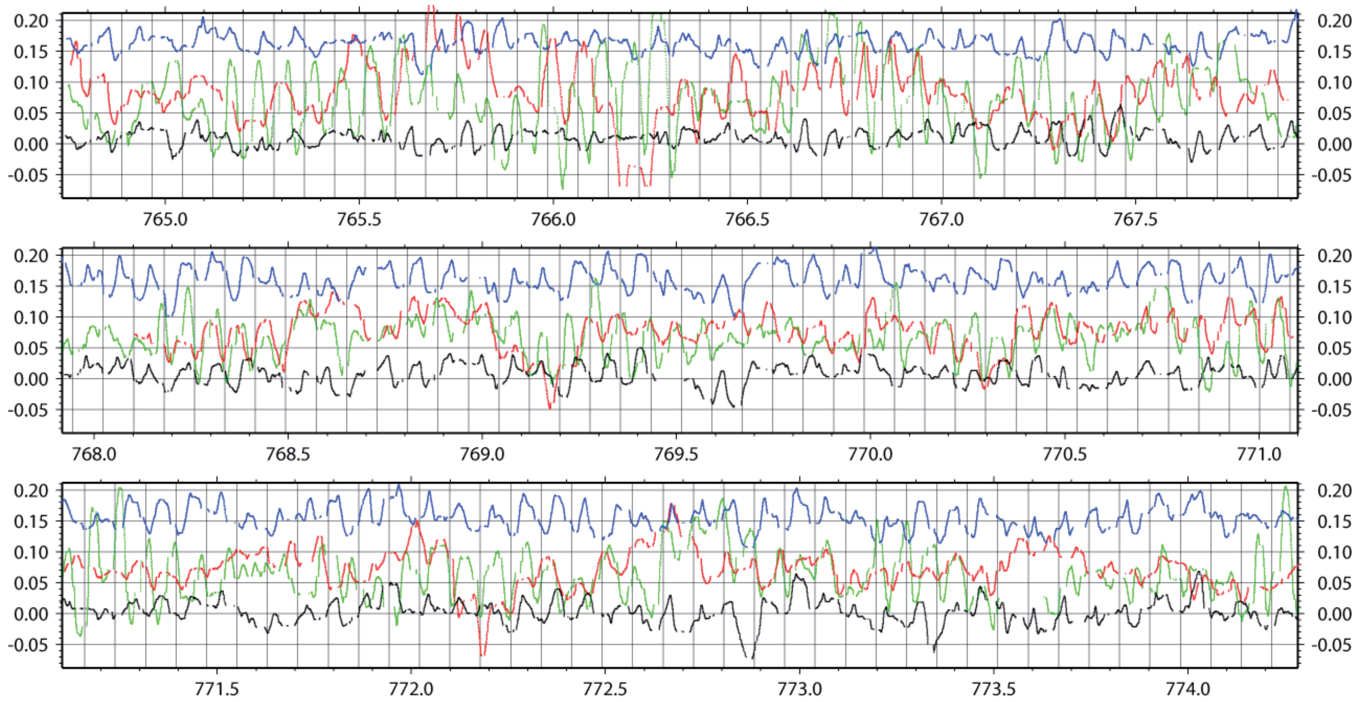

Fig. 2.3.1: Radial error estimates of TOPEX (black), ERS-2 (red), GFO (green) and Jason1 (blue) for one of the analysis periods during the tandem flight of TOPEX and Jason1.The time series of errors for TOPEX and Jason1 show a significant high correlation – due to the tandem flight and the fact that the orbits of both satellites are based on the same gravity field (JGM3).

The approach realizes a "discrete crossover analysis" (DCA) as described earlier. It is shown that the DCA has a rank defect of just one. Here, the rank defect is removed by constraining the sum of all TOPEX errors to be zero. The number of unknowns is twice as large as the number of crossovers. Thus, the normal equations to be solved are huge with a tri-diagonal plus sparse coefficient matrix. These equations are solved iteratively by a standard "conjugate gradient projection" algorithm slightly modified in order to optimize the repeated vector-matrix multiplication.

Analysis Results

The analysis is performed for a sequence of 10-day periods (coinciding with the repeat cycles 001 – 481 of TOPEX spanning more than 13 years) with 3 days overlap to neighbouring periods. Within the overlapping period the error estimates disagree to at most 1-2 mm. Consequently, temporal sequences of radial errors were performed for all satellites by simply concatenating the error estimates of the central 10-day periods. Figure 2.3.1 shows for one of the analysis periods the error estimates of four altimeter systems operating simultaneously.

As for all analysis periods the sum of TOPEX errors was forced to zero, the time series of radial errors of TOPEX always varies around zero – with a scatter of 1-2 cm (c.f. Figure 2.3.1). As a consequence, the radial errors of all other satellites carry – on average – the range biases relative to TOPEX. Jason1, for example, has a relative range bias of about 16.5 cm. By a postprocessing, the mean of radial errors was estimated for all analysis periods in order to investigate the stability of these relative range biases.

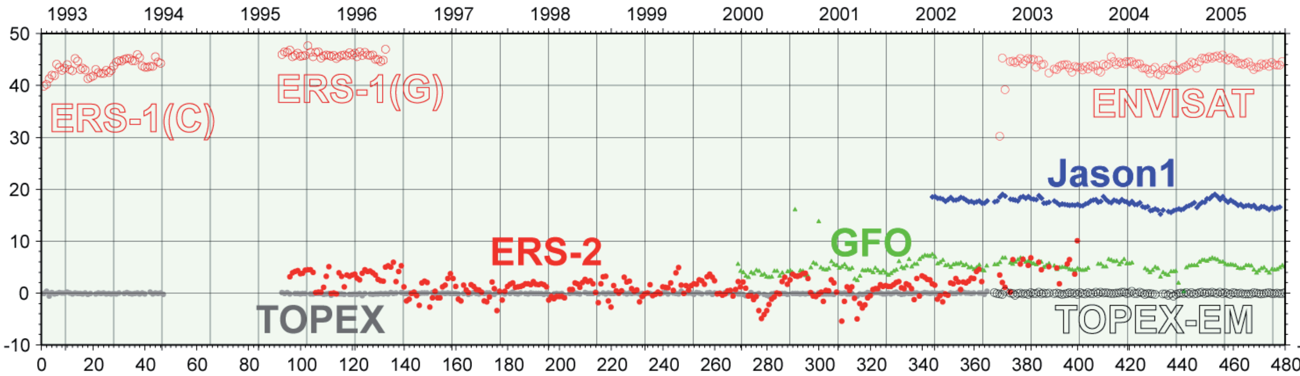

Fig. 2.3.2: Relative range biases (cm) for all missions and 10-day periods analysed. The range biases are relative to TOPEX (later T/PEM) because the sum of TOPEX (T/P-EM) errors was forced to zero. Note, all biases show weak annual oscillations with similar phasing and amplitude for ENVISAT, Jason1, and GFO since late 2002 – an indication for systematic variations in the TOPEX (T/P-EM) orbits.

Relative range biases

The result is shown in Figure 2.3.2. The order of magnitude of the relative range biases is widely consistent with independent calibrations and cross-calibrations performed by other groups. However since late 2002, the approach followed here shows for all relative biases weak annual oscillations with similar phasing and amplitude. This indicates that the mean bias of TOPEX, forced to be zero within every analysis period, might have an annual variation by itself – a topic that requires further investigations.

Centre-of-origin shifts

The postprocessing of radial errors was also used to investigate if there are conspicuously large-scale error patterns that can be explained by centre-of-origin shifts for *x*, *y*, and *z*. These shifts, estimated together with the relative range biases, are shown in Figure 2.3.3. They are predominantly within ±10 mm – except the *y* and *z* shifts of GFO, which have a magnitude of up to 20 mm. The annual variations, in particular the reversed shifts showing up for ERS-2 and TOPEX, are outstanding, not completely understood and need also further investigations.

Fig. 2.3.3: Centre-of-origin shifts (mm) derived for every 10-day analysis period from the radial error estimates of each mission. Notable the reversed shifts of ERS-2 and TOPEX. The scatter of the shifts increases significantly from 2000 on. Striking the large z-shifts for GFO - possibly caused by sea state bias errors in the southern ocean.

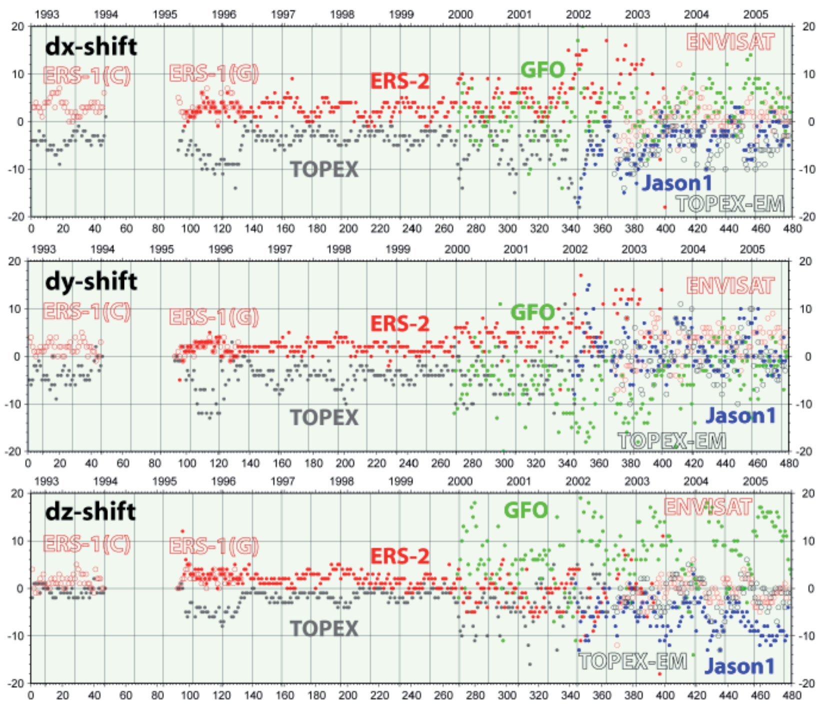

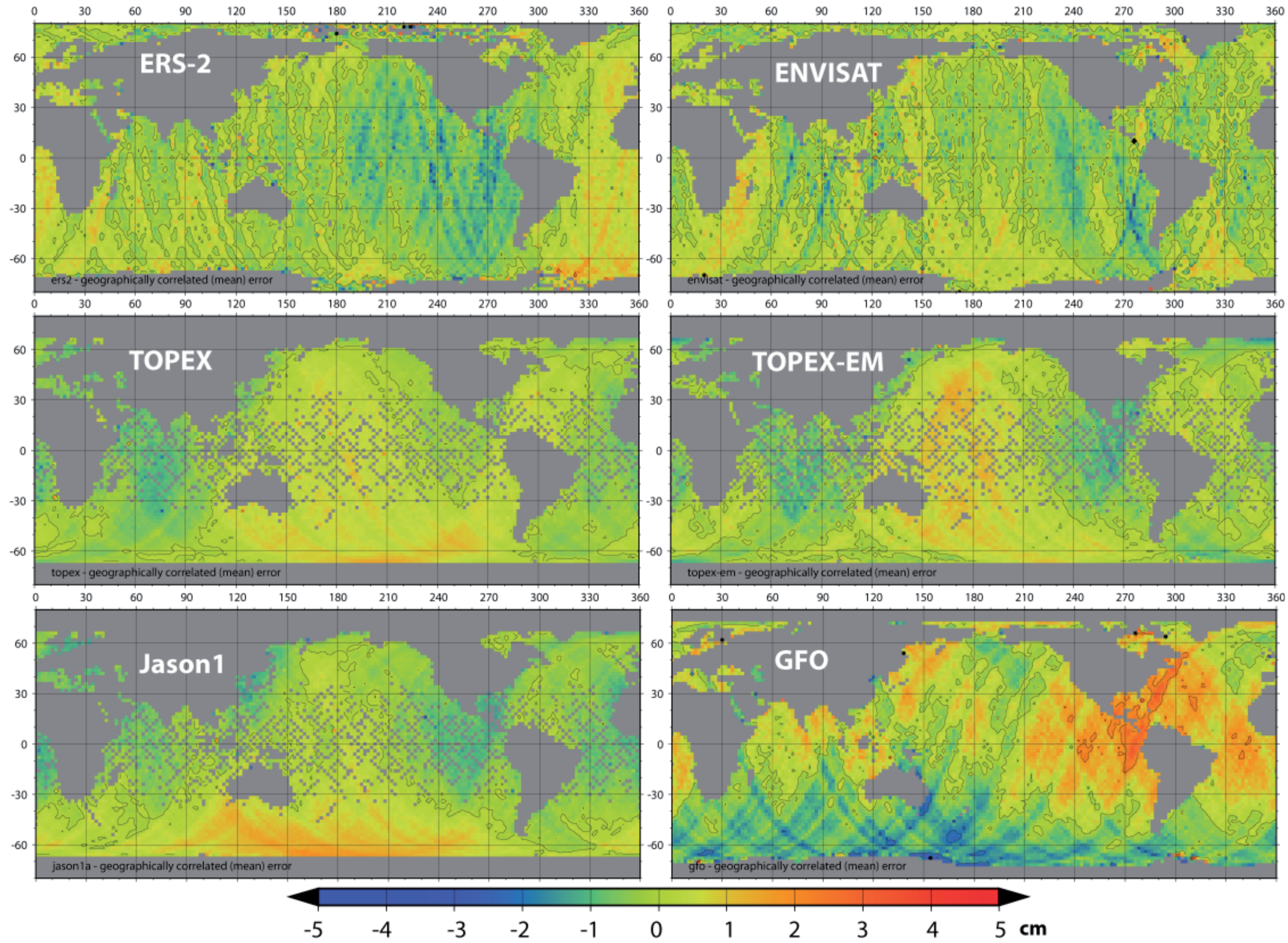

Fig. 2.3.4: Geographically correlated mean errors (centimetre) for ERS-2 and ENVISAT (top row), TOPEX and TOPEX-EM (middle row), and Jason1 and GFO (bottom row). The mean error pattern for TOPEX and TOPEX-EM are – as expected – very similar. However the mean error of Jason1 differs significantly from TOPEX although Jason1 orbits are also based on JGM3. This is an indication that not only gravity field errors, but also other errors (e.g. for sea state bias) map into the mean error. GFO exhibits the most outstanding mean error pattern with up to 4-5 cm around Central America and negative values (between -2 and -4 cm) at all southern oceans.

Geographically correlated error pattern

Finally, the complete time series of radial errors were taken to assess the dangerous geographically correlated errors for all altimeter satellites. From Kaula's first order analytic solution of satellite motions and investigations of Rosborough, it is known that the errors of ascending and descending passes are composed of sum and difference of a "mean" and a "variable" component respectively. If the errors of ascending and descending passes are known separately, the arithmetic mean of both immediately gives the mean or geographically correlated error component. To estimate the mean errors, the crossover analysis was supplemented by a simple book-keeping to distinguish errors of ascending and descending tracks. For each mission the errors of ascending and descending tracks were then spatially averaged – independent of each other on a 2° x 2° grid. This led to satellite specific mean error patterns for both ascending and descending tracks. The arithmetic means of these error pattern were performed for each satellite and give the satellite-specific geographically correlated error patterns shown in Figure 2.3.4.

2.4 Effects of mass displacements

Since March 2002 the Gravity Recovery and Climate Experiment (GRACE) satellite mission allows an unprecedented monitoring of the Earth's gravity field and its temporal variations. The observed gravity field variations reflect the integral effect of geophysical processes within the various components of the Earth system. There are three GRACE science processing centres, namely the Center for Space Research (CSR), the GeoForschungsZentrum (GFZ) and the Jet Propulsion Laboratory (JPL) which process the raw measurements and provide monthly sets of gravity field coefficients up to degree and order 120 (CSR_RL01, GFZ_RL03, and JPL_RL02 respectively).

Time-variable gravity field observations from GRACE

Among the published data sets are the so-called Level 2 GSM products which contain the geopotential coefficients of monthly static gravity fields that have been reduced by tidal effects (ocean tides, solid Earth tides, pole tide) as well as non-tidal gravity signals of oceans and atmosphere. The corresponding Level 2 GAC products contain the monthly mean geopotential coefficients of the applied atmospheric and non-tidal oceanic reductions which are derived from operational ECMWF analyses and the global ocean circulation model OMCT, respectively. Variations of the "observed" geopotential coefficients that include non-tidal oceanic and atmospheric effects can be computed by subtracting the mean values of the coefficients $\overline{GSM}$ and $\overline{GAC}$ from the sum of GSM and GAC:

$$\left.\begin{matrix}\Delta C_{nm} \\ \Delta S_{nm}\end{matrix}\right\} = \left\{\begin{matrix}\Delta C_{nm}^{GSM} - \Delta C_{nm}^{\overline{GSM}} + \Delta C_{nm}^{GAC} - \Delta C_{nm}^{\overline{GAC}} \\ \Delta S_{nm}^{GSM} - \Delta S_{nm}^{\overline{GSM}} + \Delta S_{nm}^{GAC} - \Delta S_{nm}^{\overline{GAC}}\end{matrix}\right. . \qquad (1)$$

However, besides the desired effects of geophysical processes such as hydrology, the "observed" variations ΔC_{nm} and ΔS_{nm} of the geopotential coefficients are affected by errors of the GRACE measurements, by aliasing effects and deficiencies of the applied reduction models. Consequently, prior to a geophysical interpretation, the monthly gravity field solutions must be revised, and some data corrections must be performed.

Smoothing and destriping of observations

The geopotential coefficients contain conspicuous systematic errors which appear as north-south oriented stripes in the maps of monthly gravity field changes. This error pattern is caused by several reasons, e.g., aliasing effects due to tides, ocean circulation and other geophysical effects, i.e., by mass redistributions at time-scales which are short compared to the monthly resolution of the GRACE fields. In order to obtain representations of the geopotential that can be viewed as monthly mean fields, these undesired signals have to be removed. Different filter methods have been discussed recently in the literature. The results presented below were derived from a combination of an isotropic Gaussian filter and a correlated error filter which turned out to be effective for the reduction of the stripe pattern. Figure 2.4.1 displays observed variations ΔC_{nm} and ΔS_{nm} of the potential coefficients up to degree and order 60 (top panels) in three different stages of the reduction procedure. In addition the corresponding maps of gravity field variations are displayed (lower panels) in units of generating pressure variations (cf. Equation 2.4.2). As it is clearly visible, the uncorrected gravity field variations suffer from large errors. Since mass redistributions on time scales of a few days are regionally restricted, predominantly higher degree coefficients (degree 40 and above) are affected by aliasing. In order to smooth the coefficients, a Gaussian filter with a radius of 500 km is applied. Remaining errors on larger spatial scales are eliminated from the respective coefficients by the correlated error filter (destriping).

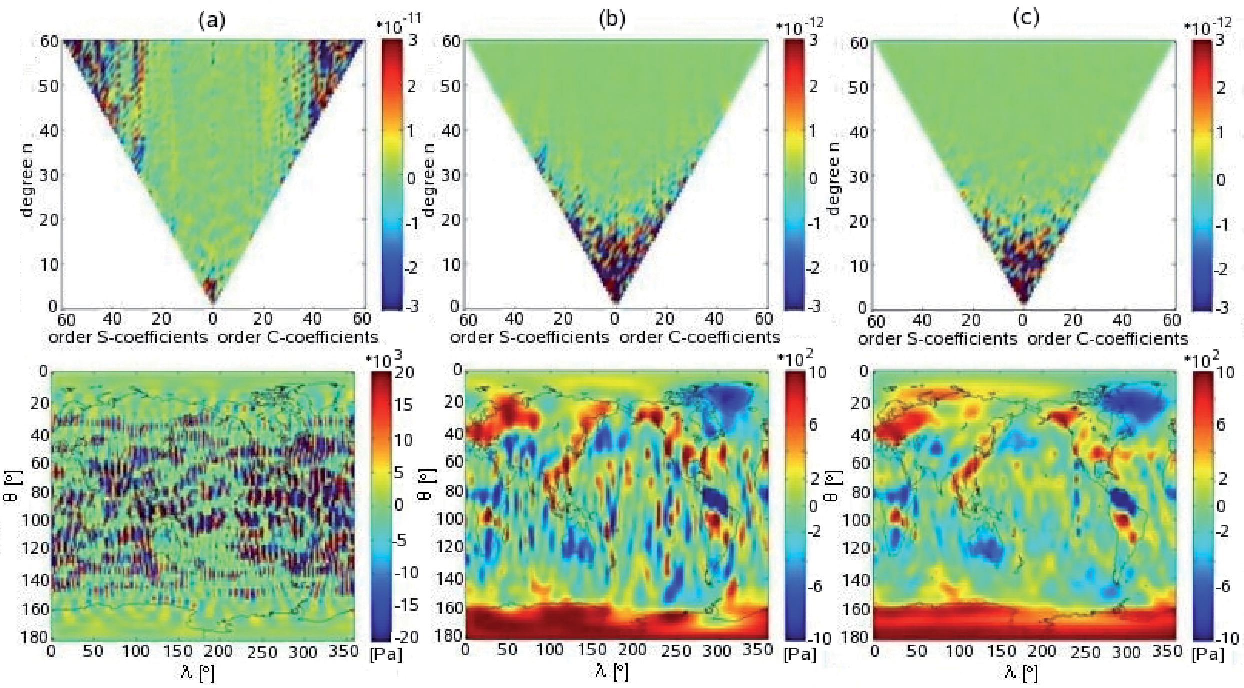

Fig. 2.4.1: Observed variations ΔC_{nm} and ΔS_{nm} of the potential coefficients up to degree and order 60 (top panels: (a) unfiltered coefficients; (b) after the application of a Gaussian filter with radius 500 km; (c) after the application of correlated error and Gaussian filter) and corresponding maps of gravity field variations (lower panels) in units of generating pressure variations [Pa].

Pressure field changes from geopotential coefficients and geophysical models

The monthly variations ΔC_{nm} and ΔS_{nm} of geopotential coefficients can be expressed in terms of generating pressure changes $p(\theta,\lambda)$, which are computed by a global spherical harmonic synthesis over a sphere with mean Earth radius R:

$$\Delta p(\theta,\lambda) = \frac{ag\rho_E}{3}\sum_{n=0}^{N}\sum_{m=0}^{n}\frac{2n+1}{1+k_n}P_{nm}(\cos\theta)\left[\Delta C_{nm}\cos(m\lambda)+\Delta S_{nm}\sin(m\lambda)\right] \quad (2)$$

In this equation θ and λ denote the co-latitude and longitude of the computation point, g is the gravitational acceleration, ρ_E is the mean density of the Earth and $P_{nm}(\cos\theta)$ is the associated Legendre polynomial of degree n and order m. To account for the effect of surface deformation of the solid Earth due to pressure variations, the degree n Love number k_n is applied.

In order to interpret the observations geophysically the monthly fields are compared with pressure fields from external data sources like reanalysis data or model simulations of mass redistributions within or between individual subsystems of the Earth. In the following the combined effect of pressure variations due to atmospheric, oceanic and hydrological effects is regarded.

The applied consistent representation of atmosphere and ocean dynamics comprehends reanalysis data of the National Centers of Environmental Prediction (NCEP) and a constrained version of the global ocean circulation model ECCO. Continental hydrological variations and snow fields were taken from the Land Data Assimilation System (LDAS). In order to provide a comparable basis, the geophysical data sets were adapted temporally (monthly mean fields) and spatially (application of the Gaussian filter with smoothing radius 500 km) to the GRACE fields.

Comparison of observed and modelled pressure field changes

In order to compare the dominant spatial patterns of variability, principal component analyses (PCA) were performed for both the observed and the modelled monthly pressure field changes. In Figure 2.4.2 the first two modes of the respective analyses are displayed. Both the observations (left panels) and the combination of the models (right panels) feature a strong annual variability in the first mode. While the corresponding curves are in good agreement, the spatial patterns and their amplitudes differ from each other. While annual pressure variations explain more than 60% of the entire model variability, the first mode accounts for only 45% of the observed signal. Discrepancies between the patterns are obvious especially in regions dominated by continental

Fig. 2.4.2: Time-variable principal components and corresponding eigenvectors of the pressure field changes from GRACE (left) and geophysical models (right) for the first and second mode.

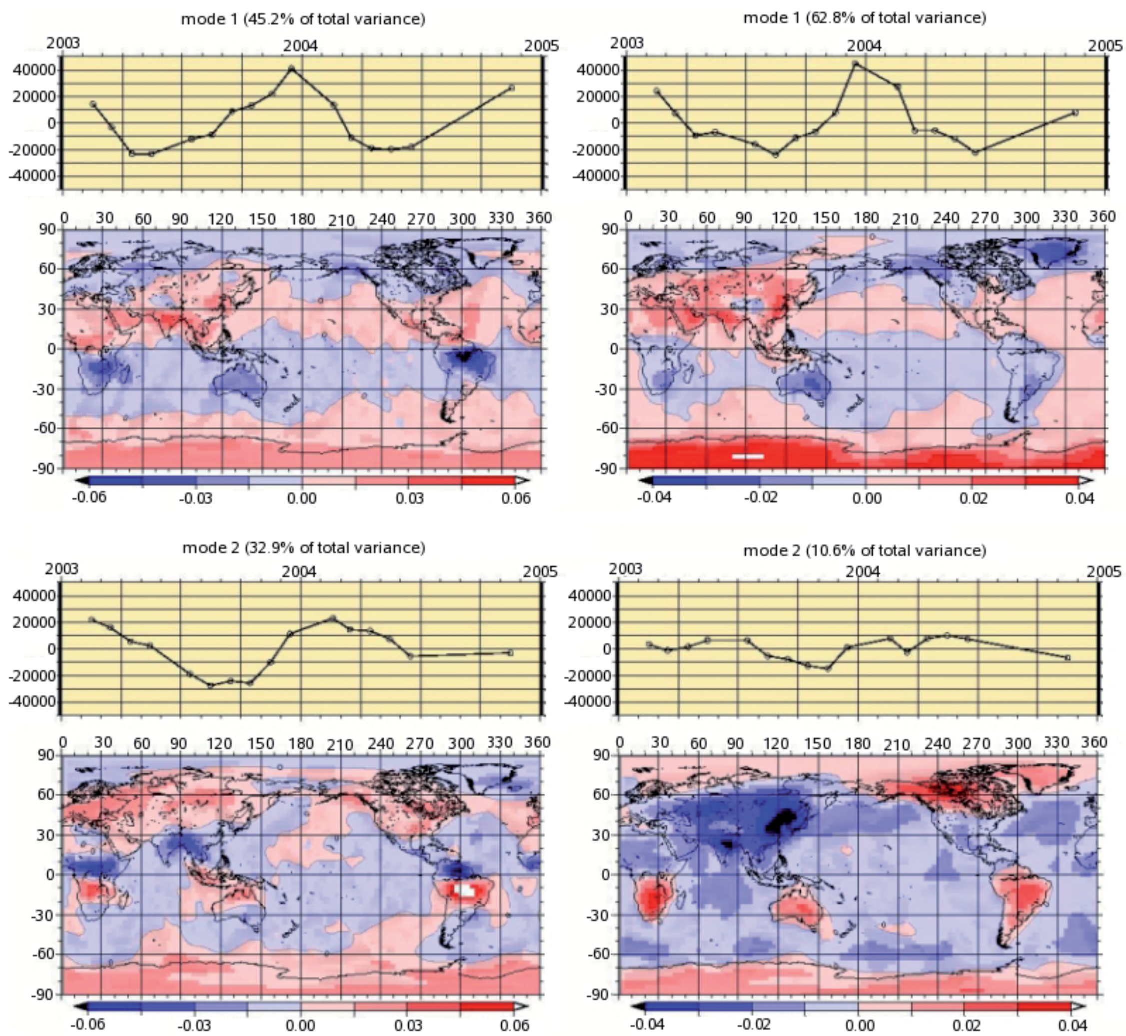

hydrology or snow variations. For example the observed signal in the Amazon region cannot be explained by the geophysical data sets. On the other hand, modelled annual pressure variations in Greenland are clearly overestimated. In constrast to the models, the second mode of the observed fields features a clear annual signal, too. But it differs from the first mode with respect to its phase. Nevertheless, the two modes tend to compensate each other partially since the colorbars of mode 1 and mode 2 seem to be inverted in the regions where dominant annual signals appear (Central and South Africa, Amazon basin). Therefore the sum of the first two modes of the observations might resemble the first mode of the model pressure fields better than the first mode alone. This is confirmed since strong signals in East Asia and Canada in mode 2 of the model pressure fields are partially apparent in the third mode of the observed pressure fields (not shown).

Figure 2.4.3 (left) displays the correlation coefficients of observed and modelled pressure field changes. In general the correlation is higher over the continents, i.e., patterns and phases of modelled atmospheric and hydrological variability agree largely with GRACE observations. In contrast, observed pressure variations over the oceans do not match the results of ECCO in many regions. The map of RMS differences between observed and modelled pressure fields (Figure 2.4.3; right) reveals that the largest discrepancies between observations and geophysical models are in regions which are strongly influenced by continental hydrology, e.g., the river basins of the Amazon, Ganges and Congo. In addition there are clear discrepancies in Siberia and Greenland.

In order to study if the discrepancies can be explained by deficiencies of the applied geophysical models, the analysis will be extended to alternative data sets like pressure variations of ECMWF (atmosphere), OMCT (ocean) and LaD (hydrology). With respect to the analysis of GRACE observations, further investigations regarding the methods used for smoothing and destriping are necessary.

Fig. 2.4.3: Correlation coefficients (left) and RMS differences (right) of observed and modelled pressure changes.

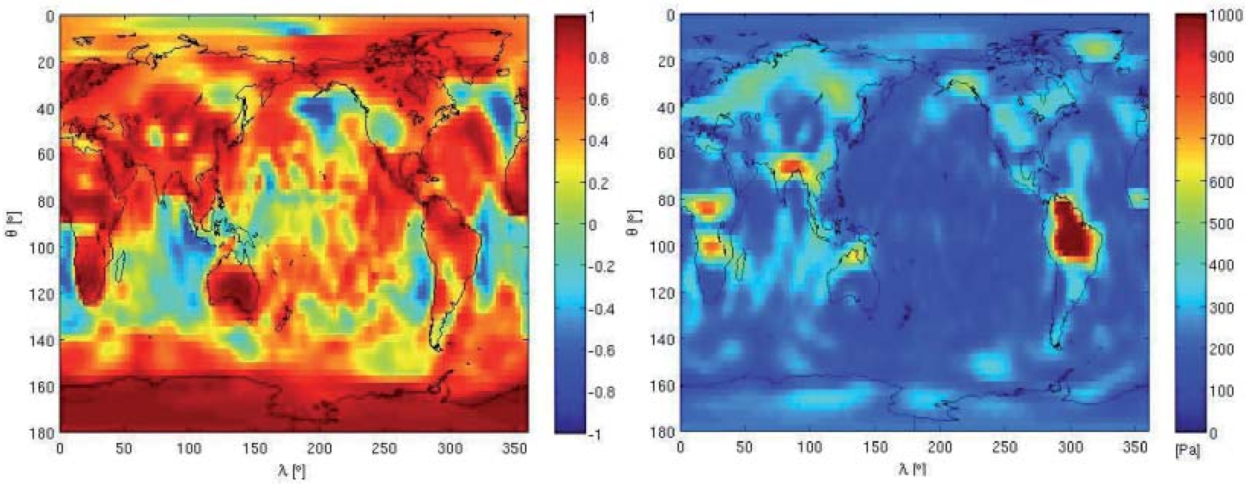

2.5 Modelling of the ionosphere

The ionosphere is generally defined as a thick shell of electrons and ions, which envelopes the Earth from about 60 to 1000 km height. In the last year's annual report we presented a three-dimensional (3-D) model of the electron density distribution mathematically based on wavelet strategies and physically controlled by the International Reference Ionosphere (IRI) model. To be more specific, in that approach we described the electron density by means of 3-D wavelet expansions w.r.t. space and time-dependent series coefficients. In order to demonstrate the procedure we presented last year the multi-resolution representation (MRR) of a 2-D data set of vertical total electron data over South America.

Electron density model based on B-splines

Now we start our considerations with the series expansion

$$N(\mathbf{x},t) = \sum_{k=0}^{K_I-1} \sum_{l=0}^{K_I-1} \sum_{m=0}^{K_I-1} d_{I;k,l,m}(t)\, \phi_{I,k}(\lambda)\, \phi_{I,l}(\varphi)\, \phi_{I,m}(h) \tag{1}$$

of the spatio-temporal, i.e. 4-D electron density $N(\mathbf{x},t)$ ($\mathbf{x}$ = spatial position vector, t = time) with time-dependent level-I scaling coefficients $d_{I;k,l,m}(t)$. As spatial base functions we choose 3-D tensor-product B-splines, i.e. products of three 1-D B-splines $\Phi_{I,k}$ depending on longitude λ, latitude φ and height h; cf. Fig. 2.2.1. Since the slant total electron content (STEC) is defined as the integral of the electron density along the ray path between the transmitting satellite S and the receiver R, we obtain with Eq. (1) the relation

$$STEC(t) = \sum_{k=0}^{K_I-1} \sum_{l=0}^{K_I-1} \sum_{m=0}^{K_I-1} d_{I;k,l,m}(t)\, b_{k,l,m}(R,S) \tag{2}$$

with

$$b_{k,l,m}(R,S) = \int_R^S \phi_{I,k}(\lambda)\, \phi_{I,l}(\varphi)\, \phi_{I,m}(h)\, ds \quad , \tag{3}$$

which basically can be interpreted as the observation equation for geometry-free GNSS observations. Since the observations are generally scattered, an unknown scaling coefficient $d_{I;k,l,m}(t)$ is computable only if observations are given close to the peak of the corresponding 3-D base function in the integrand of Eq. (3). Hence, in case of large data gaps, many scaling coefficients are not calculable and the corresponding addends can be excluded from the observation equation (2). If only a few observations support the computation of a coefficient, prior information could be introduced in order to stabilize the estimation process. With the estimated scaling coefficients the decomposition of the electron density into so-called step-j detail signals (j = 1, 2, ... , j') using wavelet techniques can be started; the related step-j approximations are a low-pass filtered version of the electron density. The different steps of the procedure, i.e. the adjustment based on variance component estimation and the decomposition into detail signals, are visualized in Fig. 2.5.1. Since usually many wavelet coefficients are numerically very small, the wavelet decomposition into detail signals, i.e. the establishment of a MRR, is also a very advantageous method for data compression.

Fig. 2.5.1: Flowchart of the 4-D multi-resolution model: the green-coloured boxes are the input data, the orange-coloured boxes represent the output components of the MRR.

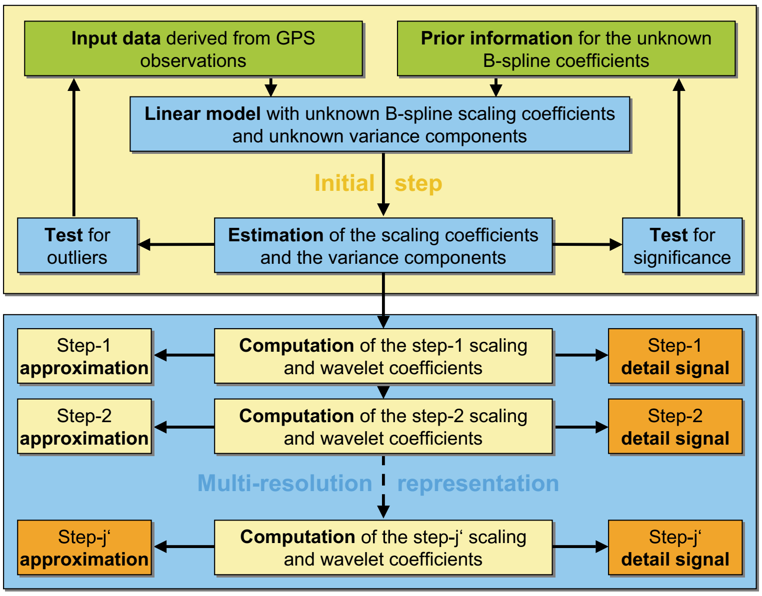

In order to demonstrate our procedure we apply it to electron density values over South America. The data were computed for one specific day from IRI with a spacing of 2° in longitude and latitude, 25 km in the height and 1 h in time. Choosing $I = 5$ for

Fig. 2.5.2: Electron density values from IRI (left panels), the corresponding estimated level-5 B-spline approximations (mid column) and the differences (right panels) for selected heights at 14:00 UT.

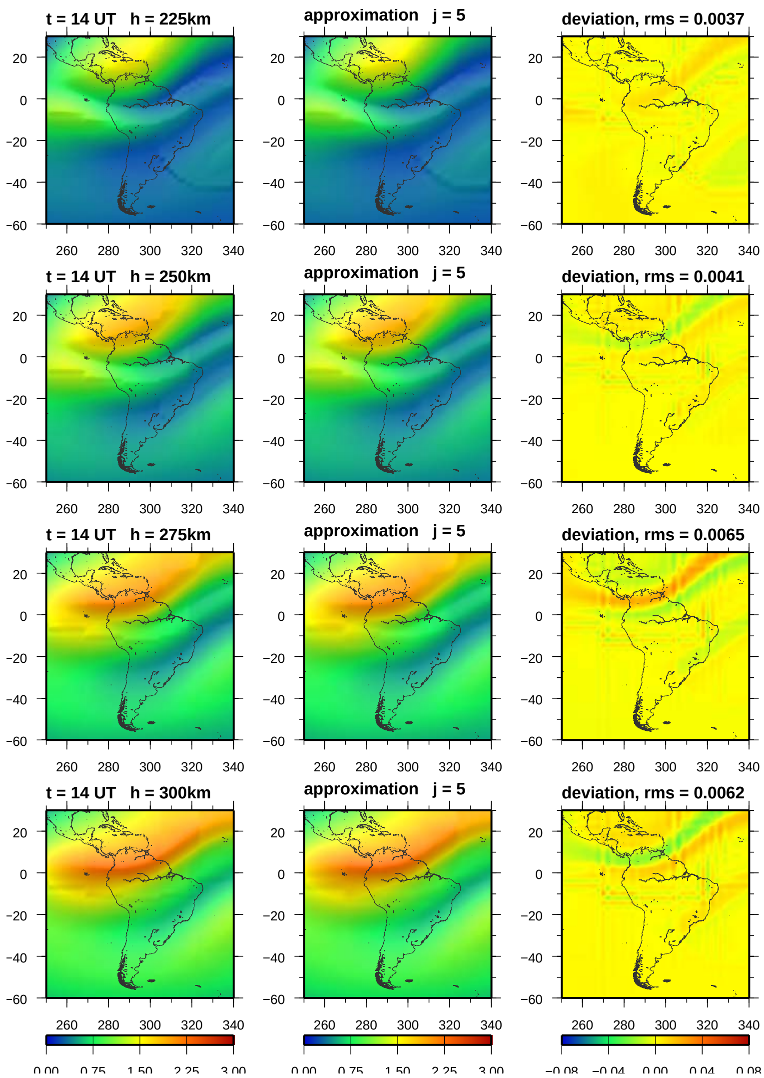

the highest level and with K_5 = 34, we estimate according to Eq. (1) altogether 34^3 = 39,304 time-dependent scaling coefficients $d_{5;k,l,m}(t)$ for each hour following the initial step shown in Fig. 2.5.1, but without considering prior information.

Figure 2.5.2 shows the electron density input data from IRI for 14:00 UT and selected heights, the corresponding level-5 estimations (approximations) as well as the deviations. The root mean square (rms) values of the deviations are between 0.002 x 10^6 electrons/cm^3 and 0.007 x 10^6 electrons/cm^3.

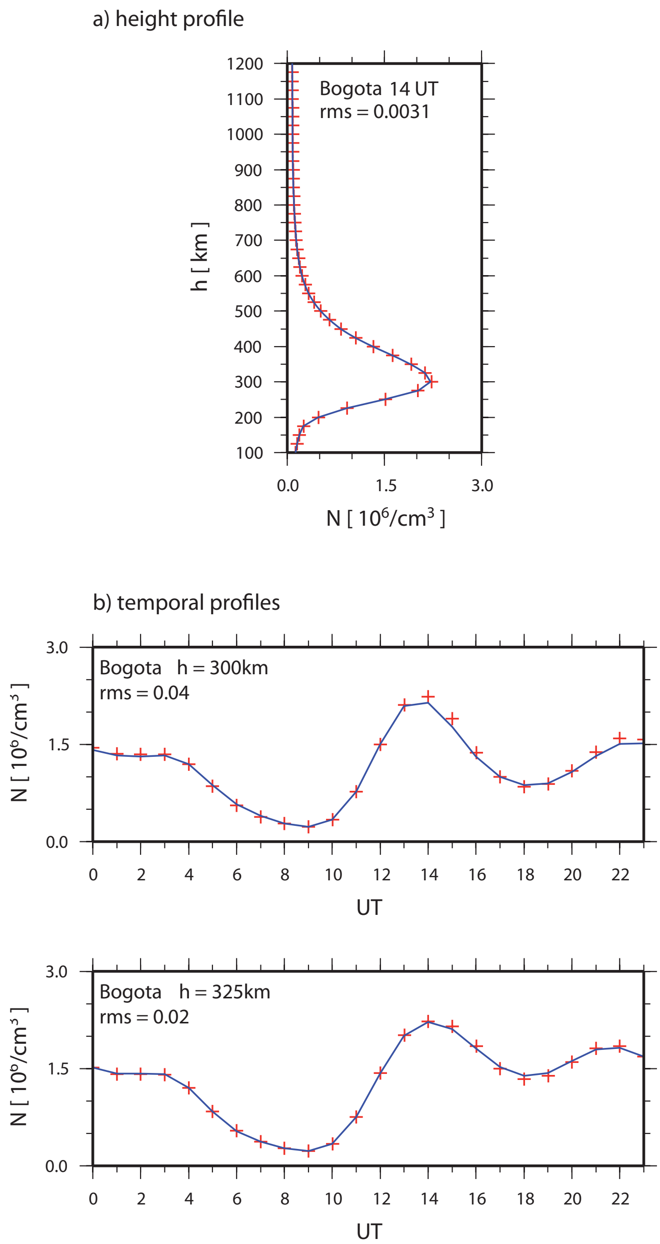

Fig. 2.5.3: Profiles of the electron density from IRI (red crosses) and from the estimated level-5 B-spline approximations (blue lines) w.r.t. a) height and b) time.

Panel a) of Fig. 2.5.3 depicts a height profile of the electron density for Bogota/Colombia. The red crosses are computed from IRI input data, the blue curve means the level-5 approximation from the B-spline approach. The rms value of the deviations amounts around 0.003 x 10^6 electrons/cm^3. Panel b) of Fig. 2.5.3 shows selected temporal profiles for 24 hours at heights h = 300 km and h = 325 km for Bogota; again the red crosses are the electron density input data from IRI model, the blue line, however, is the level-4 approximation. As can be seen from the rms values of the deviations, the level-4 approximation is much more inaccurate than the level-5 approximation since the high-frequency signal parts are suppressed.

Electron density model based on B-splines and empirical orthogonal functions

In Eq. (1) we model the height-dependency of the electron density by means of 1-D B-spline functions $\Phi_{I,m}(h)$. As an alternative we may replace these base functions by empirical orthogonal functions (EOFs). In this 2-D B-spline/1-D EOF approach we rewrite Eq. (1) as

$$N(\mathbf{x},t) = \overline{N(\mathbf{x})} + \sum_{k=0}^{K_I-1} \sum_{l=0}^{K_I-1} \sum_{m=1}^{M} d_{I;k,l,m}(t)\, \phi_{I,k}(\lambda)\, \phi_{I,l}(\varphi)\, EOF_{k,l,m}(h) \quad (4)$$

wherein the first term on the right-hand side is the mean value of the electron density w.r.t. time at position **x**. The EOFs are calculated for each point *(k,l)* of the longitude-latitude grid by applying the method of principal component analysis (PCA) to the reference model, i.e. IRI, in a preprocessing step. Approximately 98% of the electron density is considered by the first two modes of the PCA. Figure 2.5.4 shows exemplarily the corresponding eigenvectors of a specific *(k,l)* position.

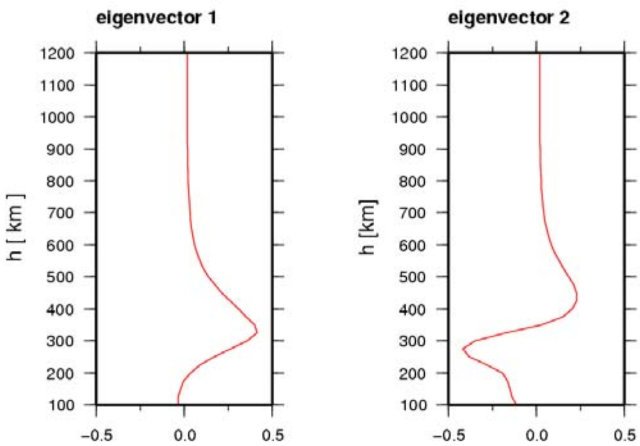

Fig.2.5.4: The first two eigenvectors (EOFs) for a specific (k,l) position. The first and the second eigenvector consider about 88% and 10% of the total energy of the electron density, respectively; the shape of the first eigenvector defines mainly the height profile of the electron density; cf. Fig. 2.5.3a.

For our computations we introduce the first five eigenvectors as $EOF_{k,l,m}(h)$ into Eq. (4). The number of unknown series coefficients $d_{I;k,l,m}(t)$ is generally much less than in the 3-D B-spline approach. In case of $K_5 = 34$ and $M = 5$ we have to solve for $34^2 \times 5 = 5{,}780$ unknowns for each hour; cf. the 39,304 unknowns of the level-5 3-D B-spline approach. Besides this issue the main advantage of this approach over the 3D B-spline approach is the consideration of the insensitivity of the GPS observations to the height dependency; on the other hand an important disadvantage is that the shape of the EOFs cannot be changed within the adjustment, i.e. the reference model strongly effects the height dependency of the estimated electron density. Applying this method to the same data set mentioned before (see Fig. 2.5.2, left panels), similar results (not shown here) are obtained.

Besides these 3-D series expansions according to the Eqs. (1) and (4), we also derived a 4-D model by considering a fourth 1-D B-spline function related to time. The main advantage of this approach is that the observations do not need a temporal discretization anymore. On the other hand large linear equation systems have to be solved, but fortunately, due to the compact support of the B-splines, the resulting normal equation system is of block-diagonal structure and can be solved efficiently.

Evaluation of GNSS measurements of the Slant Total Electron Content

Recall, the main objective of our investigation is the estimation of scaling coefficients from geometry-free GNSS observations. In the following we present a first simple example for applying the observation equation (2) in order to estimate the coefficients $d_{I;k,l,m}(t)$ from generated observations. By forward modelling we computed STEC values according to Eq. (2) using the coefficients we estimated before in evaluating the IRI electron density values and adding white noise. The configuration of receivers and satellite orbits can be taken from the panels a) and b) of Fig. 2.5.5. Panel c) depicts some selected signal paths of altogether approximately 1100 ray-paths. Such a scenario in combination with the observation equation (2) is known as the ionospheric tomography problem. In our numerical investigation, we set $I = 2$ and solve with $K_2 = 6$ the altogether $6^3 = 216$ unknown scaling coefficients of this inverse problem by applying the adjustment procedure shown in the upper part of Fig. 2.5.1. Prior information can be used to stabilize the normal equation system. As the result of this procedure we recover the input data with the desired accuracy (not shown here).

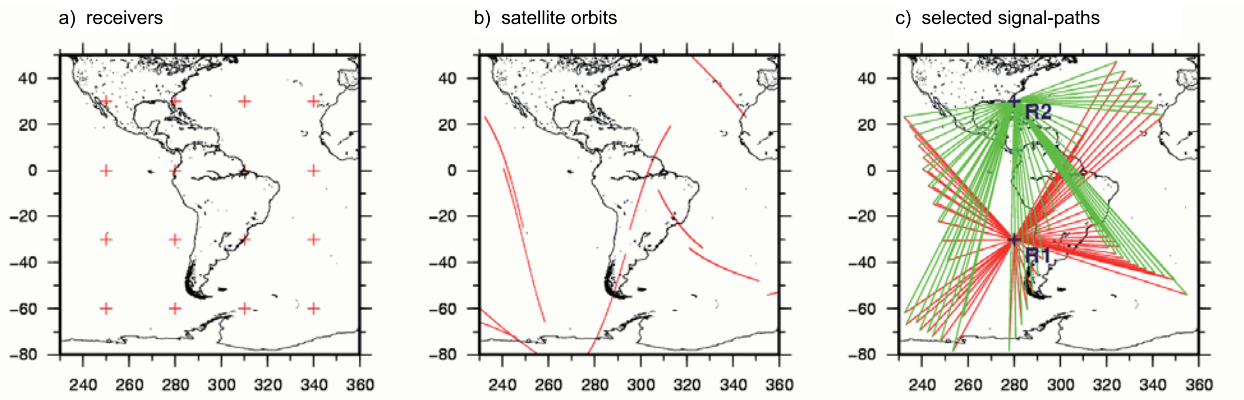

Fig. 2.5.5: Distribution of receivers (a) and satellite orbits (b) of the simulated example; panel c) shows ray-paths for two selected receiver locations.

2.6 Models of crustal deformation

The series of DGFI Actual Plate Kinematic and crustal deformation Models (APKIM) was continued in 2006 by computing two models APKIM2005 based on the space geodetic observations (GPS, SLR, VLBI, DORIS) provided by the corresponding IAG Services for the International Terrestrial Reference Frame 2005 (see 3.1). One model uses as input data the horizontal station velocities of solution ITRF2005P of Institute Géographique National (IGN), Paris, the other one the corresponding DGFI solution. The final data used are summarized in Table 2.6.1. All velocities included in the solutions were considered, i.e., if different velocities at a site were estimated and not equated, all of them entered into the processing. The aim is to realize the present-day kinematic no-net-rotation (NNR) constraint of the ITRF and to provide a new geodetic model for geophysical interpretation.

In a first step the station velocities were attributed to a rigid plate or a deformation zone, respectively. For this purpose the geometry of the geologic-geophysical plate model PB2002 (Bird 2003) was used. A total of 16 plates (see Table 2.6.2) and four deformation zones (Alpine-Mediterranean, Persia-Tibet-Burma, Gorda-California-Nevada, and Andes) of this model were covered by a sufficient number of stations. The rotation vectors of the rigid plates were computed by a least squares adjustment eliminating iteratively outliers, i.e., those velocity vectors that differ significantly from the estimated plate rotation. This may be due to unrepresentative station velocities in the ITRF solutions (e.g., multiple velocities at a site) or caused by stations not moving with the rigid plate (intra-plate deformation).

Tab. 2.6.1: Input data for two APKIM2005P computations. The different number of velocities is due to different equating at sites with more than one occupation.

	no. of velocities on rigid plates	no. of velocities in deformation zones
APKIM2005P IGN	303	125
APKIM2005P DGFI	465	148

The deformation zones were modelled by a least squares collocation approach. Covariance functions of the velocities in north and east direction as well as cross-covariances between north and east direction were computed empirically from the observations. Rigid plate motions were added as boundary conditions in case of not sufficient observations available in boundary zones (Fig. 2.6.2).

To realize the NNR condition all velocities of a global grid of 1° latitude * 1° longitude were computed as rigid plate rotations or deformations, respectively. From this complete velocity field a common rotation vector was estimated (of course weighting the grid velocities according to the different size due to meridian convergence) and subtracted from the originally estimated rotation vectors. The final result is given in Table 2.6.2 for both ITRF solutions and as a comparison with PB2002, which is identical with NNR NUVEL-1A for the major tectonic plates. There are no significant differences between the IGN and DGFI solutions. With respect to the geophysical model, however, there appear the well-known considerable discrepancies between present-day and geological plate motions. A graphical comparison is shown in Figure 2.6.1.

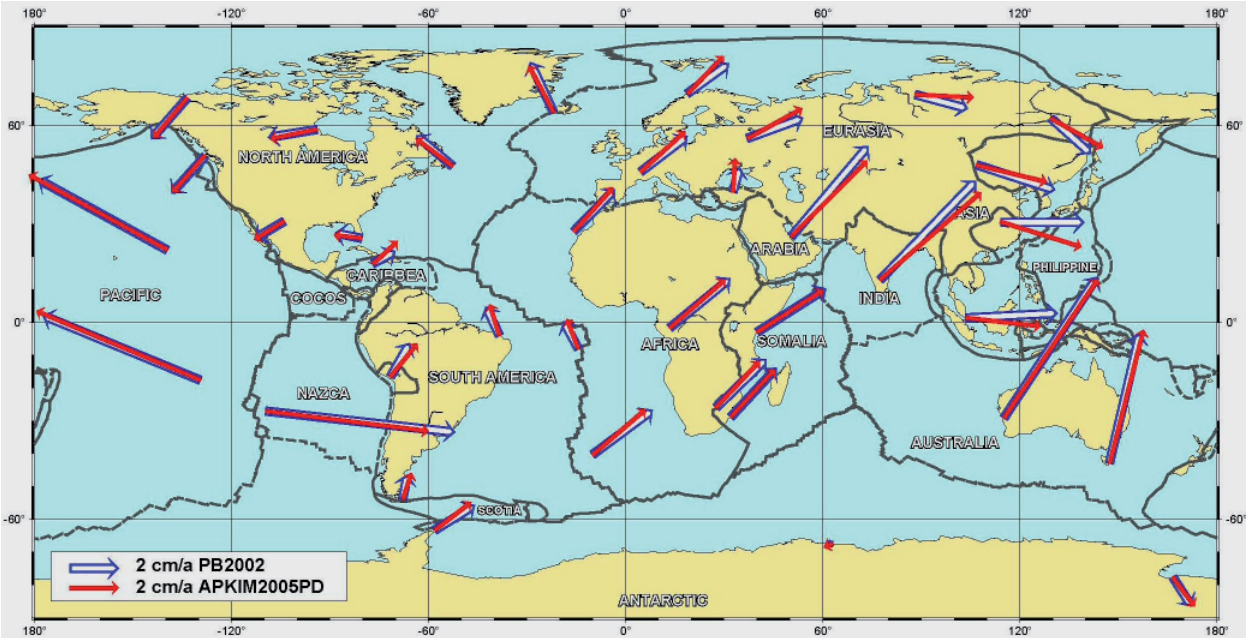

Fig. 2.6.1: Comparison of APKIM2005P (DGFI) solution and geophysical model PB2002.

Fig. 2.6.2: Deformation of the Gorda-California orogene as an example.

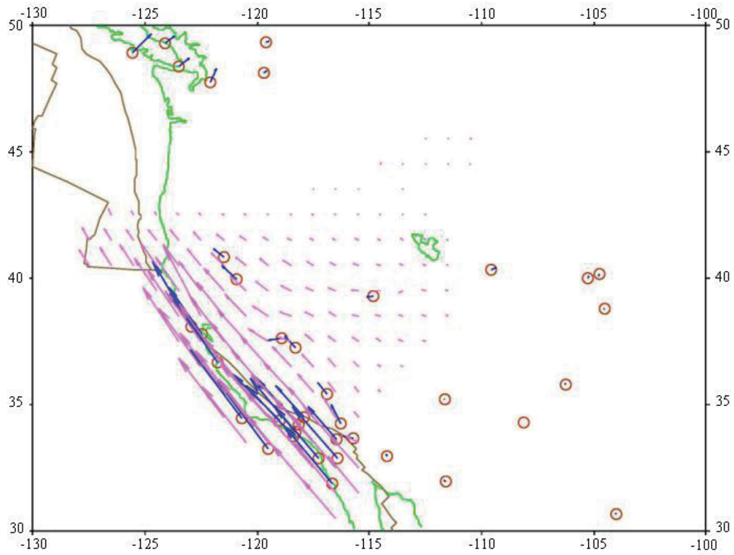

Tab. 2.6.2: Comparison of APKIM solutions for ITRF2005 and geophysical model PB2002.

Plate Abbr.	APKIM2005P (IGN)			APKIM2005P (DGFI)			PB2002 (geophysical)		
	Latitude [°]	Longitude [°]	Velocity [°/Ma]	Latitude [°]	Longitude [°]	Velocity [°/Ma]	Latit. [°]	Longit. [°]	Veloc. [°/Ma]
AFrc	48.9 ± 0.3	280.2 ± 0.7	0.278 ± 0.001	48.8 ± 0.3	280.1 ± 0.8	0.274 ± 0.002	50.6	286.0	0.291
AMur	57.4 ± 12.	262.2 ± 16.	0.278 ± 0.023	55.6 ± 3.3	263.3 ± 4.2	0.280 ± 0.005	44.3	261.6	0.308
ANta	61.1 ± 0.3	239.4 ± 0.7	0.236 ± 0.003	60.9 ± 0.4	236.9 ± 0.7	0.234 ± 0.004	63.0	244.3	0.238
ARab	49.4 ± 0.5	3.6 ± 2.2	0.592 ± 0.018	48.9 ± 0.5	4.2 ± 1.4	0.599 ± 0.015	46.7	353.8	0.593
ATol	40.0 ± 0.1	28.1 ± 0.3	2.037 ± 0.100	40.0 ± 0.1	28.2 ± 0.2	2.000 ± 0.060	40.9	27.2	1.210
AUst	32.7 ± 0.1	37.0 ± 0.2	0.636 ± 0.001	32.8 ± 0.2	37.2 ± 0.3	0.636 ± 0.002	33.9	33.2	0.646
CArb	42.0 ± 4.5	247.7 ± 28.	0.208 ± 0.064	40.4 ± 3.3	253.6 ± 15.	0.219 ± 0.041	34.0	272.4	0.291
EUra	53.6 ± 0.3	263.1 ± 0.4	0.258 ± 0.001	53.8 ± 0.3	264.2 ± 0.4	0.259 ± 0.001	50.6	247.7	0.234
INdi	29.5 ± 6.6	296.3 ± 7.8	0.602 ± 0.065	28.2 ± 5.3	294.9 ± 6.1	0.614 ± 0.054	45.5	0.3	0.545
NAme	-5.4 ± 0.5	275.3 ± 0.2	0.192 ± 0.001	-5.2 ± 0.5	276.3 ± 0.2	0.196 ± 0.001	-2.4	274.1	0.207
NZca	44.9 ± 0.8	259.9 ± 0.3	0.649 ± 0.006	45.1 ± 0.8	260.2 ± 0.4	0.646 ± 0.008	47.8	259.9	0.743
PAcf	-63.6 ± 0.1	110.3 ± 0.8	0.675 ± 0.002	-63.6 ± 0.1	111.1 ± 0.5	0.673 ± 0.001	-63.0	107.3	0.641
SAme	-15.8 ± 0.8	234.0 ± 1.6	0.121 ± 0.001	-17.6 ± 0.9	236.2 ± 2.3	0.120 ± 0.001	-25.3	235.6	0.116
SOma	52.2 ± 1.0	272.3 ± 2.5	0.316 ± 0.006	49.7 ± 1.1	267.2 ± 2.0	0.333 ± 0.007	49.8	266.7	0.348
SUma	45.2 ± 6.0	274.4 ± 2.6	0.380 ± 0.039	37.0 ± 3.9	278.6 ± 1.2	0.452 ± 0.045	45.2	286.8	0.476
YAng	53.5 ± 9.8	262.9 ± 11.	0.317 ± 0.002	56.6 ± 5.7	261.6 ± 7.4	0.316 ± 0.004	66.8	209.5	0.393

2.7 Analysis of time series of geodetic parameters

Two aspects were investigated in this project:
- The influence of time-variable effects, especially seasonal variations on the reference frame.
- The improvement of an ocean tide model in shallow water areas from altimetry data.

Influence of time-variable effects on the reference frame

In the context of the ITRF2005 computation (see 3.1) we investigated the influence of time-variable effects on terrestrial reference frame (TRF) solutions. Modern TRF solutions are computed from weekly/session-wise data which allows to study time-variable effects in station positions and to account for them in the combination.

Besides discontinuities, mainly caused by earthquakes and instrumental changes, periodic effects can be found in the time series of station positions. For example in GPS time series, annual variations are found mainly in the height component, with an average amplitude of 4-6 mm, for some stations up to 1 cm, like the station Irkutsk (see figure 2.7.1). This annual signal has a systematic effect on the velocity estimation (see table 2.7.1). Therefore it is necessary to use only stations for a TRF with long enough time spans (> 2.5 years) to minimize this effect.

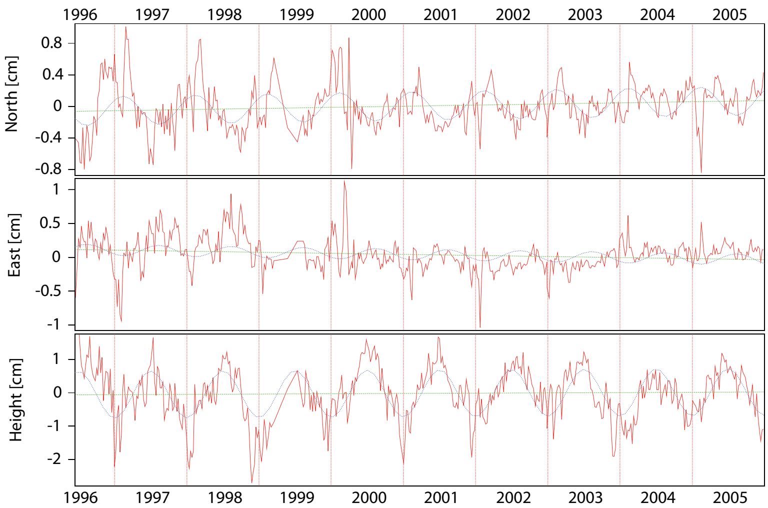

Fig. 2.7.1: Time series of station positions at Irkutsk computed from the GPS input data for ITRF2005.

Tab. 2.7.1: Influence of the annual signal in the height component of the station Irkutsk.

Data time span [yrs]	0,5	1,0	1,5	2,0	2,5	3,0	3,5	4,0	7,0
Δ Velocities [mm/yr]	-37,5±3,2	-3,7±2,3	0,1±1,0	2,7±0,8	1,0±0,6	-0,1±0,5	-1,1±0,4	-0,5±0,3	0,03±0,1

Improvement of tide models in shallow water areas

Global ocean tide models still exhibit considerable errors in shallow water areas. Sufficiently long times series of altimeter measurements can be used, however, to improve the knowledge on most of the ocean tide constituents. In contrast to tide gauge registrations, sampled hourly or with even higher frequency, the sparse sampling of tidal signals through satellite altimetry triggers the so called “alias-effect”: if dayly or half-dayly tidal signals are scanned only every few days, the signal appears to vary with a signifcant longer alias-period. This implies that the amplitude of tidal signals can only be estimated from sufficiently long time series - sometimes several years are necessary. Moreover, the separation of tidal signals is even more complicated and often requires much longer, so called “Rayleigh” periods. Tables 2.7.1 and 2.7.2 show for TOPEX (Jason1) and ERS (ENVISAT), respectively, the alias and Rayleigh periods for the most important semi-diurnal, semi-annual and annual tide signals.

Tab. 2.7.1: Alias periods (bold) and Rayleigh periods (both in days) of some important tidal constituents for a) TOPEX (Jason1) with a repeat period of 9.9156 days and b) ERS (ENVISAT) with a repeat period of 35 days.

	M_2	S_2	N_2	K_2	S_{sa}	S_a
M_2	**62**	1084	245	220	94	75
S_2		**59**	316	183	87	70
N_2			**50**	116	68	57
K_2	a) TOPEX/ Jason1			**87**	165	114
S_{sa}					**183**	365
S_a						**365**

	M_2	S_2	N_2	K_2	S_{sa}	S_a
M_2	**95**	95	3169	196	196	128
S_2		∞	97	183	183	365
N_2			**97**	209	209	133
K_2	b) ERS / ENVISAT			**183**	∞	365
S_{sa}					**183**	365
S_a						**365**

The key requirement for a successful ocean tide analysis of satellite altimetry data is the length of the altimeter time series. This can only be achieved by concatenating data of different missions. By the harmonization of data and the multi-mission cross calibration, described in theme 2.3, it was possible to construct consistent 13-year time series for TOPEX and Jason1 and for ERS-1, ERS-2 and ENVISAT. Figure 2.7.1 shows the time series of sea level anomalies for two locations at the Patagonian shelf.

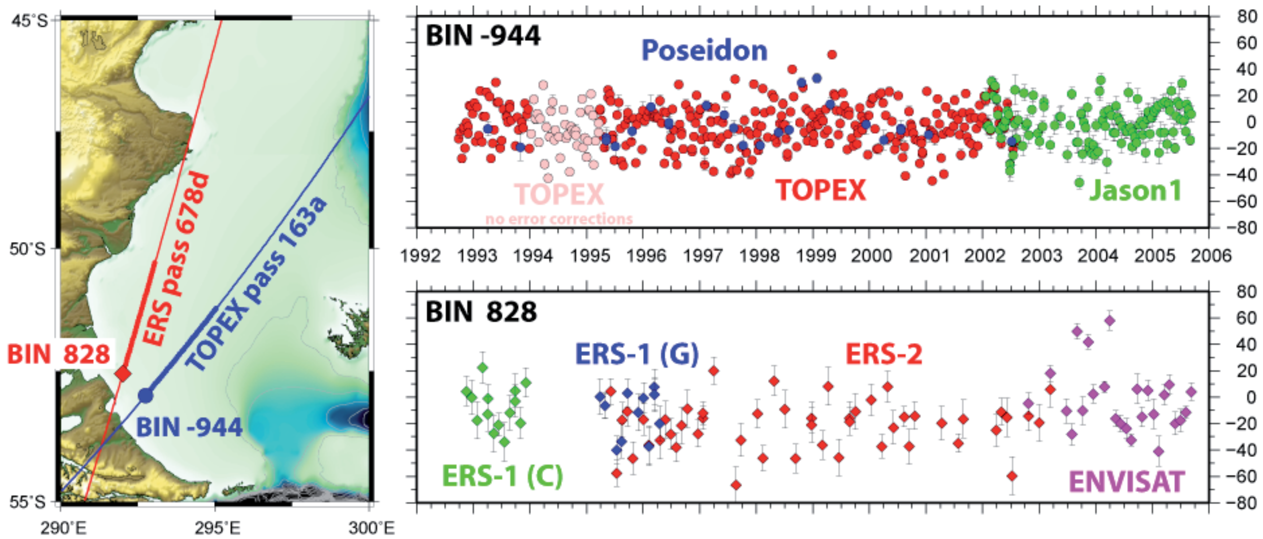

Fig. 2.7.1: Time series of sea level anomalies for two cells (BINs) located close to the coast (see left panel) on the ground tracks of TOPEX/Jason1 (upper plot) and of ERS/ENVISAT (lower plot). Although the ERS/ENVISAT time series is less accurate (indicated by the error bars) and infrequently sampled, it allows separation of M_2 and N_2.

Such time series were generated for small equidistant cells (BINs) defined on the nominal ground track. The slopes of a mean sea surface model were used to refer all sea level anomalies to the centres of these cells. For all measurements within these cells, harmonic analyses were then performed for the alias periods of S_2, M_2, and M_4 , a non-linear resonance period in shallow water. The result is shown in Figure 2.7.2. The S_2 and M_4 constituents were consistently estimated on both the ground tracks of TOPEX and the shifted ground tracks of TOPEX-EM, the extended mission period for the final three years. The spatial resolution for M_2 could be further improved by additional analyses on the ground tracks of ERS.

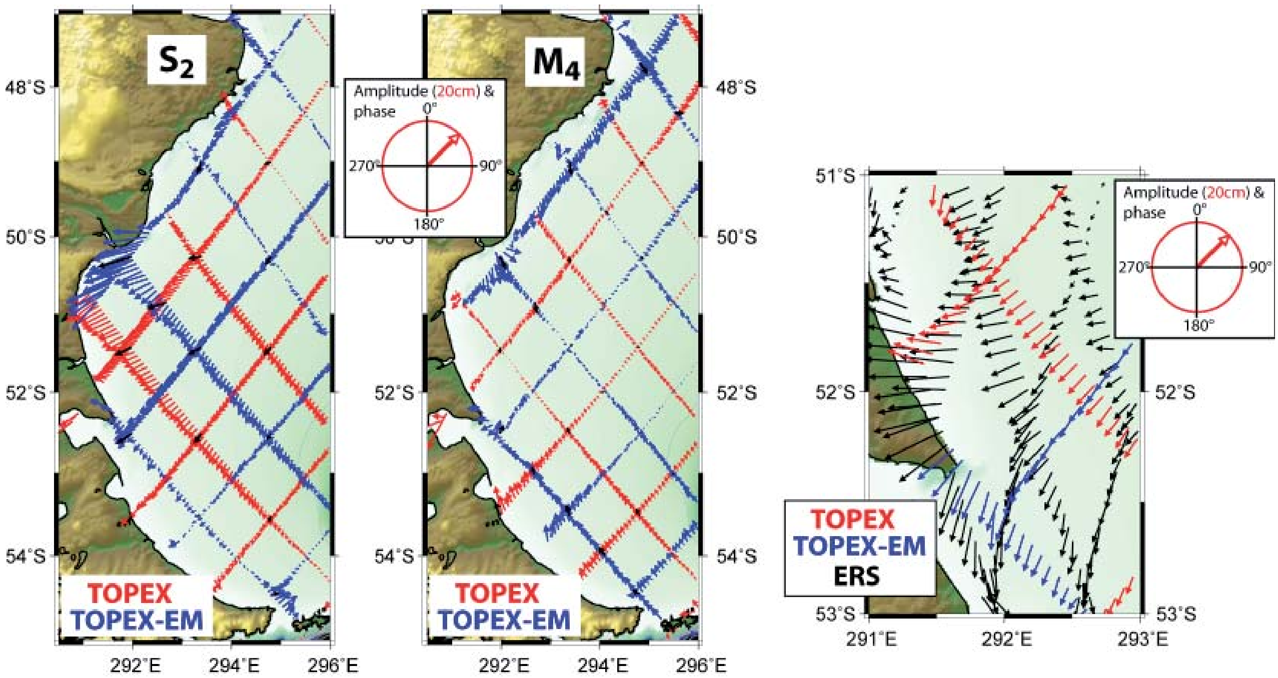

Fig. 2.7.2: Results of ocean tide analyses for altimeter time series on the tracks of both TOPEX/Jason1 (red) and the shifted tracks of TOPEX-EM (blue). The S_2 tide (left panel) and the M_4 tide (centre panel) are consistently resolved as indicated at the crossover of both ground track systems. Right panel: The M_2 tide could be resolved from TOPEX/Jason1, TOPEX-EM and the ERS/ENVISAT time series.

3 International Services and Projects

Scientific services and projects are the fundamental part of international cooperation. DGFI participates regularly in these activities. It has taken the responsibility for data centres, analysis centres and other functions in several services of the International Association of Geodesy (IAG). The results from the basic research (Chapters 1 and 2) enter thereby directly into the application for routine product generation. Within the International Earth Rotation and Reference Systems Service (IERS) DGFI is one of the three official Combination Centres for the realization of the International Terrestrial Reference System (ITRS) as well as a Combination Research Centre (CRC). In the International GNSS Service (IGS) DGFI operates the Regional Network Associate Analysis Centre for Latin America (RNAAC-SIR). For the International Laser Ranging Service (ILRS) DGFI acts as one of the two Global Data Centres (EUROLAS Data Centre, EDC), as an Analysis Centre (AC), and as a Combination Centre (CC). In the International VLBI Service for Geodesy and Astrometry (IVS) DGFI operates an Analysis Centre (AC). DGFI has also got the leading role for the installation of the planned International Altimetry Service (IAS). In IAG's Global Geodetic Observing System (GGOS) DGFI participates in particular in the Working Group on Conventions, Analysis and Modelling. Furthermore DGFI is active in some international projects by operating permanent GPS stations and data analysis, e.g., in the IGS Tide Gauge benchmark monitoring project (TIGA) and the EC INTERREG Alpine Space Project for detection and control of crustal deformations in the Alpine region (ALPS-GPS QUAKENET).

3.1 ITRS Combination Centre / IERS Combination Research Centre

During 2005/2006 the DGFI activities concentrated on the computation of the ITRF2005 solution and the validation of the ITRF2005 results. The establishment of the ITRS Combination Centre at DGFI was supported by the Federal Ministry of Education and Research (BMBF), Grant (IERS)03F0336C within the programme GEOTECHNOLOGIEN of BMBF and DFG.

Margin: Input data sets for ITRF2005

Table 1 displays the characteristics of the ITRF2005 input data. The official GPS, SLR and VLBI single-technique combined solutions were submitted by the Techniques' Combination Centres: NRCan for the International GNSS Service (IGS), the Geodetic Institute of the University Bonn (GIUB) for the International VLBI Service for Geodesy and Astrometry (IVS), and the Agenzia Spaziale Italiana (ASI) for the International Laser Ranging Service (ILRS). Until now, no combined DORIS solution is available from the International DORIS Service (IDS). Two individual solutions of DORIS Analysis Centers (IGN/JPL, LCA) were provided. Besides, the SINEX solutions the Technique Centres also provided information about discontinuities (e.g. equipment changes, earthquakes) in station positions, which are used by the ITRS Combination Centres. Furthermore updated local tie information was provided by the ITRS Product Centre, hosted at the Institute Géographique National (IGN, France).

Tab. 3.1.1: Input data sets for ITRF2005.

Technique	Service AC	Data	Time period	Parameters	Constraints
GPS	IGS NRCan	weekly solutions	1996 - 2005 from June 1999 from March 1999	Station positions EOP (pole rates, LOD) geocenter	NNT: 0.1 mm NNR: 0.3 mm NNS: 0.02 ppb
VLBI	IVS GIUB	24h sessions free NEQs	1984 - 2005	Station positions EOP (pole, UT1 + rates)	none
SLR	ILRS ASI	weekly solutions	1993 - 2005	Station positions EOP (pole + LOD)	1 m
DORIS	IGN LCA	weekly solutions weekly solutions	1993 -2005 1993 - 2005	Station positons EOP (pole, UT1 + rates) Station positions EOP (pole)	loose loose

Combination methodology

The methodology of the ITRS Combination Centre at DGFI is based on combining datum-free epoch normal equations (weekly/24 h data sets) and the common adjustment of station positions, velocities and Earth Orientation Parameters (EOP). The computations are performed with the DGFI Orbit and Geodetic Parameter Estimation Software (DOGS). Figure 3.1.1 shows the data flow and combination methodology, which was applied for the ITRF2005 computation.

Fig. 3.1.1: Data flow and procedure for the ITRF2005 computation.

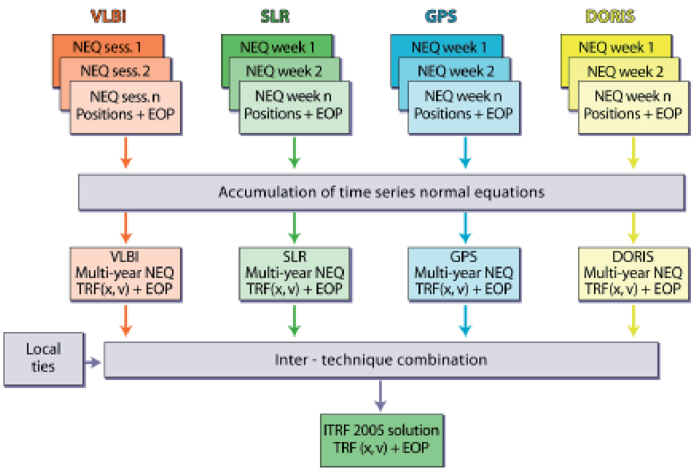

Accumulation of time series solutions

For each technique the epoch normal equations were accumulated separately to compute multi-year solutions with station positions, velocities and EOP. In the case of discontinuities (provided by the Technique Centres) new position and velocity parameters for the corresponding station were introduced. Epoch solutions were computed by applying minimum datum constraints w.r.t. the multi-year solutions. The resulting time series of station positions and datum parameters were analysed in detail. As an example Fig. 3.1.2 shows the time series of weekly position estimates along with the velocity estimations for the GPS station Höfn (Iceland). A discontinuity in the station height of 5 cm was caused by an antenna and receiver change which led to two different solutions on this station. Especially in short time intervals (e.g. less than 2.5 years), annual signals may affect the linear approach with station positions and velocities (see 2.7).

The repeatabilities of the weekly (daily) position estimates provide valuable information to assess the internal accuracy of the space geodetic solutions. The results obtained for the different space techniques using a subset of good reference stations for each technique are summarized in Table 3.1.2.

Fig. 3.1.2: Position time series and velocity estimates for the height component for the GPS station Höfn (Iceland).

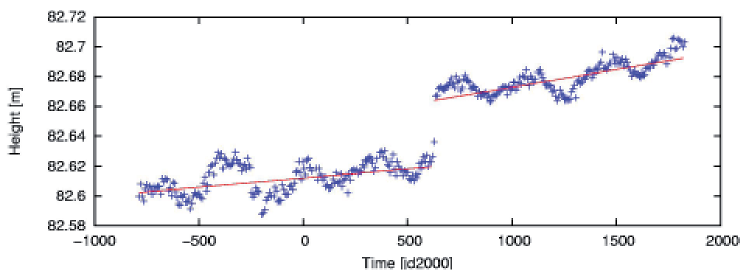

Tab. 3.1.2: Repeatability of station position estimates for different space techniques. Note that in case of VLBI daily sessions were used, whereas the other technique solutions are weekly.

Technique	TC/AC	North [mm]	East [mm]	Up [mm]
GPS	IGS	2.4	3.0	7.8
VLBI	IVS	6.7	6.9	12.5
SLR	ILRS	9.4	9.0	9.7
DORIS	IGN/JPL	24.3	32.3	22.5

Inter-technique combination

Input for the combination of the different space techniques are the accumulated intra-technique normal equations of VLBI, SLR, GPS and DORIS solutions. The parameters comprise station positions, velocities and daily EOP. Concerning the combination of the EOP of the different space techniques it has to be considered that the VLBI estimates are referred to the midpoint of a daily VLBI session (from 17 hr to 17 hr), whereas the EOP values of the other techniques are referred to 12 h. Thus, the VLBI EOP estimates have to be transformed to the reference epochs of the other techniques. A key issue within the inter-technique combination is the implementation of local tie information. For this purpose the EOP are essential to validate the local tie selection and to stabilize the inter-technique combination as additional "global ties" (see 1.2). Other issues include the weighting between different techniques and the equating of station velocities of co-located instruments. The weighting is done by estimating relative scaling factors for the normal equations based on the station position repeatabilities for the different techniques. For equating station velocities at co-location sites, tests are applied to decide whether the velocity estimates are statistically identical or different.

ITRF2005 solution of DGFI

The combined inter-technique normal equations are completed by pseudo-observations for the selected local ties and for equating station velocities at co-location sites. To generate the final combined solution, we add datum conditions and invert the resulting normal equation system. The origin (translations and their rates) is realized by the contributing SLR solutions, and the scale and its rate by SLR and VLBI. The orientation of the ITRF2005 is realized by no-net-rotation (NNR) conditions w.r.t. ITRF2000 using "good" reference stations to ensure consistency with the Bureau International de l'Heure (BIH) orientation at 1984.0. The realization of the orientation rate in the ITRF2005 will be given by an actual plate kinematic and crustal deformation model (APKIM) derived from the geodetically observed station position variations. A new model (APKIM2005) was computed from the ITRF2005 input data (see 2.6).

The final ITRF2005 solution comprises station positions, velocities and daily EOP estimates as primary results. In addition, epoch position residuals and geocenter coordinates are obtained from the time series combination. The reference epoch of station positions is 2000.0. The rather inhomogeneous data quality and quantity of the space geodetic observation stations is reflected in the accuracy and reliability of the ITRF2005 station position and velocity estimations. This holds in particular for a number of

SLR and VLBI stations, but also for some GPS and DORIS stations with few observations. Another aspect is that the new type of ITRF2005 solution contains many stations with several solution IDs. As a consequence the station positions and velocities are valid only for a certain period of time, which has to be known and considered by the users. Furthermore, co-location sites may have different station velocities for co-located instruments, if their estimated velocities differ significantly. Figure 3.1.3 shows, as an example, the station velocities of the DGFI ITRF2005P solution.

Comparison between IGN and DGFI ITRF2005 solutions

Combined inter-technique solutions for ITRF2005 were computed by the ITRS Combination Centres at IGN and DGFI. We performed similarity transformations between both solutions, namely ITRF2005P_IGN and ITRF2005P_DGFI. These transformations were done for each space technique separately by using good reference stations. Most of the transformation parameters agree within their estimated standard deviations, except for the scale and its rate of the SLR network, for which a significant difference of about 1 ppb (offset) and 0.13 ppb/yr (rate) between the DGFI and IGN solution was found. The RMS differences for station positions and velocities show that both ITRF2005 solutions are in general in a very good agreement (see Tab. 3.1.3).

Tab. 3.1.3: RMS differences for station positions and velocities for the reference frame stations (25 VLBI, 22 SLR, 57 GPS, 40 DORIS).

ITRF2005P IGN - DGFI	VLBI	SLR	GPS	DORIS
Position [mm]	± 0.79	± 1.82	± 0.31	± 3.32
Velocities [mm/yr]	± 0.34	± 0.66	± 0.14	± 1.11

Thus the major problem in the ITRF2005 is the significant difference in the SLR scale. The analysis of weekly SLR solutions in 2006 showed that the scale is in reasonable good agreement with the ITRF2005P solution of DGFI, whereas there is a significant scale bias of about 2 ppb w.r.t. the IGN solution (see Fig. 3.1.4), which is equivalent to a difference of 1.3 cm in SLR sta-

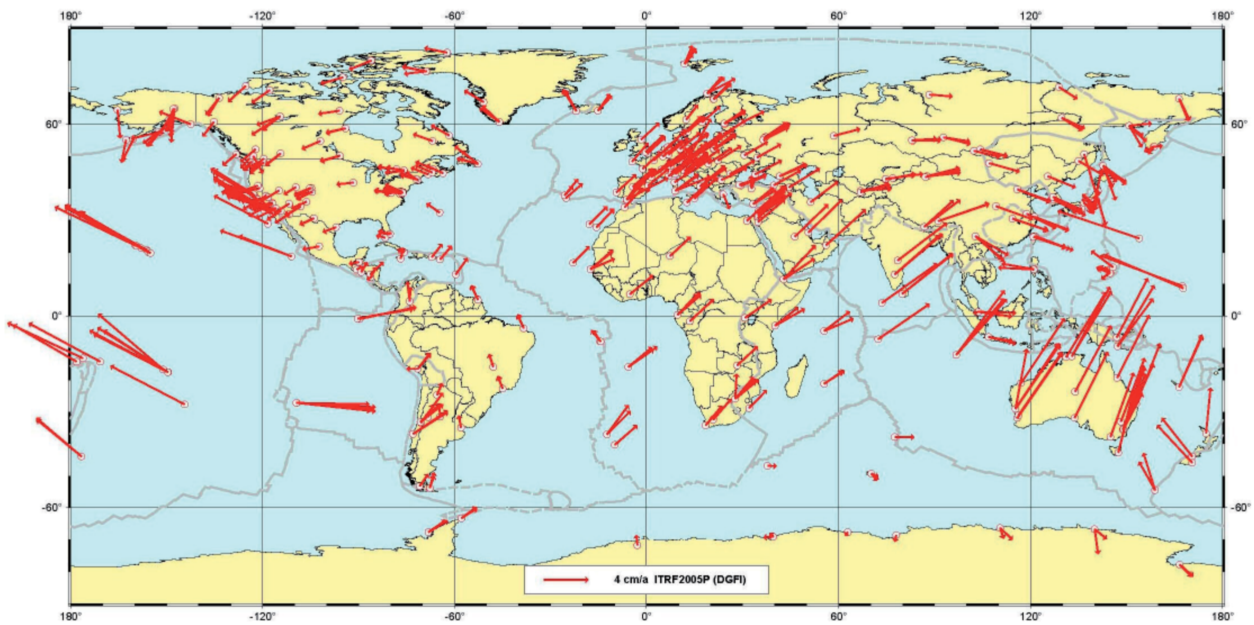

Fig. 3.1.3: Horizontal station velocities of the ITRF2005 (DGFI) solution.

Fig. 3.1.4: Scale of ITRF2005P solutions of IGN and DGFI w.r.t. weekly combined SLR solutions (ILRSA).

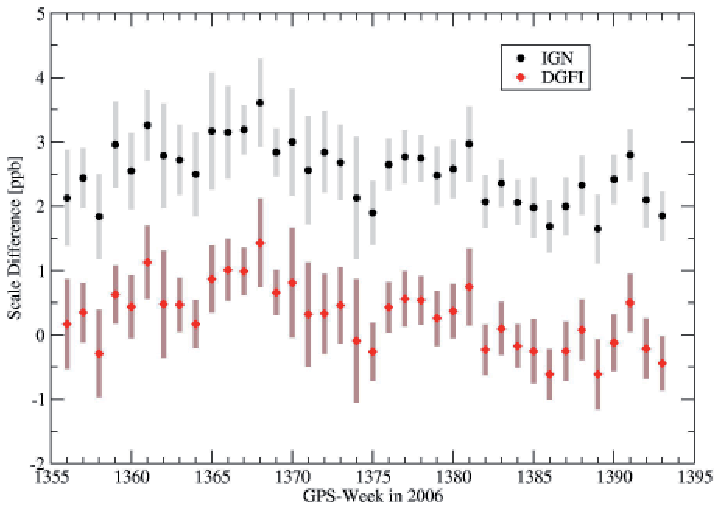

tion heights. It was argued by IGN that this "scale problem" is a consequence of a scale bias between VLBI and SLR, and the ITRF2005 scale of the IGN solution was realized by VLBI only.

Investigations on the ITRF2005 scale of VLBI and SLR

We used the intra-technique solutions of the DGFI combination for ITRF2005 to investigate the scale of VLBI and SLR. Since the number and spatial distribution of good co-location sites between VLBI and SLR is not sufficient to get reliable results for a direct comparison of the scale, we used an "indirect" approach via the GPS network and we consider the GPS intra-technique solution as reference for this specific study. We used "good" co-location sites and local ties to refer the VLBI and SLR solutions to the "arbitrary" GPS reference frame (see Fig. 3.1.5). This was done by adding the local tie measurements to the SLR and VLBI station coordinates; thus these "transformed" station coordinates refer to the GPS markers for the respective co-location sites. Then we performed 14-parameter similarity transformations between the "transformed" VLBI and SLR solutions and the GPS solution. The station position residuals for the 18 co-location sites between GPS and VLBI as well as for the 16 co-location sites between SLR and GPS are shown in Fig. 3.1.6 and 3.1.7.

Fig. 3.1.5: Co-location sites used for the integration of VLBI and SLR solutions w.r.t. GPS.

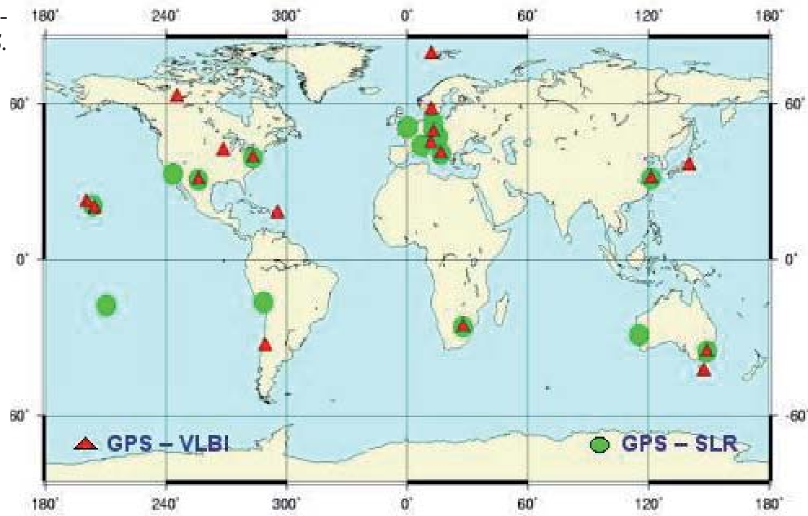

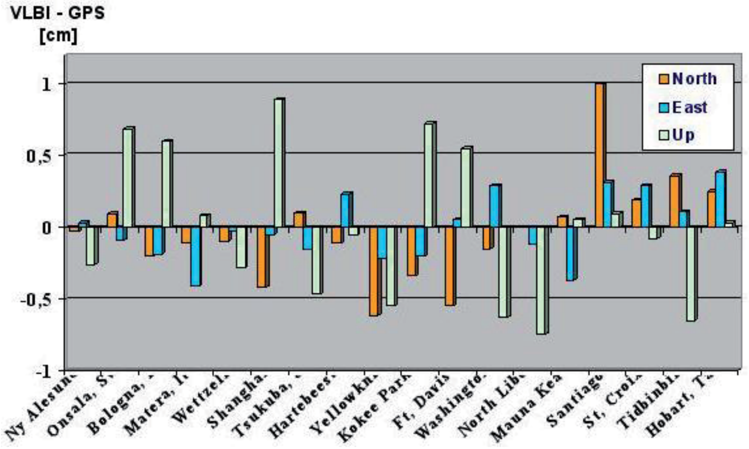

Fig. 3.1.6: Station position residuals at 18 co-location sites of VLBI and GPS (r.m.s. of residuals is 2.9 mm).

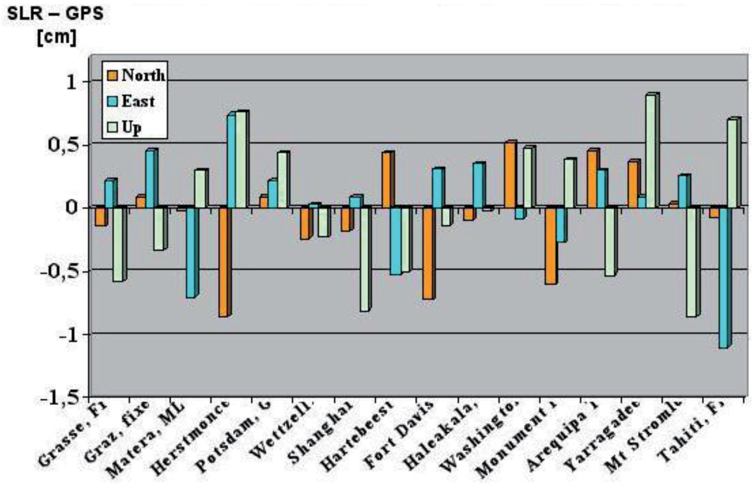

Fig. 3.1.7: Station position residuals at 16 co-location sites of SLR and GPS (r.m.s. of residuals is 3.6 mm).

The scale parameters obtained from the similarity transformations of the SLR and VLBI solutions w.r.t. GPS are arbitrary numbers, but the difference of the scale parameters is independent from the "arbitrary" GPS scale. The estimated scale difference between VLBI and SLR is 0.26 ± 0.41 ppb for the offset and 0.03 ± 0.09 ppb/yr for the drift. Thus the results of the DGFI ITRF2005P solution do not indicate any evidence for a scale bias between VLBI and SLR.

3.2 IGS Regional Network Associate Analysis Centre for SIRGAS

The DGFI has acted as an IGS Regional Network Associate Analysis Centre for Latin America (IGS RNAAC SIR) for more than ten years. Weekly coordinate solutions including all available observations of this network are generated and delivered to the IGS Global Data Centres.

RNAAC SIR network status

During the ten years of RNAAC SIR processing, the number of included stations increased from 12 stations in 1996 to 120 by the end of September 2006 (see fig. 3.2.1). Some of the stations ceased operation, and some delivered their data not always in time for the processing. Therefore the average number of processed stations in the weekly free network adjustment is between 85 and 90. The number of participating stations will still increase dramatically, especially in Argentina, Brazil and Colombia.

Changes in processing of the weekly coordinate solutions

The IGS RNAAC SIR processing at DGFI is presently done with the Bernese Processing Engine, version 5.0 (BPE). The elevation cutoff angle was set from previously 5° to 3°. In parallel the processing with the BPE version 4.2 is still continued for analysing the resulting differences between both versions.

Weekly position solutions

DGFI is providing weekly position solutions as support to all South and Central American countries. These solutions are referred to IGb00 by applying no net rotation and translation conditions to nine selected stations.

New position and velocity solution DGF06P01

A new accumulated solution DGF06P01 was computed including data from June 30, 1996 to June 17, 2006 (GPS weeks 0860 to 1379). It provides positions of 85 stations and velocities of 71 stations which have contributed to at least 52 weekly solutions. The details of the processing are as in the previous solution DGF04P01. The reference epoch is 2004.0.

Figures 3.2.1 and 3.2.2 show the horizontal and vertical velocities compared to the DGFI preliminary ITRF2005PD solution.

Experimental Analysis Centres for SIRGAS

At the last workshop of the SIRGAS Working Group I “Reference System” in Rio de Janeiro, August 16-18, 2006, it was decided to install Experimental Analysis Centres (EAC) for SIRGAS under the responsibility of Latin American institutions. The test phase of the one-year experiment will start in October 2006, in order to prove the operational capacity of the EACs to provide weekly station coordinate solutions and to support the IGS RNAAC SIR processing.

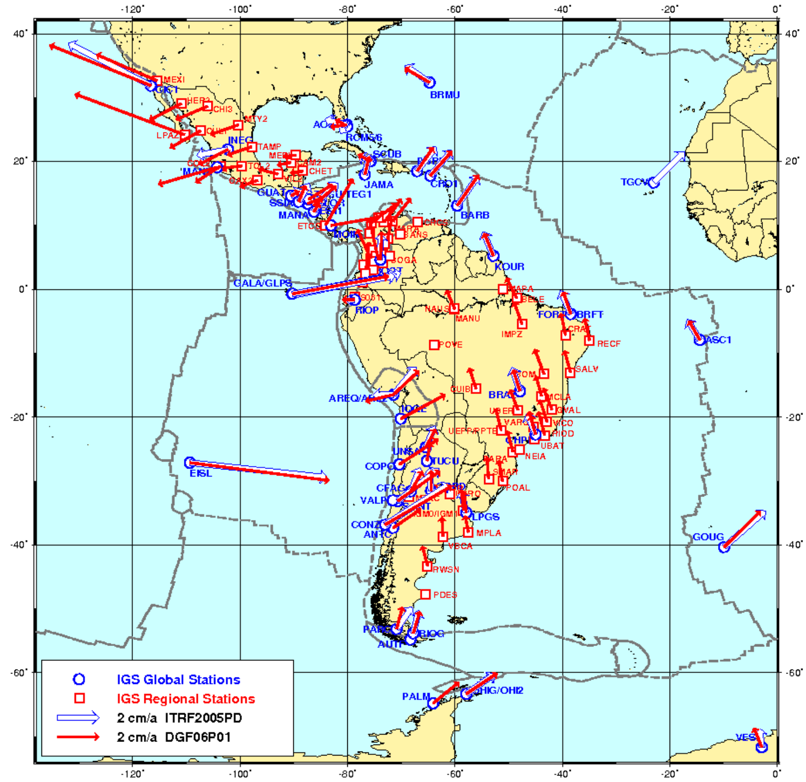

Fig. 3.2.1: IGS RNAAC SIR network and horizontal velocities from solution DGF06P01.

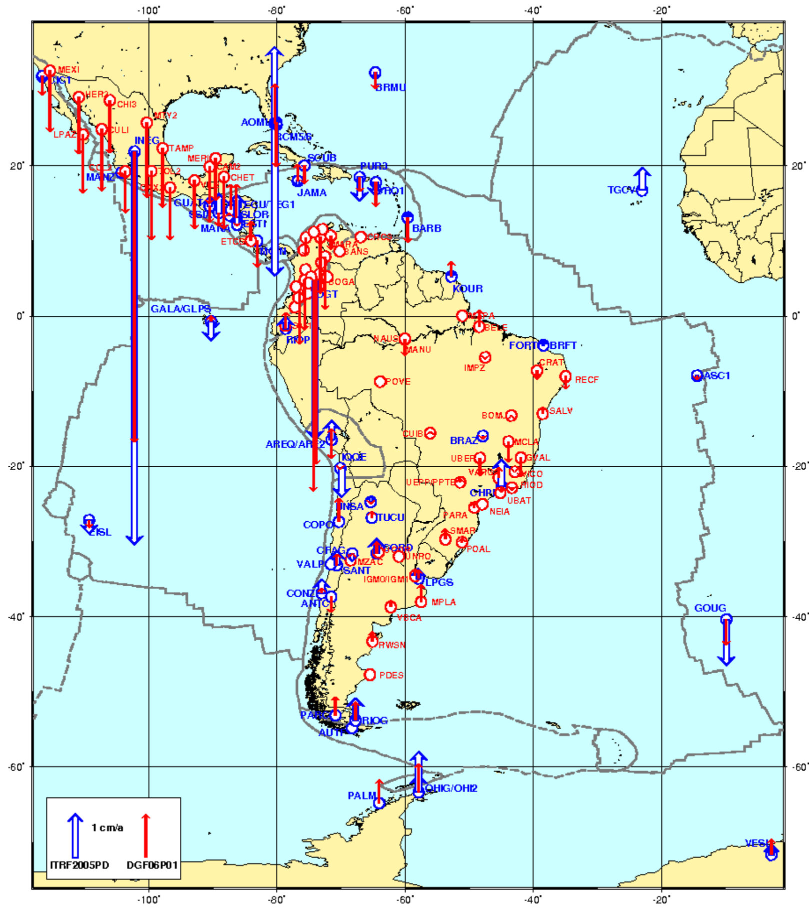

Fig. 3.2.2: Vertical velocities of IGS RNAAC SIR stations from solution DGF06P01.

3.3 Continuously operating GPS stations

DGFI operates 13 GPS permanent stations in cooperation with different national organizations in South America and Europe. The stations are installed in such a way that they are remotely controlled as far as possible. In some cases, the observational data present gaps (figure 3.3.1) due to the poor technical infrastructure at specific sites (e.g. CART, TORS) or due to extreme weather conditions, which even damaged the communication equipments of the stations through lightning (e. g. HRIE, BRIE).

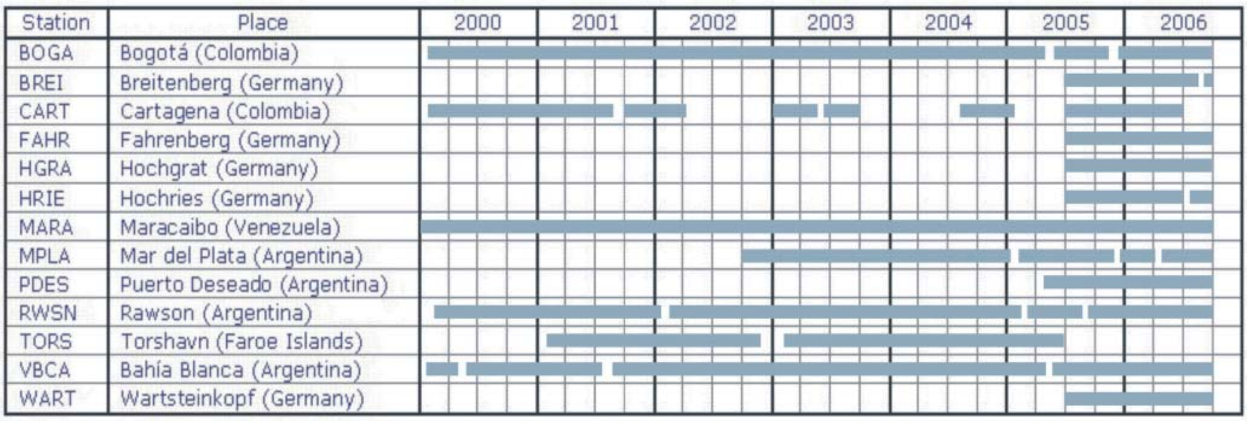

Fig. 3.3.1 Operational performance of the GPS permanent stations installed by DGFI.

All the permanent stations operated by DGFI are integrated in specific projects such as the IGS TIde GAuge benchmark monitoring project (TIGA), the EC INTERREG IIIB Alpine Space crustal deformation project (ALPS-GPS QUAKENET), the densification of the international reference frame (RNAAC-SIR, see Theme 3.2), and the definition and realization of vertical reference systems (SIRGAS-WGIII, see Theme 1.6).

TIde GAuge benchmark monitoring project

DGFI contributes to the TIGA project of the International GNSS Service (IGS) by operating some GPS permanent stations at (or close to) tide gauges and by processing a network of 54 sites covering the entire North and South Atlantic (figure 3.3.2). This network is weekly processed with the Bernese GPS Software v. 5.0 following the general IGS strategy. Since October 2005, it was decided to introduce absolute calibration values for the antenna phase centre corrections. To get reliable height positions and velocities of the included stations, the weekly solutions computed previously with relative phase centre corrections (from March 2000 until September 2005) were reprocessed. The SINEX files of the free net adjustment are provided to the TIGA Associated Analysis Centres (TAAC) and to other users through the web site http://adsc.gfz-potsdam.de/tiga/index_TIGA.html.

Tab. 3.3.1: Differences between the velocities obtained from DGFI06P01T and IGb00.

Station	North [mm/yr]	East [mm/yr]	Up [mm/yr]
CHUR	1.8	0.4	-0.2
CRO1	2.8	-2.9	3.2
FORT	0.6	-1.5	-0.9
GOUG	-0.9	-0.2	4.0
NKLG	-0.3	-0.1	-1.6
OHI2	2.7	-1.7	-2.2
STJO	0.4	-0.1	-0.7
Mean	1.0 ± 1.4	-0.9 ± 1.2	0.2 ± 2.4

A multi-year solution (DGF06P01T) of this network was computed from almost 300 daily solutions, which are regularly distributed over the six years of data analysis. Stations with short time series (less than 2 years) were excluded. The geodetic datum being defined by constraining ten IGS global stations to their IGb00 values. Table 3.3.1 presents the differences between the velocities of DGFI06P01T and IGb00 for those common stations that were not included as fiducials for the datum definition.

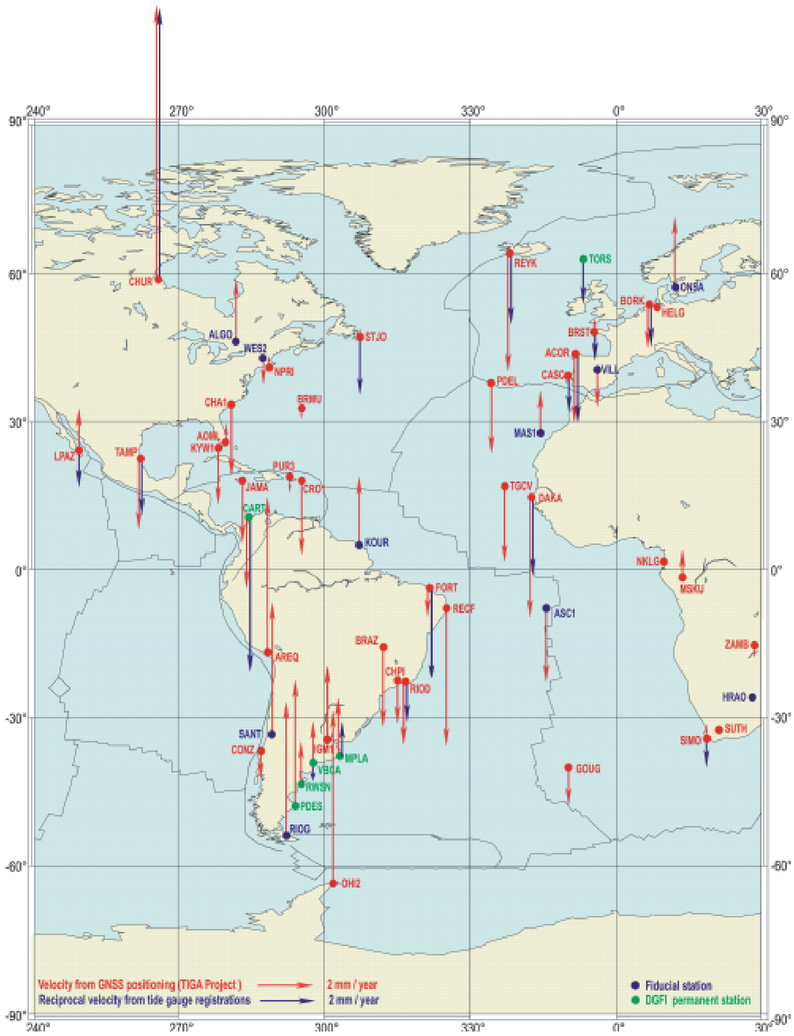

Fig. 3.3.2 GPS network processed at DGFI within the TIGA Project. The vertical velocities of the solution DGFI06P01T are compared with the reciprocal height velocities derived from tide gauge records.

The obtained vertical velocities are compared with those derived from the tide gauge registrations provided by the PSMSL (Permanent Service for the Mean Sea Level, http://www.pol.ac.uk/psmsl/). These comparisons (table 3.3.2) allow to distinguish vertical displacements of the Earth's crust (in which the tide gauges are embedded) from secular sea level changes. The true sea level change is the sum of the velocity recorded by the tide gauge and the vertical crustal movement observed by GNSS. Assuming that the obtained velocities are linear, we can reduce both, the geometrical position of the tide gauge rods, and the registered sea levels to the same epoch. In this way, the unification of the classical height systems will be feasible with high accuracy.

Besides the well-known problems associated to the measurements at tide gauges because of their regional locations (bays, creeks, etc.), the time periods covered by the different kinds of data (GNSS positioning and tide gauge observations) included here are not identical (figure 3.3.3). Therefore, it is necessary to complement these results by integrating the sea surface variations derived from the satellite altimetry data analysis (see Theme 2.3).

Tab. 3.3.2: Comparison of the vertical velocities derived from tide gauge records and the solution DGF06P01T.

Site	Tide Gauge Records		DGF06P01T	Sum [mm/yr]
	Period	dh/dt [mm/yr]	dh/dt [mm/yr]	
ACOR	1992 - 2003	2,3 ± 1,9	-2,4 ± 0,1	-0,1
BORK	1949 - 1986	1,2 ± 0,5	-1,5 ± 0,0	-0,3
BRST	1807 - 2004	1,0 ± 0,0	0,4 ± 0,2	1,4
CART	1949 - 1993	5,3 ± 0,1	-2,5 ± 0,2	2,8
CASC	1882 - 1993	1,3 ± 0,0	-0,2 ± 0,0	1,1
CHUR	1940 - 2003	-9,7 ± 0,2	9,8 ± 0,0	0,1
DAKA	1992 - 2003	2,9 ± 1,0	-4,3 ± 0,1	-1,4
FORT	1948 - 1968	3,3 ± 0,7	-1,0 ± 0,1	2,3
HELG	1951 - 1986	0,1 ± 0,5	0,1 ± 0,2	0,2
LPAZ	1952 - 1984	1,3 ± 0,3	1,5 ± 0,3	2,8
MPLA	1957 - 1980	-1,3 ± 0,5	2,1 ± 0,1	0,8
PDES	1912 - 1995	0,0 ± 0,6	4,5 ± 0,6	4,5
RECF	1948 - 1968	-0,2 ± 0,4	-4,9 ± 0,2	-5,1
REYK	1951 - 2003	2,5 ± 0,2	-4,2 ± 0,0	-1,7
RIOD	1949 - 1968	1,4 ± 1,0	-2,2 ± 0,1	-0,8
SIMO	1956 - 1996	1,1 ± 0,1	0,5 ± 0,1	1,6
STJO	1935 - 2003	2,1 ± 0,2	0,2 ± 0,1	2,3
TAMP	1952 - 1966	1,9 ± 3,1	-2,5 ± 0,3	-0,6
TORS	1957 - 2002	1,6 ± 0,2	0,1 ± 0,1	1,7
VBCA	1914 - 1938	0,7 ± 0,5	1,4 ± 0,1	2,1
Mean				0,7± 2,1

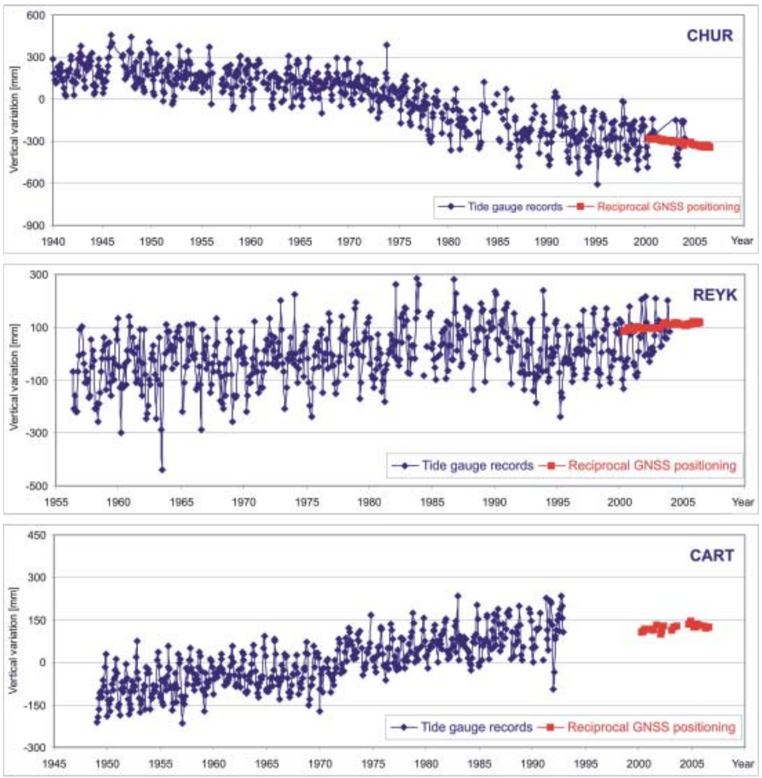

Fig. 3.3.3: Vertical variations derived from tide gauge registrations and GNSS positioning at some TIGA stations.

EC CIP INTERREG IIIB: Alpine Space Programme, Project ALPS-GPS QUAKENET

DGFI is involved, together with nine other institutions in Italy, Germany, France and Slovenia, in the ALPS-GPS QUAKENET Project, which is a component of the Alpine Space Programme established in the frame of the European Community Initiative Programme (CIP) INTERREG IIIB. The main objective of the ALPS-GPS QUAKENET project is to study crustal deformations in near real-time in order to improve natural disaster prevention in this region. To this end, a GPS permanent network composed of 30 sites was installed. Five of these stations, located along the northern Alps boundary, are provided and managed by DGFI (figure 3.3.4). They were established on stable bedrock in altitudes of 1600 m to 2000 m to represent the motion of the surrounding region. The observation data are directly transferred to the operation data centre at DGFI and then copied to the GPS QUAKENET project data base in Trieste, Italy. Three data processing centres process and analyse the data. The results will be used to formulate a continental deformation model in the Alps Region for earthquake hazard reduction, landslides monitoring and meteorology effects.

Fig. 3.3.4: Northern part of the ALPS-GPS QUAKENET network (DGFI stations).

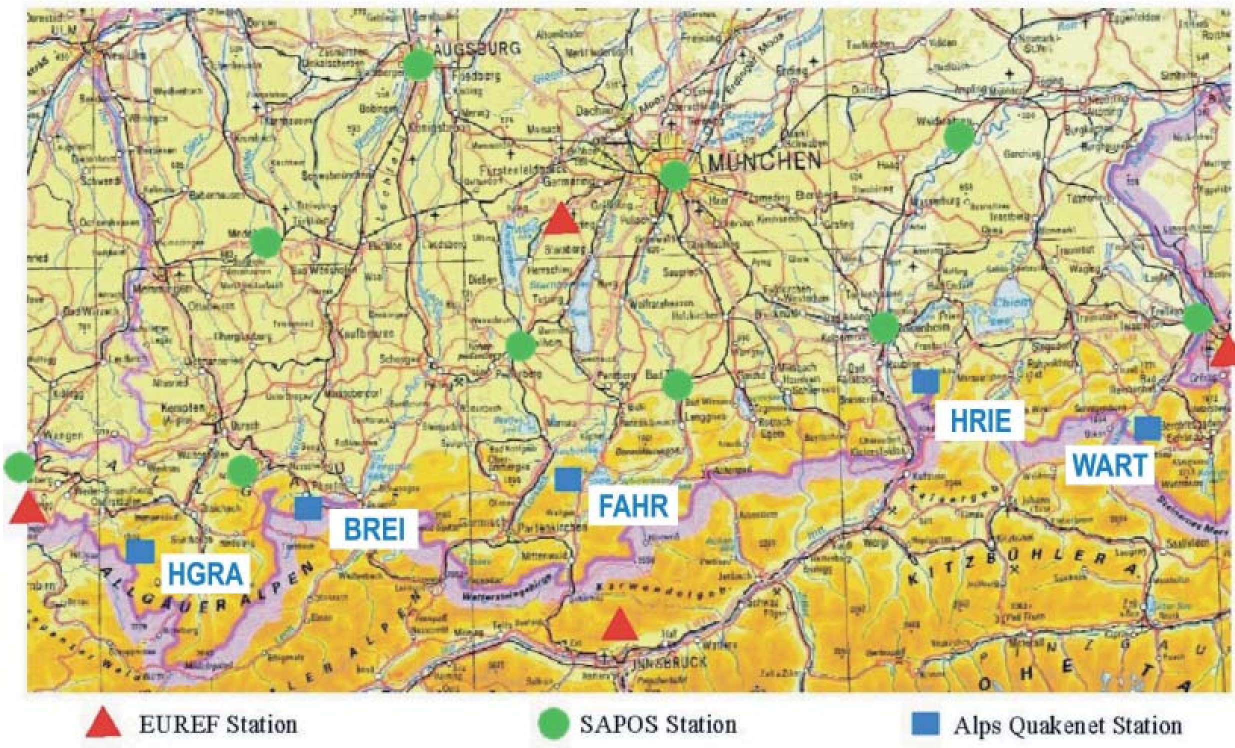

3.4 ILRS - International Laser Ranging Service

DGFI has contributed for a long time to the ILRS global SLR (Satellite Laser Ranging) network processing as

- Data Centre,
- Analysis Centre,
- Combination Centre (backup).

The ILRS Analysis Working Group (AWG) supervises all computations using SLR tracking data which produce offical ILRS products.

ILRS Global Data Centre / EUROLAS Data Centre

DGFI runs the ILRS Global Data Centre as the EUROLAS Data Centre (EDC). Another ILRS Global Data Centre is hosted by CDDIS/NASA.

Since November 1995 the SLRmail and SLReport exploders at EDC distributed 1497 SLRmails (113 during the last 12 month) and 7606 SLRreports (1551) to the permanently updated distribution lists. The exploder URGENT Mail circulated 98 e-mails (43) since August 15, 2003.

The ILRS Data Format and Procedures Working Group agreed to develop a new so-called Consolidated Prediction Format (CPF), which was confirmed by the ILRS Governing Board. These CPF predictions became necessary to track the upcoming transponders. Therefore new ftp directories had to be installed for these CPF predictions and for developing new prediction exploders. The old IRV predictions are still distributed until all SLR stations will have switched over to the new format. To avoid double distribution predictions (e.g. with the IRVs), it was decided which of the different prediction providers for the CPFs is the primary or backup CPF provider for the different satellites (see fig. 3.4.1).

Observation Campaigns

The ETALON-1/2, ENVISAT and LARETS campaigns are continued, a new GIOVE-A campaign was appointed.

Observed Satellite Passes

In the time period from September 01, 2005 to September 30, 2006, 35 SLR stations observed 33 satellites (including the four moon reflectors). Table 3.4.1 shows the EDC data base content at September 30, 2006. This content is compared with that of the CDDIS data base and has to be updated at EDC and/or CDDIS due to missing data.

Figure 3.4.1: Primary/backup Consolidated Prediction Format (CPF) provider.

SATELLITE	HTSI	NSGF	CODE	ESOC/ ESA	GFZ	GSFC	JAXA	MCC
AJISAI	P	B					B	
BEACON-C	P							
CHAMP					P			
ENVISAT	B			P				
ERS-2	B			P				
ETALON-1, -2	P	B						
GFO-1	B					P		
GIOVE-A, -B				P				
GLONASS	B		P					
GP-B	P							
GPS	B		P					
GRACE-A, -B					P			
JASON-1	P	B						
LAGEOS-1, -2	P	B					B	
LARETS	P	B						B
METEOR-3M	B					P		
OICETS							P	
STARLETTE	P	B						
STELLA	P	B						

Note: P - primary CPF provider, B - backup CPF provider in red: not ready

Table 3.4.1: Contents of ILRS/EDC data base at September 30, 2006 for the product normal points (including Lunar Laser Ranging (LLR) observations to four moon reflectors).

Satellite	number of passes		Satellite	number of passes		Satellite	number of passes	
	increase 06	2006		increase 06	2006		increase 06	2006
ADEOS		671	GLONASS-69		945	ICESAT	1695	2270
AJISAI	11694	104007	GLONASS-70		1430	JASON-1	8770	35355
ALOS	91	91	GLONASS-71		2617	LAGEOS-1	9983	78877
BEACON-C	6455	43995	GLONASS-72		3260	LAGEOS-2	9184	69565
CHAMP	1762	9672	GLONASS-74		39	LARETS	4701	11737
DIADEME-1C		1393	GLONASS-75		300	LRE/H2A		75
DIADEME-1D		1585	GLONASS-76		301	METEOR-3		409
ENVISAT	6175	24178	GLONASS-77		343	METEOR-3M	180	1756
ERS-1		10524	GLONASS-78		2712	MOON-1	13	397
ERS-2	6407	54744	GLONASS-79		3237	MOON-2	11	309
ETALON-1	1806	12591	GLONASS-80		4466	MOON-3	59	2446
ETALON-2	1874	12780	GLONASS-81		275	MOON-4		594
FIZEAU		4243	GLONASS-82		244	OICETS	115	115
GEOS-3		2237	GLONASS-84		6442	REFLECTOR		3728
GFO-1	5888	33081	GLONASS-86	23	1255	RESURS-01-3		2011
GFZ-1		5606	GLONASS-87	2110	6756	STARLETTE	9452	78855
GIOVE-A	410	410	GLONASS-88		114	STARSHINE-3		48
GLONASS-62		963	GLONASS-89	1711	5559	STELLA	4813	48558
GLONASS-63		1952	GLONASS-95	1530	1536	SUNSAT		1864
GLONASS-64		81	GPS-35	889	6626	TIPS		1849
GLONASS-65		397	GPS-36	754	5901	TOPEX/POS.	1435	86423
GLONASS-66		1544	GRACE-A	2387	8633	WESTPAC-1		5620
GLONASS-67		4299	GRACE-B	2304	7844	ZEIA		146
GLONASS-68		875	GRAVITY PROBE-B	1453	3156	Sum of all	106134	840620

ILRS Analysis Centre

An ongoing task is the weekly processing of the SLR tracking data to the geodetic satellites Lageos-1/2 and Etalon-1/2, which runs mostly automated. The solutions contain station positions and Earth orientation parameters (pole coordinates and LOD). The results are delivered as SINEX files to the ILRS data centres CDDIS and EDC. This processing includes the processing of pass-dependent biases, which are published in the DGFI Homepage http://www.dgfi.badw.de/dgfi/ILRS-AC/quality/index.html.

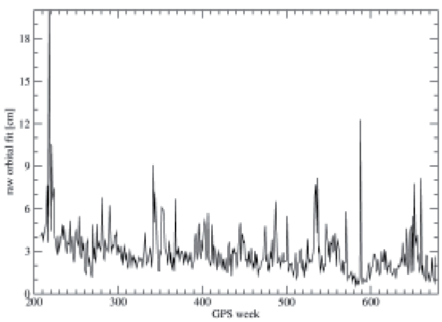

Fig. 3.4.2: Raw weekly orbital fit for Lageos-1 from 1984 to 1992.

An additional task in this year was the preparation of the backward compution of SLR data to 1984. Therefore the existing normal points from various sources were compared, and a reliable data set of Lageos-1 normal points was provided. To verify the quality of these data, all weeks from 1984 to end 1992 were processed. In figure 3.4.2 the raw weekly rms fit of the Lageos-1 orbits over this period is shown, without extra screening of the data, only blunders were eliminated. The figure shows that the quality of data prior to 1993 is significantly worse than the present one with an orbital fit of below 1 cm, though the accuracy of the older data could be improved by carefull data screening.

The ITRF2005 solutions from IGN and DGFI show a significant difference for the scale of the SLR network (see 3.1). It was found that the actual SLR results are consistent with the ITRF2005 solution of DGFI, whereas there is a bias of about 2 ppd compared to the IGN solution. Further test computations were performed by the ILRS Analysis Centre of DGFI. To test the effect of this scale difference on the actual computations we computed a Lageos-1 arc during October 1-7, 2006 with fixed station coordinates. In a first step we solved for one range bias per pass. The biases referring to the IGN solution differed from those computed with the DGFI solution and with ITRF2000 in the same way. In a second step we did not solve for any bias and compared the resulting orbits. The scale difference of (equivalent to 1.1 cm) is not visible completely in the radial orbit component, but a slight drift in the along-track component indicates that parts of the difference moved into other arc dependent parameters (fig. 3.4.3).

Fig. 3.4.3: Comparison of Lageos-1 orbit with station coordinates fixed to ITRF2005 solutions of IGN and DGFI, respectively, in the period October 1-7, 2006.

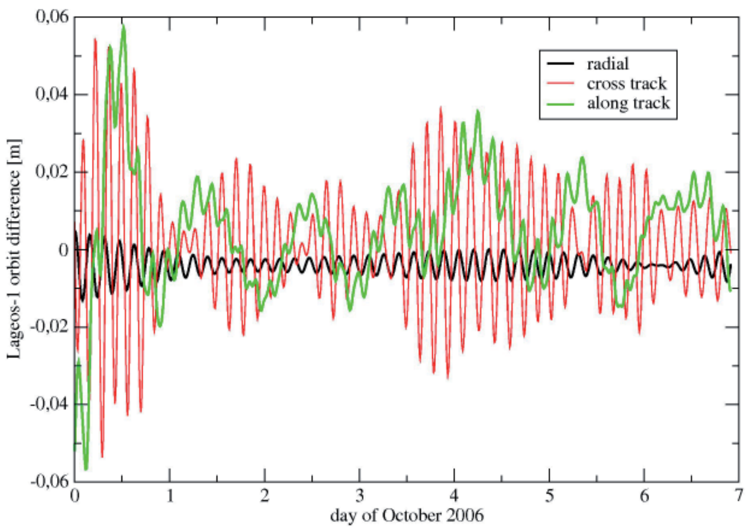

Fig. 3.4.4: Relative range bias between red and blue Laser at the SLR tracking station Zimmerwald.

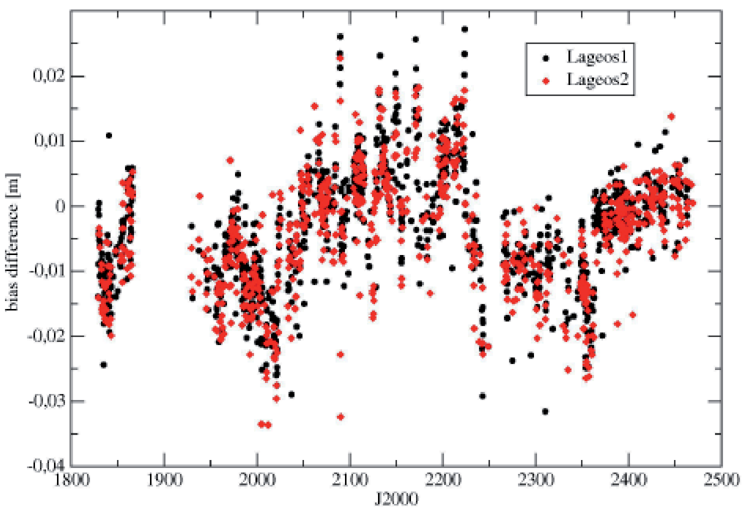

The Zimmerwald SLR station requested to validate the new calibration scheme for their two-frequency Laser. Therefore we reprocessed all Zimerwald SLR tracking data since January 2005, solving simultaneously for station coordinates and a range bias for the blue and one for the red Laser. The bias difference between red and blue is a measure for the calibration quality and should contain only the different tropospheric delay, which is very small. As shown in figure 3.4.4, the switch to a new external calibration on June 21, 2006 (J2000: 2364) reduced the relative bias between the two colours significantly.

ILRS Combination Centre (ILRSB)

DGFI as the official ILRS Backup Combination Centre (ILRSB) continued to routinely process weekly combination solutions and to store them at CDDIS and EDC. New features of the software and the processing are described in Theme 1.4.

ILRSB also contributed to the validation of ITRF2005 solutions. Weekly combined solutions from 1993 to 2006 were computed w.r.t. ITRF2000 (routine solutions), to ITRF2005D (DGFI solution), and to ITRF2005 (IGN solution). The most crucial topic was the handling of the SLR scale in ITRF2005. DGFI used the SLR and the VLBI input data for fixing the scale, whereas the scale of the IGN solution is defined by VLBI only. The figures 3.4.5a to 3.4.5c reveal that the ITRF2005 (IGN) scale leads to an offset of about -2 ppb for 2006, whereas the other two solutions fit much better to the actual SLR observations.

Fig. 3.4.5a: Scale after Helmert transformation of the input and ILRSB solutions with resprect to ITRF2000 for year 2006.

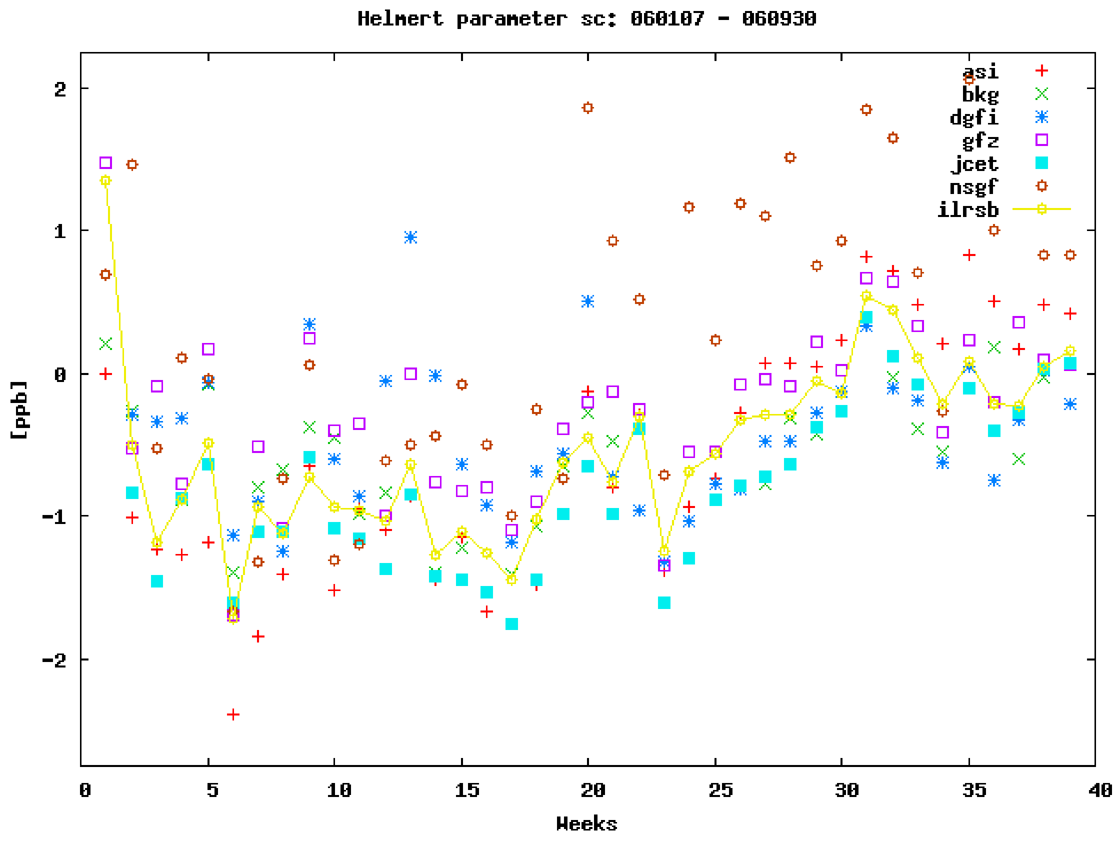

Fig. 3.4.5b: Scale after Helmert transformation of the input and ILRSB solutions with respect to ITRF2005D (preliminary solution of DGFI) for year 2006.

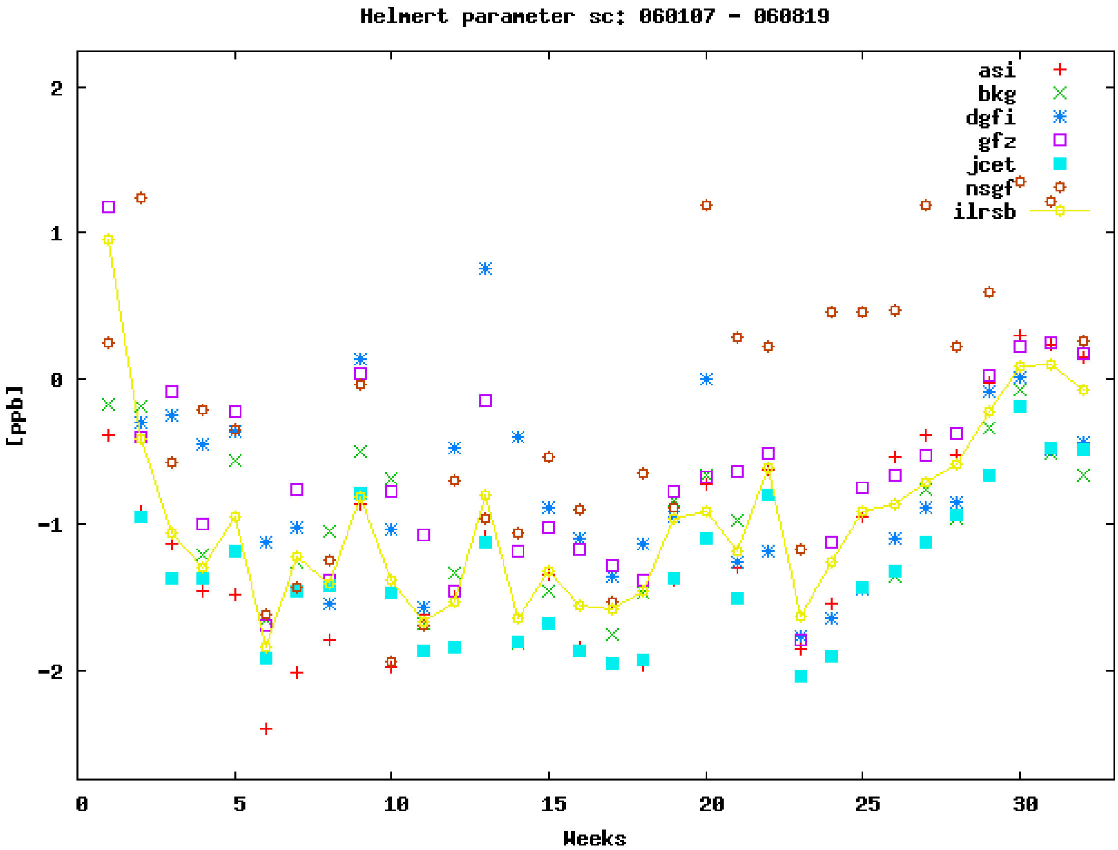

Fig. 3.4.5c: Scale after Helmert transformation of the input and ILRSB solutions with respect to ITRF2005 (official solution of IGN) for year 2006.

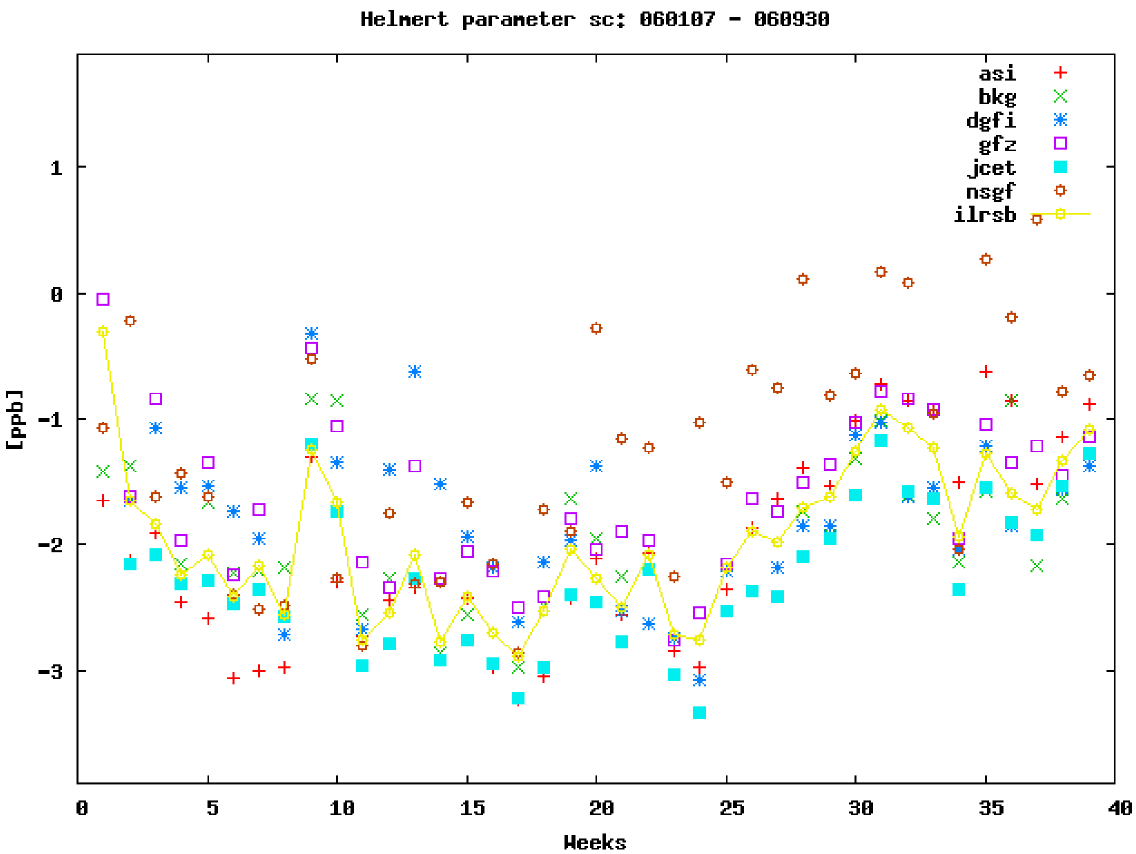

3.5 IVS Analysis Centre

IVS OCCAM working group

The VLBI software OCCAM is the central tool for DGFI's work as IVS Analysis Centre. It is maintained, refined and adapted to the current requirements in close collaboration within the IVS OCCAM Working Group, chaired by Oleg Titov, Geoscience Australia (Canberra, Australia). Leading members are scientists from the Vienna University of Technology, Austria, the St. Petersburg University and the Institute of Applied Astronomy, Russia, and DGFI. The actual version 6.0 of the software was released in February 2004 during the IVS General Meeting in Ottawa, Canada. Since then, especially the code solving the equation systems with the least squares approach was updated in many parts, mostly in very close cooperation with the Vienna University of Technology.

IVS VLBI contribution to the ITRF2005

The release of the ITRF2005 in October 2006 is a major step towards more consistent, routinely generated IERS products (for details see 3.1). The DGFI IVS Analysis Centre contributed to this effort in two different ways: Firstly, SINEX files for 2666 daily sessions between 1984 and 2005 were submitted to the IVS, which is now maintained on a quasi operational basis. These files contain the Earth orientation parameters and station positions for each 24-hour session as decomposed normal equations in the SINEX format. To test the procedure of the IVS Analysis Coordinator (GIUB, Geodetic Institute of the University Bonn) for the VLBI intra-technique combination, several test solutions series were also submitted. This was a special project as GIUB uses DGFI's software package DOGS-CS (see also 1.4 and 3.1).

Secondly, the two independent solutions of the ITRF2005, computed by DGFI and the IGN (Institut Géographique National, France) were validated before the official release. This enabled to compare geodetic results computed with OCCAM (EOP, station position time series) using the two indenpendent ITRF2005 solutions as a reference. It turned out that the VLBI parts of both ITRF2005 solutions were quite well adapted to VLBI-only results and did not differ significantly.

Towards a new realization of the International Celestial Reference Frame (ICRF)

Today, the International Celestial Reference System (ICRS) is realized by the coordinates of several hundred radio sources observed by VLBI (for the last realization "ICRF-Ext1", data until 1998 were used). The IERS as well as the IVS aim for a new realization of the ICRS in the next years, which shall, if feasible, be generated by combining several VLBI solutions. To be able to better understand expected systematic differences, the effect of various analysis options on VLBI determined CRF (celestial reference frames) were investigated in detail by comparing 13 CRF solutions computed with the VLBI software OCCAM 6.1 (least-squares method), using 2847 daily sessions between 1984 and 2006. For details see topic 1.3.

3.6 Planning and realization of an International Altimeter Service

In 2003 a Planning Group for the International Altimeter Service (IAS-PG) was initiated by a call of C.K. Shum, Phil Woodworth, Gary Mitchum and Wolfgang Bosch (chair). The group, hosted by IAG's Commission 1 "Reference Frames", studies the rationale, feasibility and scope of an International Altimeter Service (IAS) and develops an implementation plan for it. IAS-PG got formal endorsements for the establishment of an International Altimeter Service (IAS) by

Endorsements by GLOSS, IAG IAPSO

- Global Sea Level Observing System GLOSS (IOC),
- International Association of Geodesy, IAG,
- International Association of the Physical Sciences of the Oceans, IAPSO.

As the IAS-PG is not funded, discussions were organized by business meetings, a mailing list (now suspended because of massive spam mail), and a so called 'WIKI', a collaborative web site, see `http://www.dgfi.badw.de/wiki`. Business meetings were held in Paris (Oct 2003), Nice (Apr 2004), Vienna (Apr 2005), Cairns (Aug 2005), and Venice (March 2006).

Conclusions of IAS-PG

The most important results of the work performed so far within the IAS Planning Group are summarized by the conclusions in the text box below.

- There is a general agreement that an International Altimeter Service (IAS) is necessary and should be created as soon as possible.
- The IAS shall integrate the envisaged altimetry services into the Global Earth Observing System of Systems (GEOSS) and let altimetry become an essential element of Global Ocean and Geodetic Observing Systems (GOOS, GGOS).
- IAS shall provide a unique point-of-contact for altimeter users and support all applications of satellite altimetry, including, for example, applications for oceanography, coastal zones, hydrology, geodesy, cryosphere.
- IAS shall support calibration and validation activities, assess data and product quality, and recommend improvements for generation and delivery of data and products.
- IAS will not replace but be based on the voluntary contribution of the many existing data, analysis, and product centres already providing service functions. Thus, IAS will have to coordinate a network of centres. User request are to be re-directed to and resolved by these centres, which keep the desired data.
- IAS must ensure that intellectual property rights remain with and proper referencing is made to the generating node, whenever data, products or algorithms are provided or used in publications.
- A unification of data formats is neither feasible nor desirable. Instead, IAS shall provide generic tools, which keep the necessary meta data to inform about data content and allow extracting data with content and format upon user request.
- IAS shall integrate and share distributed resources (data bases) from multiple institutions, each with their own policy and mechanism on the bases of standard, open, and general-purpose protocols and interfaces.

Terms of References of IAS-PG

For the Venice meeting, Terms of References (ToR) for the envisaged IAS were drafted. The ToR designed an Executive Committee, responsible for decisions, policies, control and coordination, and representation to external organizations and a Central Bureau for the day-to-day operation, running an Information Centre, publishing documents, and organizing meetings. Together with the ToR, a preliminary call for participation was issued seeking proposals for data and analysis centres and addressing in particular the need for an organization with sufficient resources to host the Central Bureau.

No one to host the Central Bureau

Before the Venice meeting there were a few groups who indicated their general interest. The discussion at the Venice splinter meeting, however, was controversial – partly positive, partly negative, but in essence with no perspective for an applicant who is able and willing to host the IAS Central Bureau. It was therefore meaningless to submit an IAS Call for Participation.
The reasons for the failure to appoint an IAS:

- The general objective of IAS is widely accepted, but a specific and well-focussed work plan was not presented.
- Existing centres claim that a rather complete and gradually improved service to altimeter users is already provided.
- The existing centres are not willing to be organized or coordinated by an organization like the IAS Governing Board

Pilot Projects - suggestions for the next step

According to the results of the Venice meeting, it is not adequate to appoint an IAS now – with an organization imitating those of other, already existing services like IGS, ILRS and IVS. In addition the work plan of IAS has to become more specific. It must be clearly stated what shall be done and what will be the benefits of an IAS. The best solution seems to be specific service elements (pilot projects) that could be realized by small groups and might migrate at a later date to an IAS. The following is a possible list of such projects:

a. Inform and document – better than it is done presently. Tell the user where to get what data or products. Compile and provide associated meta data (XML). Give advice how to read and transform data and products (code snippets).

b. Strengthen the upgrade capability. Install procedures for a fast distributed upgrade of GDR/level-2 data. Here GRID-technology could be applied.

c. Provide quality-controlled and well-documented products. Develop standards for quality control and documentation. Compile products and meta data (again XML).

d. Allow user-defined data extracts. Set up and maintain electronic version of data element dictionaries e.g. for GDR/level-2 data. Let the experienced user decide what record parameter he wants to get. Give inexperienced users recommended extract formats for specific applications.

3.7 Contributions to the Global Geodetic Observing System (GGOS)

After a two-years initial definition phase, the Global Geodetic Observing System (GGOS) of the International Association of Geodesy (IAG) was installed for operation during the IAG Scientific Assembly in August 2005 in Cairns, Australia. There are five Working Groups in the GGOS structure:

- Data and information systems,
- Ground networks and communication,
- Satellite missions,
- Conventions, models, analysis,
- User linkage and outreach.

DGFI is concentrating its activities on the WG "Conventions, models and analysis". The objective is to actualize the conventions and to homogenize the models and analyses used in all geodetic data processing and product generation. At present there are some contradictions, e.g., of IAG resolutions and IERS conventions such as the tidal reduction and fundamental constants. The use of constants and models in services and individual products is not always consistent with the resolutions and conventions.

In the first phase of activities, the use of constants and conventions in common software packages shall be analysed and evaluated. This includes in particular the following fundamental constants:

- geocentric gravitational constant GM,
- speed of light c,
- Earth rotation velocity ω,
- equatorial radius a,
- flattening f;

conventions and models:

- time system (TT, TCG),
- solid Earth tidal model,
- ocean tide and loading model,
- pole tides,
- permanent tide treatment,
- atmospheric loading,
- troposphere model,
- ionosphere model,
- relativity model;

and parameterizations for

- station coordinates (epoch time),
- nutation, UT1 and polar motion,
- troposphere parameters,
- gravity field models.

All institutions participating in the international cooperation are invited to document the parameters used in their software packages. The effect of deviations from the official IAG values will then be estimated. As a consequence, a change of significantly differing parameters will be proposed.

The work is done in close connection with the Project "Integration of Space Techniques as a Basis for a Global Geodetic-Geophysical Observing System (GGOS-D)" financed by the German Ministry of Education and Technology (BMBF).

4 Information Services and Scientific Transfer

Scientific research needs to achieve its results within a certain time span and to meet the requests of society. This is especially valid for geo-sciences which describe the planet Earth. Considering the fact of decreasing funds and other restrictions, we have to sustain the permanent and long-term work in the field of geodesy. This requires a system of clear and accessible information. The information can either be provided by personal contacts or by written documents. Research is more and more based on broad cooperation, therefore careful documentation of data and results is requested. The internet has proven to serve as a fast and worldwide accessible tool for information exchange. This tool is fully used, however, for many other requests we still produce printed reports especially for long-term documentation.
The DGFI maintains a homepage (http://www.dgfi.badw.de/) in which all activities of the institute are presented in detail. Moreover links to the IAG entities lead to the international geodetic organisation, especially to Commission 1 – Reference Frames, as an intensive research field of DGFI. Other links point to national/international projects. Furthermore, the German Geodetic Commission (Deutsche Geodätische Kommission – DGK) maintains its homepage (http://dgk.badw.de/) informing especially on the commission and its activities but also on various topics of geodesy such as conferences, education in geodesy, job offers in geodetic research, links to other geodetic institutions etc. In this homepage the publications of the German Geodetic Commission (Veröffentlichungen der Deutschen Geodätischen Kommission – DGK) with up to 1000 volumes are listed in detail as well.

4.1 Internet representation

Internet is more and more used as a medium to exchange data and scientific information. Solving growing demands to inform about different scientific aspects, DGFI set up and maintains several independent Internet sites. The administration of multiple Internet representations is solved by means of the Typo3 Content Management System (CMS).

Typo3 Content Managament System

A CMS administrates the pages of an Internet site by a data base system, ensures a common layout by pre-defined templates and provides simple interfaces to the editors - which are in the present case scientists, responsible for the page content. With Typo3, any computer connected to the Internet can be used, to create, modify or delete pages by means of a browser interface – without experiences in Internet specific “mark up” languages like HTML or CSS. Typo3 is an ‘Open Source’ project and as such available free of charge. It is one of the most actively developed content management systems, applied by many commercial sites. Typo3 provides comfortable functions to handle graphics - a necessary feature for the presentation of scientific results.

Web sites set up and maintained by DGFI

The Typo3 Content Management System is used by DGFI to inform about

- the institute and its research programme (DGFI home page),
- its involvement in the Commission 1 of the International Association of Geodesy (IAG),
- the “Deutsche Geodätische Kommission (DGK)”, and
- a Geodesy Information System GeodIS.

DGFI used the same system also for new Websites, dedicated to

- the new DFG priority program “Mass transport and mass distribution in the Earth system” (SPP1257), and
- the International IAG/FIG symposium on “Geodetic Reference Frames” (GRF2006).

Moreover, Internet is in addition used to maintain

- several file transfer servers for extensive data exchange, required for DGFI acting as data and analysis centres,
- mailing lists for services and international projects,
- collaborative Internet site for specific projects, and an
- Intranet site to support compilation and distribution of internal information (blackboard, calendar, library).

DGFI home page

The DGFI home page, available under

`http://www.dgfi.badw.de`

informs about structure and results of the actual research programme, ongoing research topics and the national and international projects, DGFI is involved in and the multiple contributions of DGFI to international services. The home page also provides a complete list of papers and reports published since 1994 by the employees and a compilation of all posters and presentations. Most recent publications and posters are – as far as possible – available in electronic form (mostly with the portable document format, pdf).

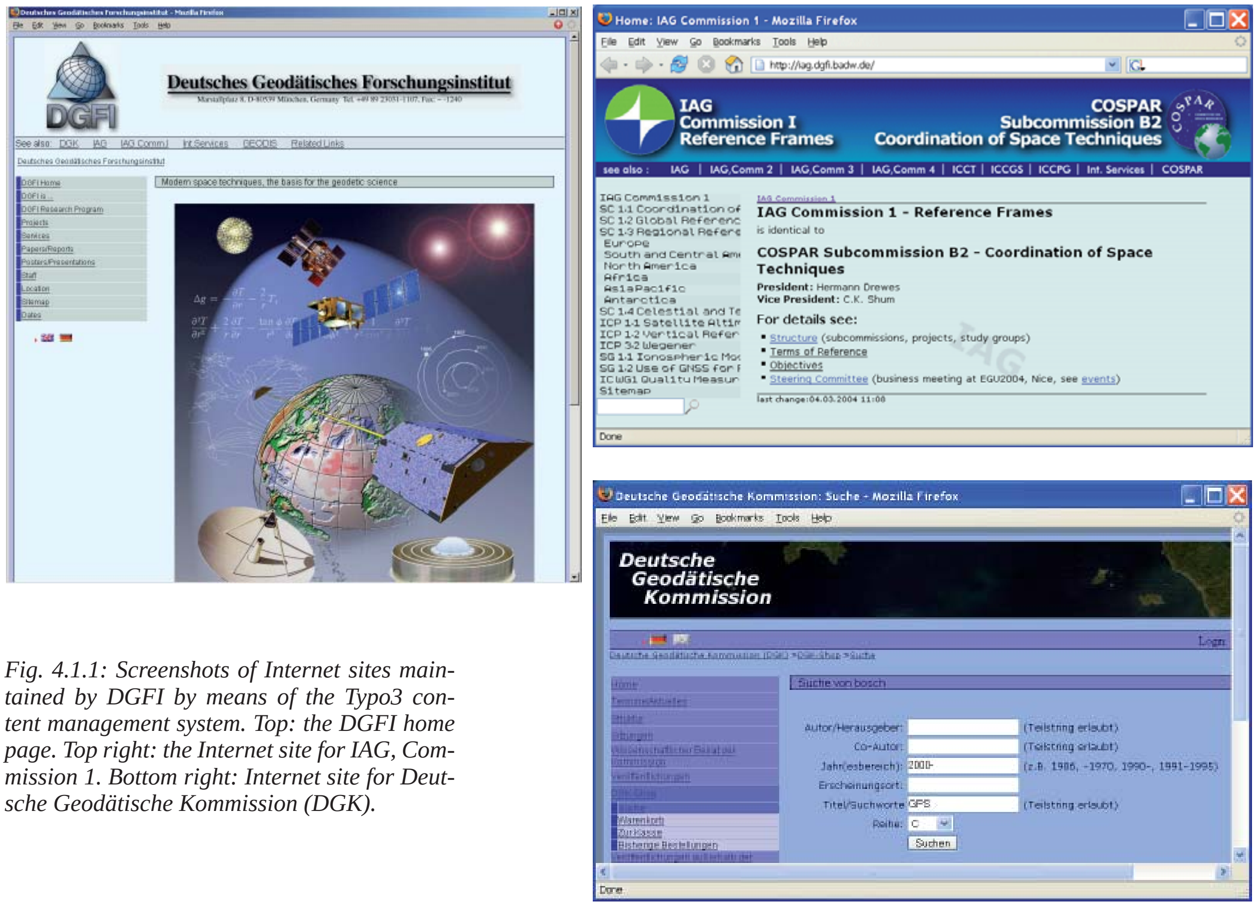

Fig. 4.1.1: Screenshots of Internet sites maintained by DGFI by means of the Typo3 content management system. Top: the DGFI home page. Top right: the Internet site for IAG, Commission 1. Bottom right: Internet site for Deutsche Geodätische Kommission (DGK).

Internet site for IAG, Commission 1

DGFI scientists contribute significantly to the Commission 1 "Reference Frames" of the IAG which is identical to the COSPAR Subcommission B2, "Coordination of Space Techniques". The leading role, given by presidency, chair of an Intercommission Project, and chair of a Study Group, requested a self standing internet presentation, available under

`http://iag.dgfi.badw.de .`

The site provides general informations about structure, organisation and general objectives of the Commission 1 and compiles an overview to all sub-commissions, inter-commission projects and study groups with numerous subpages, giving the terms-of-references and the objectives of all entities.

Geodesy Information System GeodIS

The geodesy information system GeodIS, located at

`http://www.dgfi.badw.de/~geodis`

is further maintained by DGFI with the objective to compile informations about the most important areas of physical geodesy. The intention of GeodIS is to help people in finding information on and data relevant to geodesy. GeodIS provides, for example, a summary about relevant scientific organizations and international services with direct links to the corresponding home pages.

Internet site for Deutsche Geodätische Kommission (DGK)

Another Internet site is maintained for the "Deutsche Geodätische Kommission" (DGK). The site is available at location

`http://dgk.badw.de`

and informs about the structure of the DGK, the membership, working groups, geodetic research institutes in Germany, and – above all – the numerous publications of DGK. The complete catalogue of DGK publications can be downloaded as pdf file.

The list of DGK publication is administrated by means of a MySQL data base system. On top of this system is a comfortable search function allowing to look for author(s), year or period of years, keywords and substrings within the title of publication (see figure 4.1.1). The search result, showing all publications fulfilling the criteria can be further edited, in order to get exactly the list of those publications that are of interest. The final list can be used to order a publication by submitting an e-mail to the DGK office.

Internet site for the International IAG/FIG Symposium on „Geodetic Reference Frames"

Typo3 has also been used for the International IAG/FIG Symposium on "Geodetic Reference Frames", organized by DGFI, October, 09-14, 2006 in Munich. The symposiums web site at

`http://iag.dgfi.badw.de/?grf2006`

informed about the scope of the symposium, the general session schedule, the meeting place, registration procedure, accommo-

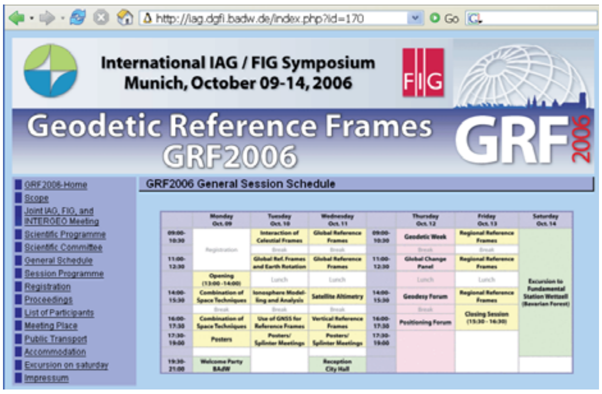

Fig 4.1.2: Screenshots of the Internet sites for the International IAG/FIG Symposium on "Geodetic Reference Frames", GRF2006 (left) and the new DFG priority program "Mass transport and mass distribution in the Earth system", SPP1257 (right).

dation, and public transport. Abstracts could be submitted by an online registration form by which a background data base was updated. This data base was later used to set up and display the detailed session schedule.

Internet site for the new DFG priority program „Mass transport and mass distribution in the Earth system"

Finally, an Internet site for the new DFG priority program "Mass transport and mass distribution in the Earth system", SPP1257, is under development. It resides on a DGFI server, but has got it's own domain name

`http://www.massentransporte.de` .

The site shall make the SPP-program known to the public and other scientists (outreach), but provide also a basis for internal communication, compile and provide thematic expertise and establish links to data and products that are relevant for the priority program.

Mailing lists

Several mailing lists are maintained by DGFI to fulfil the requirements for information exchange within the ILRS Global Data Centre or to support discussions within the Planning Group of the International Altimeter Service. The mailing lists are partly realized by a set of 'bash'-scripts, which are automatically executed according to pre-defined schedules or by the 'mailman' program, which transforms submitted e-mails to a specific format which can then be viewed by any Internet-browser sorted according to date, thread, or author.

Intranet

Finally it should be mentioned that another server behind a firewall is used to provide Intranet functionality – again on the basis of the Typo3 content management system. The internal information exchange is supported by a black board, a meeting calendar, the access to the library data base, and numerous pages which can be created, modified or deleted by any of the employees. The pages compile internal information for the work of particular research topics, links to data sets, formats, internal documentation, and the necessary meta data.

4.2 Publications

ANGERMANN, D., H. DREWES, M. GERSTL, M. KRÜGEL, B. MEISEL, H. MÜLLER, W. SEEMÜLLER: ITRS Combination Centre at DGFI. IERS Annual Report 2004, 88-92, Verlag des Bundesamts für Kartographie und Geodäsie, Frankfurt a.M., 2005 (online at www.iers.org).

ANGERMANN, D., H. DREWES, R. KELM, M. KRÜGEL, B. MEISEL, V. TESMER: IERS Combination Research Centre at DGFI. IERS Annual Report 2004, 100-101, Verlag des Bundesamts für Kartographie und Geodäsie, Frankfurt a.M., 2005 (online at www.iers.org).

ANGERMANN, D., R. KELM, M. KRÜGEL, B. MEISEL, H. MÜLLER, V. TESMER, D. THALLER, R. DILL: Towards a rigorous combination of space geodetic observations for IERS product generation. Observation of the Earth System from Space, J. Flury, R. Rummel, C. Reigber, M. Rothacher, G. Boedecker, U. Schreiber (Eds.), Springer, 2006.

BEUTLER, G., H. DREWES, A. VERDUN: The Integrated Global Geodetic Observing System (IGGOS) viewed from the perspective of history. J. of Geodynamics (40) 414-431, 2005.

BOSCH, W.: Dynamic Planet 2005, Joint Assembly of IAG, IAPSO and IABO, Cairns, Australien, 22.-26. August 2005, Session GP2: Global sea-level change: Altimetry, GNSS and tide gauge measurements. ZfV (130) 399-400, 2005.

DREWES, H. (Ed.): The Global Geodetic Observing System. J. of Geodynamics (40) Issues 4-5, 47pp, DOI 10.1016/j.jog.2005.10.002, 2005.

DREWES, H.: The ILRS: An important service for science and practice. In: ILRS 2003-2004 Annual Report, 1-3, NASA/TP-2005-212780, 2005.

DREWES, H.: IAG-Commission 1 – Reference Frames, Mid-term report 2005. IAG Commission 1 Bulletin No. 19, 7-9, 2005.

DREWES, H.: Dynamic Planet 2005, Joint Assembly of IAG, IAPSO and IABO, Cairns, Australien, 22.-26. August 2005, Session G5: Global Geodetic Observing System (GGOS), ZfV (130) 397-398, 2005.

DREWES, H.: Integration von Geometrie und Gravimetrie: Das Globale Geodätische Observations-System (GGOS). Wiss. Arb. Fachr. Geod. u. Geoinf. Hannover, Nr. 263, 159-168, 2006.

DREWES, H.: Zum Wandel in der Zielsetzung geodätischer Forschung (CD Version: The changing objectives in geodetic research). ZfV (131) 292-298, 2006.

DREWES, H., CH. REIGBER: IAG's Global Geodetic Observing System (GGOS) in its initial phase. 14th ILRS Workshop Proceedings, Boletin ROA No. 5, 11-14, San Fernando, Spain, 2005.

DREWES, H., H. HORNIK (Eds.): IAG Commission 1 – Reference Frames, Mid-term Report. IAG Commission 1 Bulletin No. 19, 43 pp., 2005.

DREWES, H., D. ANGERMANN, M. GERSTL, M. KRÜGEL, B. MEISEL, W. SEEMÜLLER: Analysis and refined computations of the International Terrestrial Reference Frame. In: J. Flury, R. Rummel, C. Reigber, M. Rothacher, G. Boedecker, U. Schreiber (Eds.): Observation of the Earth System from Space, 343-356, Springer, 2006.

FORTES, L.P., E. LAURÍA, C. BRUNINI, A. HERNANDEZ, L. SÁNCHEZ, H. DREWES, W. SEEMÜLLER: Current status and future developments of the SIRGAS project. Wiss.Arb.Fachr.Verm., Univ. Hannover, Nr. 258, 59-70, 2006.

KANIUTH, K., S. VETTER: Estimating atmospheric pressure loading regression coefficients from GPS observations. GPS Solutions 10(2), 126-135, 2006.

KRÜGEL, M.: Dynamic Planet 2005, Joint Assembly of IAG, IAPSO and IABO, Cairns, Australien, 22.-26. August 2005, Session G4: Advances in the realization of and regional reference frames, ZfV (130) 396-397, 2005.

MEISEL, B., D. ANGERMANN, M. KRÜGEL, H. DREWES, M. GERSTL, R. KELM, H. MÜLLER, W. SEEMÜLLER, V. TESMER: Refined approaches for terrestrial reference frame computations. Advances in Space Research 36 , 350-357, 2005.

MONICO, J.F., J.C. BAEZ, H. DREWES: O estado da arte em referenciais geodésicos: ITRF2000 e as próximas realizações do ITRS. Boletim de Ciências geodésicas (11) No. 2, 261-277, Univ. Fed. do Paraná, Curitiba, Brasil, 2005.

MÜLLER, H.: The SLR Tracking Data Quality Control During the Operational Processing. In: J.Garate, J. Davila, C. Noll, M. Pearlman (Eds.): 14th International Laser Ranging Workshop, Proceedings, Boletin ROA 5/2005, 395-398, 2005.

MÜLLER, H., D. ANGERMANN, B. MEISEL: A Multi-Year SLR Solution. In: Garate, J., J. Davila, C. Noll, M. Pearlman (Eds.): 14th International Laser Ranging Workshop, Proceedings, Boletin ROA 5/2005, 15-19, 2005.

MÜLLER, H., R. KELM, D. ANGERMANN: Deutsches Geodätisches Forschungsinstitut (DGFI), Germany, Associate Analysis Center. In M. Pearlman and C. Noll (Eds.): International Laser Ranging Service, Annual Report 2003-2004, NASA/TP-2005-212780, A11-12, 2005.

RUMMEL, R., H. DREWES, H. HORNIK: Deutsches Geodätisches Forschungsinstitut (DGFI). Bayer. Akademie der Wissenschaften, Jahrbuch 2005, 273-280, 2006.

SCHMIDT, M., O. FABERT, C.K. SHUM: On the estimation of a multi resolution representation of the gravity field based on spherical harmonics and wavelets. J. Geodynamics (39), 512-526, 2005.

SCHMIDT, M., S.-C. HAN, J. KUSCHE, L. SÁNCHEZ, C.K. SHUM: Regional high-resolution spatio-temporal gravity modeling from GRACE data using spherical wavelets. Geophys. Res. Lett., 33, L08403, doi:10.1029/2005GL025509, 2006.

SEITZ, F., M. SCHMIDT: Atmospheric and oceanic contributions to Chandler wobble excitation determined by wavelet filtering. Journal of Geophsical Research (110), B11406, doi:10.1029/2005JB003826, 2005.

TESMER, V.: Konsistente Realisierung von Referenzsystemen mit dem Verfahren VLBI. DGFI Report No. 78, 2006.

TESMER, V., H. DREWES, M. KRÜGEL: DGFI Analysis Center Annual Report 2005. In: Behrend, D.,K. Baver (Eds.): IVS 2005 Annual Report, NASA/TP-2006-214136, 223-226, 2006.

THALLER D., DILL R., KRÜGEL M., STEIGENBERGER P., ROTHACHER M., TESMER V.: CONT02 Analysis and Combination of Long EOP Series. In: Flury, J., Rummel, R., Reigber, C., Rothacher, M., Boedecker, G., Schreiber, U. (Eds.) Observation of the Earth System from Space, 389-411, Springer, 2006.

TORRES, J., HORNIK, H. (Ed.): Report on the Symposium of the IAG Sub-commission for Europe (EUREF) held in Bratislava, 2 – 5 June 2004; Reports of the EUREF Technical Working Group (TWG). EUREF Publication No. 14, 412 S. Mitteilungen des Bundesamtes für Kartographie und Geodäsie, Band 35, Frankfurt a.M., 2005.

4.3 Posters and oral presentations

ANGERMANN, D.: ITRF2004 computations at DGFI. IERS Workshop on Combination, Potsdam, Germany, 10.10.2005.

ANGERMANN, D.: Status of ITRF2004 computations at DGFI. IERS Directing Board Meeting No. 41, San Francisco, USA, 05.12.2005.

ANGERMANN, D., H. DREWES, M. KRÜGEL, B. MEISEL: Challenges towards a uniform terrestrial reference frame. AGU Fall Meeting 2005, San Francisco, USA, 07.12.2005 (Poster).

ANGERMANN, D.: Reference Frames: Overview and User Requirements. GAGOS/EPIGGOS Workshop, DGFI, Munich, Germany, 13.02.2006.

ANGERMANN, D., H. DREWES, M. KRÜGEL, B. MEISEL, M. GERSTL: Accuracy evaluation of the terrestrial reference frame. EGU General Assembly, Vienna, Austria, 02.-07.04.2006 (Poster).

ANGERMANN, D.: Report of ITRS Combination Center at DGFI. IERS Directing Board Meeting No. 42, Vienna, Austria, 08.04.2006.

ANGERMANN, D.: The International Terrestrial Reference Frame (ITRF2005). INTERREG III B "Alpine Space GPS Quakenet, Workshop, Brussels, Belgium, 26.-27.06.2006.

BOSCH, W. , R. SAVCENKO (2005): Gemeinsame Kreuzungspunktanalyse simultan messender Altimeter-satelliten, Geodetic Week 2005, Düsseldorf, 04.-06.10.2005 (Poster).

BOSCH, W.: Altimetry. GAGOS Workshop, DGFI, 13.02.2006.

BOSCH, W.: Data Acquisition, Data Flow, Archiving and Information Management. GAGOS Workshop, DGFI, 14.02.2006.

BOSCH, W.: Mass Transport and Mass Distribution in the Earth System – a new research program of the Deutsche Forschungsgemeinschaft, DFG. GGOS Steering Committee Retreat, DGFI, 15.02.2006.

BOSCH, W.: Combination of gravity field models and altimetry data. IAPG satellite geodesy workshop, Höllenstein (Bayerischer Wald), 09.03.2006.

BOSCH, W.: Geographically correlated errors – problem solved? 15 Years of progress in radar altimetry. ESA/CNES symposium, Venice, Italy 13.03.2006.

BOSCH, W.: Global Multi-Mission Crossover Analysis. Ocean Surface Topography Science Team, Venice, Italy, 16.-18.03.2006 (Poster).

BOSCH, W., C.K. SHUM, PH. WOODWORTH, G. MITCHUM: The International Altimeter Service (IAS) – focussing satellite altimetry for global Earth observing systems. Ocean Surface Topography Science Team, Venice, Italy, 16.-18.03.2006 (Poster).

BOSCH, W.: Mean Sea Surfaces – Determination and Calibration. Inter-Commission Project 1.2 Workshop, Prague, Czech Republic, 10.04.2006.

BOSCH, W.: Die Vermessung der Meeresoberfläche durch Satellitenaltimetrie - Technologie, Ergebnisse und Anwendungen. Deutscher Hydrographentag, Magdeburg, 14.06.2006.

BOSCH, W.: Satellite Altimetry, Sea Level variation and Gravity Field. Dynamic Earth Seminar, Dept. for Earth & Environmental Sciences, Ludwig Maximilians University, München, 16.06.2006.

BOSCH, W.: Mean sea level and the sea surface topography along the Brazilian coast. IV National Conference on Geography and Cartography (CONFEGE), Instituto Brasileiro de Geografia e Estatística (IBGE), Rio de Janeiro, Brazil, 22.08.2006.

BOSCH, W.: On the combination of gravity field models and satellite altimeter data. 1st International Symposium of the International Gravity Field Service (IGFS2006), Harbiye Military Museum and Culture Center, Istanbul, Turkey, 30.08.2006.

BOSCH W.: Robinson Crusoe sucht Anschluß – Überlegungen zur Realisierung eines globalen einheitlichen Höhensystems. DGK Arbeitskreis Theoretische Geodäsie "Vertikaldatum und Welthöhensystem", Institut für Theoretische Geodäsie, Universität Bonn, 12.09.2006.

Bosch, W., C. Schwatke: DFG priority program SPP1257 – Data management, information exchange, and outreach. Geotechnologien Statusseminar, University Bonn, 18.-19.09.2006 (Poster).

Bosch, W.: Consistent data combination and signal separation – theme 7 projects of the DFG priority program SPP1257. Geotechnologien Statusseminar, University Bonn, 19.09.2006.

Bosch, W.: From sensor data to mass signals – theme 1 projects of the DFG priority program SPP1257. Geotechnologien Statusseminar, University Bonn, 19.09.2006.

Drewes, H.: Probleme bei der Höhenbestimmung mit GPS. INTERGEO, Düsseldorf, Germany, 06.10.2005.

Drewes, H.: The kinematic reference frame for ITRF. IERS Workshop on Combination, Potsdam, Germany, 10.10.2005.

Drewes, H.: Present-day plate kinematics and crustal deformation. Geophys. Kolloquium, Ludwig-Maximilian-Universität, München, Germany, 28.10.2005.

Drewes, H.: Die Arbeiten des DGFI im Jahr 2005. Vollsitzung der Deutschen Geodätischen Kommission, München, 03.11.2005.

Drewes, H.: SIRGAS en el marco de referencia global: Estado del ITRF2005. Reunión Técnica del Proyecto SIRGAS, Caracas, Venezuela, 17.11.2005.

Drewes, H.: Sistema de Observación Geodésico Global. XX Reunión Consulta Cartografía IPGH, Caracas, Venezuela, 17.11.2005.

Drewes, H.: Integration der Raumbeobachtungsverfahren als Grundlage eines globalen geodätisch-geophysikalischen Beobachtungssystems (GGOS-D). GGOS-D Project Meeting, Potsdam, Germany, 22.11.2005.

Drewes, H.: Assessing and forward planning of the Geodetic And Geohazard Observing System for GMES applications (GAGOS). GAGOS Project Meeting, Potsdam, Germany, 23.11.2005.

Drewes, H.: Geodäsie, eine der ältesten Wissenschaften, und aktuelle Forschungsarbeiten des DGFI. Treffen der Technisch-Literarischen Gesellschaft, München, 01.03.2006.

Drewes, H.: Status of the Global Geodetic Observing System (GGOS). IAPG Satellite Geodesy Workshop, Höllenstein, Germany, 09.03.2006.

Drewes, H.: Implementation of the kinematic NNR condition for the terrestrial reference frame. EGU General Assembly 2006, Session G1, Vienna, Austria, 05.04.2006.

Drewes, H.: The actual plate kinematic and deformation model - APKIM 2005. EGU General Assembly 2006, Session G11/GD17, Vienna, Austria, 06.04.2006.

Drewes, H.: The role of the vertical reference system in IAG. Inter-Commission Project 1.2 „Vertical Reference Frame“ Workshop, Prague, Czech Republic, 10.04.2006.

Drewes, H.: Status and perspectives of the definition and realization of geodetic reference systems. Hotine-Marussi Symposium, Wuhan, China, 29.05.2006.

Drewes, H.: Status und Entwicklung des Internationalen Terrestrischen Referenzsystems (ITRF). Geodätisches Kolloquium, Technische Universität Dresden, 28.06.2006.

Drewes, H.: Integration von Geometrie und Gravimetrie: Das globale geodätische Observations-System (GGOS). Geodätisches Kolloquium, Universität Hannover, 13.07.2006.

Drewes, H.: Sistemas de referencia y geoide. Curso de Formación DIGSA, Barcelona, Spain, 19.07.2006.

Drewes, H.: Deberes y tareas de los centros de procesamiento en los servicios internacionales. Workshop of the SIRGAS Working Group I (Reference System), Rio de Janeiro, Brazil, 16.08.2006.

Drewes, H.: Estado del ITRF2005. Workshop of the SIRGAS Working Group I (Reference System), Rio de Janeiro, Brazil, 17.08.2006.

Drewes, H.: Estado actual de los sistemas de referencia terrestres. IV National Conference on Geography and Cartography (CONFEGE), Instituto Brasileiro de Geografia e Estatística (IBGE), Rio de Janeiro, Brazil, 22.08.2006.

Drewes, H.: Notwendigkeit eines vereinheitlichten Höhensystems aus der Sicht eines Globalen Geodätischen Observations-Systems (GGOS). DGK Arbeitskreis Theoretische Geodäsie "Vertikaldatum und Welthöhensystem", Institut für Theoretische Geodäsie, Universität Bonn, 12.09.2006.

Drewes, H., D. Angermann, M. Gerstl, M. Krügel, B. Meisel: The ITRF2005 realization of DGFI. Geotechnologien Statusseminar, Bonn, 18.-19.09.2006 (Poster).

Göttl, F.: Verknüpfung von Erdrotation, Schwerefeld und Geometrie mit geodätischen Raumverfahren. Kick-off meeting of the DFG research group „Erdrotation und globale dynamische Prozesse", Hannover, 06.07.2006.

Krügel, M., D. Angermann, M. Gerstl, B.Meisel: Improved consideration of local ties in inter technique combination, IERS Workshop on combination, Potsdam, 10.10.2005 (Poster).

Krügel, M.: Bernese Software Course. IGAC, Bogotá, Colombia, 14.-21.07.2006.

Kusche, J., M.Schmidt, S.-C. Han, L. Sánchez, C.K. Shum, J. Xie: Regional high-resolution spatio-temporal gravity modeling from GRACE data using spherical wavelets. AGU Fall Meeting 2005, San Francisco, USA, 07.12.2005 (Poster).

Meisel, B., D. Angermann, M. Krügel: Accumulating intra-technique solutions from epoch normal equations. IERS Workshop on Combination, Potsdam, Germany, 10.10.2005 (Poster).

Meisel, B.: TRF solution based on time series combination. Geotechnologien Statusseminar, Bonn, 19.09.2006.

Potts, L., M. Schmidt, C.K. Shum, R. von Frese, C. Zeilhofer, H. Kim: Multi-resolution ionopheric electron density and external field over Antarctica from altimetry and CHAMP magnetic observations. EGU Gen. Ass., Vienna, Austria, 02.-07.04.2006 (Poster).

Sánchez, L.: Hacia un sistema vertical de referencia unificado para América del Sur. XX Reunión de Consulta de la Comisión de Cartografía del IPGH, Caracas, Venezuela, 17.11.2005.

Sánchez, L.: SIRGAS-GTIII: Datum Vertical, Reporte 2005. Reunión SIRGAS, Caracas, Venezuela, 18.11.2005.

Sánchez, L.: Empirical determination of the global reference value W_0. IAG: Intercommission Project 1.2 (Vertical reference systems) Workshop. Prague, Czech Republic, 11.04.2006.

Sánchez, L.: Connection of the South American height systems to a global unified vertical reference frame. IAG: Inter commission Project 1.2 (Vertical reference systems) Workshop. Prague, Czech Republic, 12.04.2006.

Sánchez, L.: Approach for the establishment of a global vertical reference system. VI Hotine-Marussi Symposium. Wuhan, China, 30.05.2006.

Sánchez, L.: Curso Fundamentos teóricos para el procesamiento de información GNSS utilizando el software científico Bernese. Instituto Geográfico Augustín Codazzi (IGAC), Bogotá, Colombia, 10.-21.07.2006.

Sánchez, L.: Reporte del centro de procesamiento IGAC. Workshop of the SIRGAS Working Group I (Reference System). Rio de Janeiro, Brazil, 17.08.2006.

Sánchez, L.: Modernización de los sistemas de alturas en América del Sur. IV National Conference on Geography and Cartography (CONFEGE), Instituto Brasileiro de Geografia e Estatística (IBGE), Rio de Janeiro, Brazil, 22.08.2006.

Sánchez, L.: Advances to define and realise a World Height System. 1st International Symposium of the International Gravity Field Service (IGFS2006), Harbiye Military Museum and Culture Center, Istanbul, Turkey, 29.08.2006.

Sánchez, L.: Konzept für die Definition und Realisierung eines globalen vertikalen Referenzsystem. DGK Arbeitskreis Theoretische Geodäsie "Vertikaldatum und Welthöhensystem", Institut für Theoretische Geodäsie, Universität Bonn, 12.09.2006.

Savcenko, R.: Saisonale Variationen des Meeresspiegels aus Multi-Missions Altimetrie. Re-Organisation und De-Korrelation. Geodätische Woche 2005, Düsseldorf, 05.10.2005.

Savcenko, R.: Response Method of tidal analysis using BIN data, 3rd COSSTAGT project meeting, Darmstadt, 08.11.2005.

Savcenko, R., W. Bosch: Shallow water tides from multi-mission altimetry – a case study at the Patagonian shelf. Ocean Surface Topography Science Team, Venice, Italy, 16.-18.03.2006 (Poster).

Schmidt, M., J. Kusche, S.-C. Han, C.K. Shum: Multi-resolution representation of the gravity field from satellite and terrestrial data. EGU Gen. Ass., Vienna, Austria, 03.04.2006.

Schmidt, M., C.K. Shum, D. Bilitza, C. Zeilhofer, L. Potts, S. Ge, M. Karslioglu: Regional multi-resolution representation of the ionospheric electron density. EGU Gen. Ass., Vienna, Austria, 02.-07.04.2006 (Poster).

Schmidt, M., J. Kusche, S.-C. Han, C.K. Shum: Spatio-temporal multi-resolution representation of the gravity field from satellite and surface data. VI Hotine-Marussi Symposium of Theoretical and Computational Geodesy, Wuhan, China, 29.05.-02.06.2006 (Poster).

Schmidt, M.: Regional 4-D modeling of the ionospheric electron density. 36th COSPAR Scientific Assembly, Beijing, China, 21.07.2006.

Schmidt, M.: Multi-resolution representation of the gravity field from satellite data based on wavelet expansions with time-dependent coefficients. 1st International Symposium of the International Gravity Field Service (IGFS2006), Harbiye Military Museum and Culture Center, Istanbul, Turkey, 31.08.2006.

Seemüller, W.: Report on New Activities of IGS Regional Associate Analysis Centre for SIRGAS (IGS RNAAC SIR). SIRGAS Workshop, Caracas, Venezuela, 18.11.2005.

Seemüller, W.: Activities of IGS Regional Network Associate Analysis Centre for SIRGAS (IGS RNAAC SIR), IV National Conference on Geography and Cartography (CONFEGE), Instituto Brasileiro de Geografia e Estatística (IBGE), Rio de Janeiro, Brazil, 22.08.2006.

Seitz, F.: Atmosphärische, ozeanische und hydrologische Antriebe des Erdsystemmodells DyMEG. Meeting of the working group ‚Dynamisches Erdsystemmodell' of the DFG project ‚Rotation der Erde', Dresden, 04.05.2006.

Seitz, F.: Modellansätze zur Untersuchung zeitlicher Variationen des Schwerefelds und der geometrischen Figur der Erde. Arbeitstreffen zum Thema ‚Dynamisches Erdsystemmodell' im Rahmen des DFG Forschungsvorhabens ‚Rotation der Erde', Hamburg, 04.10.2005.

Seitz, F.: Entwicklung eines physikalisch konsistenten Systemmodells zur Untersuchung von Rotation, Oberflächengestalt und Schwerefeld der Erde. Kick-off meeting of the DFG research group "Erdrotation und globale dynamische Prozesse", Hannover, 07.07.2006.

Tesmer, V.: Simultaneous estimation of a TRF, a CRF and the EOP using VLBI. IERS Workshop on Combination, Potsdam, Germany, 11.10.2005.

Tesmer, V.: Impact of different analysis options on the TRF, CRF, and position time series estimated from VLBI, Concepcion, Chile 11.01.2006.

Tesmer, V., D. Thaller, P. Steigenberger, M. Rothacher, M. Krügel: Can low-latency UT1 estimates be improved combining VLBI intensive and daily GPS session? EGU 2006 General Assembly, Vienna, Austria, 05.04.2006 (Poster).

Tesmer, V.: Effect of different tropospheric mapping functions on the TRF, CRF, and position time series estimated from VLBI. EGU 2006 General Assembly, Vienna, Austria, 05.04.2006.

4.4 Membership in scientific bodies

International Council for Science (ICSU)
- International Lithosphere Programme (ILP) (Bureau member: H. Drewes)
- Committee on Space Research (COSPAR): Subcommission B2: International Coordination of Space Techniques for Geodesy and Geodynamics (President: H. Drewes)

International Union of Geodesy and Geophysics (IUGG)
- IUGG Representative to Panamerican Institute for Geography and History, PAIGH (H. Drewes)
- IUGG Representative to United Nations Cartographic Office (H. Drewes)
- IUGG Inter-Association Commission on Geophysical Risk and Sustainability (H. Drewes)

International Association of Geodesy (IAG)
- IAG Commission 1: Reference Frames (President: H. Drewes)
- IAG-Representative to Sistema de Referencia Geocéntrico para las Américas, SIRGAS (H. Drewes)
- Inter-Commission Project 1.1: Satellite Altimetry (Chair: W. Bosch)
- Inter-Commission Project 1.2: Vertical Reference Frames (L. Sánchez)
- Inter-Commission Committee on Theory (ICCT) Working Group “Inverse Theory and Global Optimization” (M. Schmidt)
- Subcommission 1.3a: IAG Reference Frame for Europe (Secretary: H. Hornik)
- Subcommission 1.3a: IAG Reference Frame for Europe, Technical Working Group (H. Hornik)
- Subcommission 1.3b: SIRGAS, Working Group I “Reference Frame” (W. Seemüller)
- Subcommission 1.3b: SIRGAS, Working Group III “Vertical Datum” (President: L. Sánchez)
- Working Group 1.2.3 and Inter-Commission Committee on Theory (ICCT) Working Group 3: Integrated theory for crustal deformation (B. Meisel)
- Working Group 2 “Interactions and consistency between terrestrial reference frame, Earth rotation and gravity field”, Subcommission 1.1 “Coordination of Space Techniques” (Chair: D. Angermann)
- Study Group 1.1: Ionosphere Modelling and Analysis (Chair: M. Schmidt)
- Study Group 1.3 and Inter-Commission Committee on Theory (ICCT) Working Group: Quality measures, quality control, and quality improvement (M. Krügel)
- Study Group 2.3: Satellite Altimetry: data quality improvement and coastal applications (W. Bosch)
- Project Global Geodetic Observing System, GGOS Working Group “Conventions, Analysis and Modelling” (Chair: H. Drewes)
- International Earth Rotation and Reference Systems Service (IERS): IERS Working Group on Combination (D. Angermann)
- International Earth Rotation and Reference Systems Service (IERS): ITRS Combination Centre (Chair: H. Drewes)
- International Earth Rotation and Reference Systems Service (IERS): IERS Combination Research Centre (Chair: D. Angermann)
- International Earth Rotation and Reference Systems Service (IERS): Working Group Site Survey and Co-location (D. Angermann)
- International Laser Ranging Service (ILRS): Governing Board (H. Drewes, W. Seemüller)
- International Laser Ranging Service (ILRS): Analysis Working Group (D. Angermann, R. Kelm, H. Müller)
- International Laser Ranging Service (ILRS): Data Formats and Procedures Working Group (Chair: W. Seemüller)
- International VLBI Service for Geodesy and Astrometry (IVS): Analysis Centre (H. Drewes, M. Krügel, V. Tesmer)

Group on Earth Observation (GEO)
- Committee on Capacity Building and Outreach (IAG Substitute Delegate: H. Drewes)

Centre National d‘Etudes spatiales (CNES) / National Aeronautics and Space Administration (NASA)
- Ocean Surface Topography Science Team for Jason (Joint Altimetry Satellite Oceanography Network) (W. Bosch)

Consortium of European Laser Stations EUROLAS
- Member in the EUROLAS Board of Representatives (W. Seemüller)
- EUROLAS Secretary (W. Seemüller)

Deutsche Geodätische Kommission (DGK)
- “Ständiger Gast” (H. Drewes)
- Working Groups “Rezente Krustenbewegungen”, “Theoretische Geodäsie” (several collaborators)

Deutscher Verein für Vermessungswesen (DVW), Gesellschaft für Geodäsie, Geoinformation und Landmanagement
- Working Group 7 “Experimentelle, angewandte und theoretische Geodäsie” (H. Drewes)

4.5 Participation in meetings, symposia, conferences

ILRS AWG Meeting, Eastbourne, England, 02.10.2005 (Kelm)

ILRS Fall Meeting, Eastbourne, England, 03.10.2005 (Kelm)

ILRS Fall Technical Workshop Herstmonceux, Eastbourne, England, 03.-07.10.2005 (Seemüller)

DFG-Project Meeting "Earth System Model", Hamburg, Germany, 04.-05.10.2005 (Seitz)

INTERGEO/Geodetic Week 2005, Congress Centre Düsseldorf, 04.-06.10.2005 (Angermann, Bosch, Drewes, Meisel, Savcenko, Schmidt, Seitz)

Colloquium on „50 Years Geodesy at the University Bonn", Institute of Theoretical Geodesy, Univeristy Bonn, 07.10.2005 (Bosch, Schmidt)

IERS Workshop on Combination, Potsdam, Germany, 10.-11.10.2005 (Angermann, Drewes, Krügel, Meisel, Tesmer)

Jahressitzung der Deutschen Geodätischen Kommission, München, 02.–04.11.2005 (Hornik)

3rd COSSTAGT Project Meeting, Institute of Physical Geodesy, TU Darmstadt, 07.-08.11.2005 (Bosch, Savcenko)

XXXVIII Meeting of the EUREF Technical Working Group, Berne, 07.-08.11.2005 (Hornik)

SIRGAS Workshop, Caracas, Venezuela, 16.-18.11.2005 (Drewes, Sánchez, Seemüller)

XX Reunión Consulta Cartografía IPGH y Reunión Técnica del Proyecto SIRGAS, Caracas, Venezuela, 17.-18.11.2005 (Drewes, Sánchez, Seemüller)

GGOS-D Kick-off Meeting, GFZ Potsdam, Germany, 22.-23.11.2005 (Bosch, Drewes, Krügel, Meisel)

GAGOS Kick-off Meeting, GFZ Potsdam, Germany, 23.11.2005 (Bosch, Drewes)

DFG Colloquium on "Mass Transport and Mass Distribution in the Earth System", GFZ Potsdam, 28.-29.11.2005 (Bosch)

AGU Fall Meeting 2005, San Francisco, USA, 05.-09.12.2005 (Angermann)

IERS Directing Board Meeting, No. 41, San Francisco, USA, 05.12.2005 (Angermann)

Global Geodetic Observing System (GGOS) Steering Committee Meeting, San Francisco, USA, 08.12.2005 (Angermann)

4th IVS General Meeting, Analysis Workshop and OCCAM Workshop, Concepción, Chile, 08.-13.01.2006 (Tesmer)

Coordinators Meeting DFG Priority Research Programme ‚Massenstransporte und Massenverteilungen im System Erde', IMG, Frankfurt, 23.01.2006 (Bosch)

4th COSSTAGT Project Meeting, DGFI, München, 02.-03.02.2006 (Bosch, Savcenko)

GAGOS/EPIGGOS Workshop, DGFI, Munich, Germany, 13.-14.02.2006 (Angermann, Bosch, Drewes, Seemüller)

GGOS Retreat, DGFI, Munich, Germany, 15.-16.02.2006 (Angermann, Bosch, Drewes, Seemüller)

Navigation Summit, München, Germany, 21.-23.02.2006 (Krügel, Seitz)

Group on Earth Observations (GEO), Committee on Capacity Building and Outreach, Workshop, Paris, France, 06.-07.03.2006 (Drewes)

IAPG Satellite Geodesy Workshop, Höllenstein, Germany, 09.03.2006 (Bosch, Drewes)

15 Years of Progress in Radar Altimetry. ESA/CNES Symposium, Venice, Italy 13.-18.03.2006 (Bosch)

Business Meeting of International Altimeter Planing Group, Venice, Italy, 15.03.2006 (Bosch)

Ocean Surface Topography (OST) Science Team, Venice, Italy, 16.-18.03.2006 (Bosch)

EGU General Assembly 2006, Vienna, Austria, 03.-07.04.2006 (Angermann, Drewes, Schmidt, Seemüller, Tesmer)

IAG Executive Committee Meeting, Vienna, Austria, 03.04.2006 (Drewes)

ILRS AWG Meeting , Wien, Österreich , 04.04.2006 (Kelm, Müller)

ILRS Data Formats and Procedures Working Group, Vienna, Austria, 05.04.2006 (Seemüller)

GGOS Steering Committee Meeting. Vienna, Austria, 05.04.2006 (Drewes)

ILRS Governing Board Meeting, Vienna, Austria, 07.04.2006 (Drewes, Seemüller)

IERS Directing Board Meeting No. 42, Vienna, Austria, 08.04.2006 (Angermann)

IAG Inter-Commission Project 1.2 „Vertical Reference Frame“ Workshop, Prague, Czech Republic, 10.-11.04.2006 (Bosch, Drewes, Sánchez)

GGOS-D Projekttreffen, München, 02.-03.05.2006 (Angermann, Bosch, Drewes, Göttl, Krügel, Meisel, Tesmer)

DFG-Project Meeting “Earth System Model”, Dresden, Germany, 04.-05.05.2006 (Drewes, Seitz)

IAG Hotine-Marussi Symposium, Wuhan, China, 29.05.-02.06.2006 (Drewes, Sánchez)

Deutscher Hydrographentag, Magdeburg, 12.-14.06.2006 (Bosch)

41. Meeting of the EUREF Technical Working Group (TWG), Riga, Latvia, 13.06.2006 (Hornik)

EUREF TWG meeting, Riga, Latvia, 13.06.2006 (Hornik)

Symposium of the IAG Sub-commission for Europe (EUREF), Riga, Latvia, 14.-17.06.2006 (Hornik)

Dynamic Earth Seminar, Dept. for Earth & Environmental Sciences, Ludwig Maximilians University, München, 16.06.2006 (Bosch)

INTERREG III B "Alpine Space GPS Quakenet", Workshop, Brussels, Belgium, 26.-27.06.2006 (Angermann)

Kick-off meeting of the DFG research group “Erdrotation und globale dynamische Prozesse”, Hannover, 06.-07.07.2006 (Angermann, Bosch, Drewes, Göttl, Seitz)

GGOS-D Geotechnologien, 3rd project meeting, Frankfurt am Main, 16.-17.08.2006 (Angermann, Bosch, Krügel, Meisel, Müller, Tesmer)

Workshop of the SIRGAS Working Group I (Reference System). Rio de Janeiro, Brazil, 16.-18.08.2006 (Drewes, Sánchez, Seemüller)

IAU Working Group for the International Celestial Reference Frame (ICRF), Prag, Czechia, 21.08.2006 (Tesmer)

IV National Conference on Geography and Cartography (CONFEGE), Instituto Brasileiro de Geografia e Estatística (IBGE), Rio de Janeiro, Brazil, 21.-25.08.2006 (Bosch, Drewes, Sánchez, Seemüller)

1st International Symposium of the International Gravity Field Service (IGFS2006), Harbiye Military Museum and Culture Center, Istanbul, Turkey, 28.08.-01.09.2006 (Bosch, Drewes, Sánchez, Schmidt)

Working group meeting of the DFG research group „Erdrotation und globale dynamische Prozesse“, Berlin, 04.09.2006 (Göttl)

DGK Arbeitskreis Theoretische Geodäsie “Vertikaldatum und Welthöhensystem”, Institut für Theoretische Geodäsie, Bonn, 12.09.2006 (Bosch, Drewes, Sánchez)

Work meeting with the VLBI group Bonn, Bonn, 14.-15.09.2006 (Tesmer)

Geotechnologien Statusseminar, Bonn, 18.-19.09.2006 (Angermann, Bosch, Krügel, Meisel, Tesmer)

4.6 Guests

27.10.-13.12.2005:	J. Baez, Universidad Concepción, Chile and Universidade Federal do Paraná, Curitiba, Brazil.
01.03.2006:	Presseclub TELI, München.
06.-10.03.2006:	Prof. C. Brunini, Universidad Nacional de la Plata, Argentina.
26.05.2006:	Students of ARGEOS organisation, Germany.
17.-28.07.2006:	R. Luz, Instituto Brasileiro de Geografia e Estatistica (IBGE), Rio de Janiero, and Universidade Federal do Paraná (UFPR), Curitiba, Brazil (from April to November, 2006, at Universität Karlsruhe).
18.-19.08.2006:	Dr. O. Titov, Geoscience Australia, Canberra, Australia. Dr. J. Böhm, Technical University Vienna, Austria.
23.-24.08.2006:	Prof. H. Kutterer, Universität Hannover.
29.09.2006:	Prof. H. Schuh with geodesy students of the Technical University Vienna, Austria.

5 Personnel

5.1 Number of personnel

Total staff of DGFI during the 2005/2006 period (incl. DGK Office):

Regular budget

11 scientists
9 technical and administrative employees
1 worker
7 student helpers with an average of 278 hours/year
2 minor time employees

Project funds

5 junior scientists

5.2 Lectures at universities

Hon.-Prof. Dr. H. Drewes: Geodätische Geodynamik, Technische Universität München, WS 2005/2006

PD Dr. M. Schmidt: Approximation Methods, Technische Universität München, WS 2005/2006

Dr. B. Richter: Geodätische Bezugssysteme, Universität Stuttgart, WS 2005/2006

PD Dr. M. Schmidt: Wavelets, Technische Universität München, SS 2006

5.3 Graduations and honours

Doctoral graduation:

22.02.2006: J.C. Báez, Concepción, Chile, and PhD Student at DGFI: Monitoramento das deformações da rede de referência do SIRGAS em área com atividade tectônica. Univ. Federal do Paraná, Curitiba, Brasil.

23.02.2006: R. Dalazoana, Curitiba, Brasil, and PhD Student at DGFI: Estudos dirigidos à análise temporal do Datum Vertical Brasileiro. Univ. Federal do Paraná, Curitiba, Brasil.